FISH KAIROMONE-INDUCED DEFENSES IN CRUSTACEAN ZOOPLANKTON: ON THE DIVERSITY OF STRATEGIES, MECHANISM, AND ENVIRONMENT

by

Corie L. Charpentier

A dissertation submitted to the Faculty of the University of Delaware in partial fulfillment of the requirements for the degree of Doctor of Philosophy in Marine Studies

Spring 2017

© 2017 Charpentier
All Rights Reserved

FISH KAIROMONE-INDUCED DEFENSES IN CRUSTACEAN ZOOPLANKTON: ON THE DIVERSITY OF STRATEGIES, MECHANISM, AND ENVIRONMENT

by

Corie L. Charpentier

Approved: _____
Mark A. Moline, Ph.D.
Director of the School of Marine Science and Policy

Approved: _____
Mohsen Badiey, Ph.D.
Acting Dean of the College of Earth, Ocean, and Environment

Approved: _____
Ann L. Ardis, Ph.D.
Senior Vice Provost for Graduate and Professional Education

I certify that I have read this dissertation and that in my opinion it meets the academic and professional standard required by the University as a dissertation for the degree of Doctor of Philosophy.

Signed: _____

Jonathan H. Cohen, Ph.D.
Professor in charge of dissertation

I certify that I have read this dissertation and that in my opinion it meets the academic and professional standard required by the University as a dissertation for the degree of Doctor of Philosophy.

Signed: _____

Timothy E. Targett, Ph.D.
Member of dissertation committee

I certify that I have read this dissertation and that in my opinion it meets the academic and professional standard required by the University as a dissertation for the degree of Doctor of Philosophy.

Signed: _____

Mark E. Warner, Ph.D.
Member of dissertation committee

I certify that I have read this dissertation and that in my opinion it meets the academic and professional standard required by the University as a dissertation for the degree of Doctor of Philosophy.

Signed: _____

Daniel Rittschof, Ph.D.
Member of dissertation committee

ACKNOWLEDGMENTS

I would like to thank my committee for their guidance and support. First, I thank my advisor, Jon Cohen, for encouraging me to pursue my research interests, while always maintaining an open door to entertain my thoughts, questions, and conundrums. Through Jon's mentorship, I have grown as a scientist, and been given abundant opportunities to ponder and explore the world, from Svalbard to Montevideo. I am also grateful for Tim Targett. He has guided my understanding of fish ecology and sampling, and provided ongoing support of my career through countless recommendations. Furthermore, I thank Mark Warner, who has allowed me the use of his laboratory and also provided several recommendations in my continuous pursuit of a career in science. Finally, I would like to express my appreciation for my external committee member, Dan Rittschof. His thought-provoking questions have kept me enlightened and alert.

I am also thankful for my labmates, Adam Wickline, Heather Cronin, Laura Smith, Talene Yeghissian, Haley Glos, and Ryan Pieffer as well as undergraduate research assistants, Alex Wright, Chris Angell, and Patrick Duffy. I have been quite literally stuck in the mud with many of you, and I kindly thank you for your humor, fervor, and patience. Outside of the Cohen Lab, I thank the Cai Lab, the Hanson Lab, as well as the amazing administrative staff in the School of Marine Science and Policy for their expertise and support. In addition, I am grateful for the many funding sources that have made this work possible, the Marian R. Okie Fellowship, the Joanne Currier Daiber Fellowship, the Delaware Research Foundation, Sigma Xi, and the Delaware

Environmental Institute (DENIN). In particular, the staff and students at DENIN have become a proactive part of my graduate student experience.

Finally, I would like to thank my friends and family for their ongoing dedication. Along the way, I have been fortunate in gaining lifelong friends, whose laughter and kindness can brighten even the dreariest of days, from 02882 to Eckerd and the Daiberhood. I am also grateful to Andrew. I cannot imagine maintaining such optimism throughout my dissertation without his persistent sense of humor and joy. Last but certainly not least, thank you to my mum, who has never wavered in her encouragement of my pursuits and aspirations, from my childhood days of tidal pool hopping to the defense of this dissertation. There are no words that accurately describe the weight of her support.

It truly takes a village to raise a scientist, and I continue to learn and grow from my mentors, peers, family, and friends. In my opinion, there is no greater fortune!

TABLE OF CONTENTS

LIST OF TABLES x
LIST OF FIGURES xii
ABSTRACT xix

Chapter

1 INTRODUCTION 1

1.1 Predator-Induced Defenses in Zooplankton 1
1.2 Fish Kairomones 3
1.3 The Current State of Affairs 5
1.4 Dissertation Objectives and Structure 7

REFERENCES 11

2 FISH KAIROMONES HEIGHTEN VISUAL SENSITIVITY IN LARVAL CRABS THROUGH CHANGES IN PHOTORECEPTOR STRUCTURE AND FUNCTION 18

2.1 Introduction 19
2.2 Methods 22

2.2.1 Experimental solutions 22
2.2.2 Crab collection and rearing 23
2.2.3 Behavioral experiments 23
2.2.4 Electrophysiology 26
2.2.5 Histology: Eye structure 28
2.2.6 Estimated changes to depth 31

2.3 Results 32

2.3.1 Defensive photobehavior 32
2.3.2 Electrophysiology 35
2.3.3 Eye structure 39

2.4 Discussion 41
2.5 Conclusion 49

REFERENCES 51

3 KAIROMONES FROM MARINE FISH INCREASE VISUAL SENSITIVITY IN BRINE SHRIMP FROM GREAT SALT LAKE, UTAH, USA 57

3.1 Introduction 58
3.2 Methods 60

3.2.1 Experimental solutions 60
3.2.2 Animal rearing 61
3.2.3 Photobehavior 61
3.2.4 Electrophysiology 63
3.2.5 Eye structure 66

3.3 Results 69

3.3.1 Photobehavior 69
3.3.2 Electrophysiology 70
3.3.3 Eye structure 74

3.4 Discussion 75

REFERENCES 81

4 ACIDIFICATION AND γ-AMINOBUTYRIC ACID ALTER KAIROMONE-INDUCED BEHAVIOR IN A LARVAL CRAB 86

4.1 Introduction 86
4.2 Methods 89

4.2.1 Animal collection and rearing 89
4.2.2 Behavioral experiments 89

4.2.2.1 The pH experiment 90
4.2.2.2 The gabazine dose-response experiment 93

4.2.3 Analysis of extracellular fluid 93
4.2.4 Seawater chemistry 94

4.3 Results and Discussion 97
4.4 Conclusion 102

REFERENCES 104

5 FISH KAIROMONES INDUCE SPINE ELONGATION AND REDUCE PREDATION IN MARINE CRAB LARVAE 110

5.1 Introduction 110
5.2 Methods 113

5.2.1 Morphology experiment 113
5.2.2 Predation experiment 114
5.2.3 Brood effects (combined comparison) 116

5.3 Results 117

5.3.1 Morphology experiment 117
5.3.2 Predation experiment 118
5.3.3 Brood effects (combined comparison) 120

5.4 Discussion 122

REFERENCES 126

6 QUANTIFYING FISH KAIROMONES IN ESTUARINE WATER: IS THE KAIROMONE EFFECT TO ZOOPLANKTON PHOTOBEHAVIOR A LABORATORY ARTIFACT? 130

6.1 Introduction 131
6.2 Methods 133

6.2.1 Field collection 133
6.2.2 Chemical assay 135
6.2.3 Behavioral assay 137
6.2.4 Statistical analyses 140

6.3 Results 141

6.3.1 Fish quantity 141
6.3.2 Chemical assay 143
6.3.3 Behavioral assay 145

6.4 Discussion 147

REFERENCES 152

7 CONCLUDING REMARKS 157

REFERENCES 163

Appendix

A CHAPTER 4 SUPPLEMENTARY MATERIALS 166

A.1 Supplemental Methods 166

A.1.1 The pH experiment 166
A.1.2 Analysis of extracellular fluid 166
A.1.3 Seawater chemistry 167

REFERENCES 169

B CHAPTER 5 SUPPLEMENTARY MATERIALS 170

B.1 Animal rearing and maintenance 170
B.2 Predation experiment 171

B.2.1 Fish morphology 171
B.2.2 Experimental chamber 171
B.2.3 Larval morphology and swimming speed 174

B.3 Power analysis 175

REFERENCES 177

C CHAPTER 6 SUPPLEMENTARY MATERIALS 178
D RIGHTS AND PERMISSIONS OF PUBLISHED CHAPTERS 181

D.1 Journal of Experimental Biology (Ch. 2) 181
D.2 Royal Society Open Science (Ch. 4) 183

E ANIMAL CARE APPROVAL 185

LIST OF TABLES

Table 2.1: Behavioral threshold, physiological sensitivity, and optical sensitivity in *Rhithropanopeus harrisii* and *Hemigrapsus sanguineus* exposed to control seawater (C) or kairomones (K) from *Fundulus heteroclitus* mucus (0.1 g L^{-1}) 35

Table 2.2: Response-intensity curve parameters in *Rhithropanopeus harrisii* and *Hemigrapsus sanguineus* exposed to control seawater (C) or kairomones (K) from *Fundulus heteroclitus* mucus (0.1 g L^{-1}) 37

Table 2.3: Acceptance angle calculated from eye structure across kairomone exposure time in *Rhithropanopeus harrisii* and *Hemigrapsus sanguineus* 42

Table 3.1: Response-intensity curve parameters in *Artemia* spp. exposed to the control, negative control (aged mucus), or kairomones ("kairo.") from *Fundulus heteroclitus* mucus (0.001 and 0.1 g mucus L^{-1} seawater) 72

Table 3.2: Characteristics of eye structure as well as optical sensitivity and acceptance angle in *Artemia* spp. after exposure to kairomones from *Fundulus heteroclitus* mucus (0.1 g mucus L^{-1} seawater) for 0, 0.5, 1, and 3 h. 74

Table 3.3: Characteristics of eye structure as well as optical sensitivity and acceptance angle in *Artemia* spp. after light and dark acclimation 75

Table 4.1: Parameters of the carbonate system during experiments 96

Table 4.2: Effect of gabazine on kairomone-induced photosensitivity of stage 3 *Hemigrapsus sanguineus* larvae 100

Table 4.3: Osmolality (mOsm kg^{-1}) and Cl^- concentration ($[Cl^-]$, m*M*) in extracellular fluid (ECF) of stage 1 *Hemigrapsus sanguineus* larvae after exposure to various salinities 101

Table 6.1: Environmental parameters of field water at the time of collection 135

Table A.1: Salinity of artificial seawater (Instant Ocean) at 0 and 24 h after dissolution of salt mixture into deionized water 168

Table B.1: Sizes (mm) of *Menidia menidia* used in the predation experiment, given Z3 *Rhithropanopeus harrisii* that had been previously exposed to control seawater or kairomones over two timescales, developmental (since time of hatching) and acute (1 – 3 h) 171

Table B.2: Morphology and swimming speed of Z3 *Rhithropanopeus harrisii* given control seawater or kairomones at two timescales, developmental (since time of hatching) and acute (1 – 3 h), prior to the predation experiment 175

Table C.1: Descent responses and behavioral thresholds of *Artemia* spp. nauplii after a 1 – 3 h exposure to field water from samples taken in 2014 and 2015. 179

Table D.1: Rights and permissions as described by the Journal of Experimental Biology 182

LIST OF FIGURES

Figure 1.1: Chondroitin sulfate A disaccharide, one of the amino sugars known to induce behavioral changes in marine zooplankton. The molecule is shown as it would be charged in seawater. 4

Figure 2.1: Behavioral thresholds of photobehavior. Mean ± s.e.m. percent descending (± 60°) of (A) stage 4 *Rhithropanopeus harrisii* and (B) stage 3 *Hemigrapsus sanguineus* zoeae before (swimming in the dark) and after light stimulation. Animals (~30 individuals) in each replicate (n = 5) were exposed to either control seawater (0 g L^{-1}) or kairomones from *Fundulus heteroclitus* mucus at 0.1, 0.01, or 0.001 g mucus L^{-1} seawater. Behavioral thresholds, or significant differences in percent descending before and after light stimulation, were determined by one-way repeated measures ANOVAs with Holm-Sidak *post-hoc* tests and accepted at $P < 0.05$. These thresholds are represented by asterisks of respective treatment symbol colors. Data shown here for animals swimming in the dark are the combined mean ± s.e.m. of all four treatments..... 34

Figure 2.2: Response-intensity (V – log I) curves. Mean ± s.e.m. normalized ERG responses across a log range of irradiances (photons m^{-2} s^{-1}), in (A) stage 4 *Rhithropanopeus harrisii* and (B) stage 3 *Hemigrapsus sanguineus* zoeae exposed to control seawater (n = 5) or kairomones from *Fundulus heteroclitus* mucus at 0.1 g mucus L^{-1} seawater (n = 5). Curves were modeled using the Zettler modification of the Naka-Rushton equation, and log k of each curve is indicated by a dotted line of its respective treatment color. Inset with each V – log I curve, are representative ERG response waveforms at log K of control (black) and kairomone-treated animals (red), with length of light stimulus (0.1 s) and response magnitude indicated by scale bars. The timescale of insets is positioned at the onset of the light stimulus. 37

Figure 2.3: Latency in ERG responses. Mean ± s.e.m. response latency (ms) in (A) stage 4 *Rhithropanopeus harrisii* and (B) stage 3 *Hemigrapsus sanguineus* zoeae as well as mean ± s.e.m. peak latency (ms) in the same stage *R. harrisii* (C) and *H. sanguineus* (D) across a log range of irradiances (photons m^{-2} s^{-1}). Animals were exposed to either control seawater (n = 5) or kairomones from *Fundulus heteroclitus* mucus at 0.1 g mucus L^{-1} seawater (n = 5). As indicated by the inset, response latency was defined as the time from the light stimulus onset to the response start, and peak latency as the time from the light stimulus onset to the response peak. 39

Figure 2.4: Characteristics of eye structure. (A) Semi-thin (0.2 μm) longitudinal section from a stage 4 *Rhithropanopeus harrisii* zoeae compound eye. Structural characteristics used in analysis are highlighted in white and include cone length (CL), aperture diameter (AD), rhabdom length (RL), and rhabdom diameter at the distal tip (RD). Mean ± s.e.m. rhabdom diameter (μm) in (B) stage 4 *Rhithropanopeus harrisii* and (C) stage 3 *Hemigrapsus sanguineus* zoeae, as well as mean ± s.e.m. rhabdom length (μm) in the same stage (D) *R. harrisii* and (E) *H. sanguineus*. Zoeae were exposed to kairomones from *Fundulus heteroclitus* mucus at a concentration of 0.1 g L^{-1} for 0 (control), 0.5, 1, or 3 h, and sample size at each exposure time is noted in parentheses. Significant differences in rhabdom size between control and kairomone-exposed animals (0.5, 1, 3 h) were determined by one-way ANOVAs with Holm Sidak *post-hoc* tests, accepted if $P < 0.05$, and represented by asterisks. 41

Figure 2.5: Estuarine water column depth at the larval crab behavioral threshold. Solid lines are downwelling irradiance weighted by the spectral sensitivity of *Rhithropanopeus harrisii* larvae, thereby representing the light utilized by the larval crab eye at a given depth (Crab utilized photons). Light at depth is calculated from surface irradiance of 2.9×10^{20} photons m^{-2} s^{-1} (midday; grey line) and 2.9×10^{18} photons m^{-2} s^{-1} (twilight; black line), using a diffuse attenuation coefficient (K_d) of 1.4 m^{-1}. For each time of day, the depth difference for *R. harrisii* behavioral threshold with (+ K) and without kairomones (- K) is shown as an inset thickened vertical line, with horizontal lines indicating the light level at these behavioral thresholds..... 49

Figure 3.1: Semi-thin (0.2 um) longitudinal cross-section of the *Artemia* spp. compound eye stained with Toludine Blue O and Basic Fuchsin. Each of the characteristics measured in the structural analysis are highlighted in white, including glycogen body diameter (GD), glycogen body length (GL), aperture diameter (AD), rhabdom length (RL), rhabdom diameter (RD), cone diameter (CD), and cone length (CL). All measured ommatidia were within the acute zone, described by Nilsson and Odselius (1981). 68

Figure 3.2: Kairomones alter photobehavior. Mean ± se percentage descending (nadir ± 30°) of *Artemia* spp. before (swimming in the dark, unfilled symbols) and after light stimulation (filled symbols). Prior to experiments, animals (≈ 20) from each replicate (n = 5) were exposed to control seawater (0 g L^{-1}) or kairomones from *Fundulus heteroclitus* mucus, across a concentration gradient (0.001 – 0.1 g mucus L^{-1} seawater). The behavioral threshold of each treatment, or lowest light intensity to induce a descent response, was determined using one-way repeated measures ANOVAs with Holm-Šidák *post hoc* analyses, where significant differences were accepted at $P < 0.05$. Asterisks represent these thresholds, with each given its respective treatment color. 70

Figure 3.3: Response-intensity curves. Mean ± se normalized ERG responses across a log range of irradiance stimulations in *Artemia* spp.. Prior to experiments, individuals were given control seawater (0 g L^{-1}, n = 11), a negative control (aged 0.1 g mucus L^{-1} seawater, n = 5), or two concentrations of kairomones from *Fundulus heteroclitus* mucus (0.001, 0.1 g mucus L^{-1} seawater; n = 5 and 11, respectively). Curves were modeled using the Zettler modification of the Naka-Rushton equation, and log K of the control and highest kairomone concentration (0.1 mucus g seawater L^{-1}) are highlighted with dotted lines of their respective treatment colors. Insets (right) show a representative ERG response waveform at log K for each treatment as well as the length and timing of a light stimulus (0.1 s). Scale bar (top) indicates the time and magnitude of ERG responses. 72

Figure 3.4: Effect of light and kairomones to temporal resolution. Mean ± se (A) response and (B) peak latency of *Artemia* spp. exposed to a log range of irradiance stimulations. Prior to experiments, individuals were given control seawater (0 g L^{-1}, n = 11), a negative control (aged 0.1 g mucus L^{-1} seawater, n = 5), or two concentrations of kairomones from *Fundulus heteroclitus* mucus (0.001, 0.1 g mucus L^{-1} seawater; n = 5 and 11, respectively). The inset at the top of panel B indicates the time of the light stimulus, response start ("response latency"), and response peak ("peak latency") in a representative response. 73

Figure 4.1: Tidal and diel pH cycles. Time series of pH (black), tidal height (m above mean lower low water, blue), and day (light grey) versus night (dark grey), measured on July 9th, 2015 in Roosevelt Inlet, DE, USA, adjacent to collection site, with a Sonde (6600-V2; YSI Incorporated, Yellow Springs, OH, USA). 92

Figure 4.2: Effect of pH on kairomone-induced photosensitivity. Mean ± se percent descending of larval *Hemigrapsus sanguineus* in darkness (unfilled) and after exposure to downwelling light (filled). Before experiments, animals were exposed to (*a*,*c*) ambient pH or (*b*,*d*) low pH, and to control (black), gabazine-only (10 μ*M*, gray), kairomones (red), or kairomones with gabazine (blue). Behavioral thresholds, or light intensity that elicits a descent response, are indicated with asterisks and were determined by one-way RM ANOVAs with Holm-Šidák *post hoc* tests ($P < 0.05$; n = 5 replicates with ~ 15 larvae per replicate, except n = 4 replicates in ambient, gabazine-only treatment). 99

Figure 5.1: Interspecific variation in morphology and response to kairomones in (a) Z3 *Rhithropanopeus harrisii* and (b) Z3 *Hemigrapsus sanguineus*. Mean ± SE body and spine length of *R. harrisii* (c, e respectively) and *H. sanguineus* (d, f respectively) across all zoeal stages, reared in control seawater or kairomones (n = 5 broods except for in Z2 *R. harrisii* where n = 4 broods). Asterisks indicate significant differences in morphology between control and kairomone-treated animals ($P \leq 0.05$; linear mixed models, false discovery rate *post-hoc* tests). 118

Figure 5.2: Kairomones effect predation of zoeae by fish planktivore. Mean ± SE Z3 *Rhithropanopeus harrisii* consumed (0.5 h^{-1}) by juvenile *Menidia menidia* was compared between zoeae given prior exposure to control seawater ("none") or kairomones over acute and developmental ("develop.") timescales (n = 10). Different letters indicate significant differences in the number of zoeae consumed between kairomone exposures ($P \leq 0.05$; general linear mixed effects model, false discovery rate *post hoc* tests)..... 120

Figure 5.3: Variation amongst broods. Mean ± SE of (a) body length and (b) spine length of Z3 *Rhithropanopeus harrisii* from individual broods during the morphology experiment (n = 5) and the predation experiment (n = 10). Connection between two symbols represents zoeae within the same brood. One brood exhibited kairomone-induced changes to spine length ($P < 0.05$; mixed model, false discovery rate *post hoc* test), which is shown in red. 121

Figure 5.4: Kairomone effect varies with body and spine length. Relationship between the relative kairomone effect (with/without kairomones) and initial condition (without kairomones) for (a) body length and (b) spine length of Z3 *Rhithropanopeus harrisii* (n = 15). Regressions are shown with 95% CI as well as corresponding equations, R^2, and *P* values (top right). 122

Figure 6.1: Map of field collection sites. Samples were taken from three sites in Broadkill River, Delaware, USA (within red box of panel A). Site numbers are shown in white (B) and indicate the order in which samples were collected each week, including site 1 (38.802166°, -75.201915°), 2 (38.802166°, -75.201915°), and 3 (38.802141°, -75.201633°). Scale bar is shown on the bottom left of each panel. 135

Figure 6.2: Variability in fish quantity. Mean ± se fish abundance (fish m^{-2}), mass (g m^{-2}) and surface area (cm^{-2} m^{-2}) across the sampling season in 2014 (A, C, E) and 2015 (B, D, F), respectively. Fish were collected with a 3.0 x 0.9 m bagless seine net (8 mm mesh) in 2014 and a 3 x 1.2 m seine net with a bag (6.4 mm mesh) in 2015. The scale of fish quantity is also different between 2014 and 2015. 142

Figure 6.3: Relative kairomone concentration increases with fish quantity. Mean ± se sGAG concentration (μg mL^{-1}) across log abundance (fish m^{-2}), log mass (g m^{-2}), and log surface area (cm^{-2} m^{-2}) in 2014 (A, B, C; n = 20) and 2015 (D, E, F; n = 23). For all significant relationships ($P \leq 0.05$), regression lines are shown with 95% confidence intervals, equations, and adjusted R^2 values in the bottom right of the panel..... 144

Figure 6.4: Temperature affects sGAG concentration in 2014. Mean ± se sGAG concentration (μg mL^{-1}) across temperature (°C) in 2014 field samples (n = 20). Regression line is shown with 95% confidence intervals, equation, and adjusted R^2 value (top left). Symbol gradient represents log fish abundance ("log A"; fish m^{-2}). 144

Figure 6.5: Mucus solutions resemble field sGAG concentrations. Mean ± se sGAG concentration (μg mL^{-1}) of crude mucus solutions, across a range of concentrations used in previous laboratory experiments (0.001 – 10 g mucus L^{-1} seawater). Concentrations shown are the combined results from assays conducted in 2014 (n = 2) and 2015 (n = 2). The red dashed lines represent the mean minimum and maximum sGAG concentrations of field seawater in 2014 (n = 2) and 2015 (n = 2). 145

Figure 6.6: Photosensitivity increases with fish quantity. Behavioral threshold across log abundance (fish m^{-2}), log mass (g m^{-2}), and log surface area (cm^{-2} m^{-2}) in 2014 (A, B, C; n = 10) and 2015 (D, E, F; n = 21). For all significant relationships ($P \leq 0.05$), regression lines are shown with 95% confidence intervals, equations, and adjusted R^2 value in the top right of the panel..... 146

Figure B.1: Comparison of irradiance in the field to the predation experiment chamber. Moving average (1 nm) of spectral irradiance in the Broadkill River, DE, USA at a depth of 0.5 m during (a) midday (12:00) and (b) sunset (19:11), and (c) at the center of the experimental chamber. Field irradiance measurements were also taken over time at 0.5 m (d), at ± 0.5 h around sunset and ending at the conclusion of civil twilight (integrated from 400 – 700 nm). Highlighted values represent the irradiance at the time of sunset (red) and within the animal chamber (gray). Note scale differences in irradiance for each panel. 174

Figure C.1: Determination of the behavioral threshold. Mean ± se percentage of animals descending (nadir ± 30°) before (black) and after (gray) an increase in light. Prior to experiments, animals were exposed to either (A) control or (B) field seawater for 1 – 3 h. Field seawater was collected on August 28th, 2014, and the example dataset shown here was included in my analysis. Significant differences in the percentage descending before and after light stimulation were determined by one-way repeated measures ANOVAs with Holm–Šidák *post hoc* tests and accepted at $P < 0.05$. The behavioral threshold, or lowest light increase to induce a descent response, is labeled in red. Note that animals in control seawater did not exhibit a significant descent response to increases in light. 178

Figure C.2: Tidal and diel fluctuations in pH. Time series of pH (red), tidal height (m above mean lower low water, black), and day (white) versus night (gray), measured from September 15th, 2015 to September 17th, 2015 in Broadkill River, Delaware, USA (38.802583°, -75.203183°). Measurements of pH were made with a Sonde (6600-V2; YSI Incorporated, Yellow Springs, OH, USA). 180

ABSTRACT

Predator chemical cues, or *kairomones*, induce behavioral and morphological defense strategies in zooplankton. For example, several species become more responsive to light following exposure to fish kairomones. These behavioral changes likely impact diel vertical migration (DVM). A nearly universal behavior amongst zooplankton, DVM generally describes the nighttime ascent to feed and daytime descent to avoid visual predators. Although predator avoidance was proposed as the adaptive significance of DVM decades ago, we know little about the mechanism by which kairomones alter photobehavior. In addition, several zooplankton species exhibit kairomone-induced morphological defenses (e.g. spines), although previous reports of morphological plasticity have been generally limited to freshwater zooplankters. Despite laboratory and field evidence of kairomone-induced defenses, further work is needed to quantify the effective concentration of kairomone molecules in marine environments.

Here, I first evaluated the mechanism by which kairomones enhance photoresponses in zooplankton. Comparing behavior and visual physiology (electrophysiology, eye structure), I found that kairomones altered photobehavior by increasing visual sensitivity at the photoreceptor level in the larvae of two marine crab species, *Rhithropanopeus harrisii* and *Hemigrapsus sanguineus*, as well as in a

branchiopod crustacean, *Artemia* spp. Using similar behavioral experiments, I also found that signaling by a ubiquitous neurotransmitter, γ-aminobutyric acid (GABA), is required for detection and/or processing of predator kairomones in larval *H. sanguineus*. In addition, larvae lost the ability to detect kairomones after exposure to low pH/high CO_2, over timescales that reflect diel/tidal pH cycles in coastal ecosystems (12 h). The mechanism of this pH effect differs from that described in fish, and the loss of kairomone-induced photosensitivity at low pH may be adaptive in these zooplankton under diel-cycling pH.

In addition to behavioral defenses, crab larvae have spines. In some species, including *R. harrisii*, these spines are known to aid in predator defense. The freshwater crustacean zooplankton, *Daphnia*, exhibit drastic spine elongation after exposure to predator kairomones, but similar phenotypic plasticity has not been observed in estuarine or marine crustacean zooplankton. Here, I assessed the effect of developmental kairomone exposure on the morphology of crab larvae (*R. harrisii* and *H. sanguineus*). Kairomone exposure resulted in slightly elongated spines in larval *R. harrisii* as well as decreased consumption by a planktivorous fish, *Menidia mendia*, suggesting that the observed spine elongation is an inducible defense.

The described behavioral and morphological defenses are induced by fish kairomones. In estuarine and marine systems, these signaling molecules are derived from body mucus and include sulfated glycosaminoglycans (sGAGs). Little work has been done to quantify these cues in marine environments or to assess whether kairomone concentrations used in laboratory studies reflect natural scenarios. During a

two-year field study, I applied quantitative chemical and behavioral assays to measure these kairomones in an estuarine environment. I found that sGAG concentration and zooplankton photosensitivity were positively related to fish quantity. Further, sGAG concentration was similar between field samples and mucus extracts used in previous laboratory experiments, supporting that kairomone-induced changes to zooplankton behavior are not an artifact of laboratory experiments.

The results of this dissertation have important implications to evolutionary biology, namely the evolution of sensory systems. For example, we can now compare the neural mechanisms that mediate kairomone-induced photobehavior in crustaceans to other zooplankton and ancestral defense mechanisms. More broadly, DVM impacts biogeochemical cycles and ecological interactions in aquatic environments. Hence, assessing the response of migrating zooplankton to environmental change (e.g. acidification, predator abundance) is essential in predicting ecosystem health. Although previous laboratory work has provided immense insight to zooplankton behavior in a controlled environment, there is still a great need for complementary fieldwork.

Chapter 1

INTRODUCTION

In aquatic ecosystems, chemical communication is omnipresent. From microbes to megafauna, freshwater and marine organisms use chemical signals to decode and thereby respond to information that is important to foraging, ecological interactions, and survival (Pohnert et al. 2007; Hay 2009; Von Elert 2012). In zooplankton, for example, chemical cues from fish predators induce traits that aid in predator avoidance (Lass and Spark 2003; Cohen and Forward 2009). These cues are defined as *kairomones*, because they are interspecific signaling molecules that benefit the receiver (Brönmark and Hansson 2012). Below, I introduce predator-induced defenses in zooplankton, describe the kairomone molecules that induce these defenses, discuss current interest in inducible defenses and similar chemical signaling paradigms, and finally explain the rationale and structure of this dissertation.

1.1 Predator-Induced Defenses in Zooplankton

Kairomone-induced defenses are phenotypically plastic and include alterations to life history, morphology, and behavior. For example, after kairomone exposure, freshwater cladocerans alter reproduction time, fecundity, and production of diapause eggs (Riessen 1999). In marine zooplankton, kairomone exposure results in larval cloning (*Dendraster excentricus*, Vaughn and Strathmann 2008) as well as accelerated growth at the end of larval development (*Temora longicornis*, Bjærke et al. 2014).

Kairomone-induced morphological defenses have been most thoroughly described in freshwater ecosystems. Furthermore, the cladoceran *Daphnia* has become a textbook example of phenotypic plasticity in morphological defenses. When exposed to chemical cues from predators, *Daphnia* produce various defensive structures (e.g. helmets, tail spines) via cyclomorphosis (Tollrian and Dodson 1999). Other freshwater zooplankters exhibit similar changes, including spine elongation in rotifers (Gilbert 2013) as well as increases in cell width and dorsal crests in *Euplotes* ciliates (Kuhlmann et al. 1999). Similar observations are rare in marine zooplankton, with one report of kairomone-induced changes to shell morphology in the larvae of a marine snail (Vaughn 2007).

A variety of behavioral defense responses have been observed following exposure to predator kairomones, including decreased movement (Hazlett 2000), retreating from odor sources (Diaz et al. 2003), as well as changes in photobehavior (reviewed in Cohen and Forward 2009; Ringelberg 2010). In both marine and freshwater zooplankton, kairomones increase photosensitivity, where kairomone-exposed animals respond to smaller changes in the downwelling light than they do in the absence of kairomones. Such changes in light include both differences in the magnitude and the rate-of-change (Cohen and Forward 2009; Ringelberg 2010). This increased photosensitivity likely deepens diel vertical migration (DVM; Charpentier and Cohen 2015), as light is the proximate cue for DVM. A nearly universal behavior amongst zooplankton, DVM generally describes the nighttime ascent to feed and daytime descent to avoid visual predators (e.g. fish). Given its universality, DVM is

thought to be the greatest migration of biomass on earth (Hays 2003). In addition to light and kairomones, migrations are influenced by temperature, salinity, and food availability (reviewed in Williamson et al., 2011, Epifanio and Cohen 2016). Kairomones have also been shown to result in a more dramatic avoidance of overhead shadows, so-called *shadow responses*, which likely aid in predator avoidance (Cohen and Forward 2003). Although shadow responses and DVM require the integration of multiple sensory modalities (e.g. light, chemical cues), we know little about the mechanism by which kairomones amplify photobehavior in marine zooplankton.

1.2 Fish Kairomones

Although responses to fish kairomones are comparable between marine and freshwater zooplankton, the chemical composition of these signaling molecules likely differs. In freshwater environments, fish kairomones are low-molecular weight (< 500 Da), soluble compounds of intermediate lipophilicity, and glucuronic acids, sulfate, phosphate, and carboxyl groups are not required for biological activity (Von Elert and Pohnert 2000). The origin of freshwater kairomones is still up for debate, although bacteria associated with fish are likely involved (Ringelberg and Van Gool 1998; Ringelberg 2010). In marine ecosystems, fish kairomones are degradation products from external body mucus. Mucus is composed of protein moieties and polysaccharide chains known as glycosaminoglycans (GAGs), made of repeating disaccharide units (400 – 600 Da each) of uronic acid with glycosidic linkages to substituted (often acetylated/sulfated) amino sugars (Shephard 1994; Forward and Rittschof 1999; Rittschof and Cohen 2004). Cues that induce photobehavioral responses in marine zooplankton are disaccharides and monosaccharides, released from larger mucus

molecules by hydrolysis with heparinase and chondroitinase enzymes (Rittschof and Cohen 2004). There are four basic types of GAG molecules, including hyaluronic acid, chondroitin sulfate/dermatan sulfate (Figure 1.1), heparin/heparin sulfate, and keratan sulfate. Of these, di-/monosaccharide units of hyaluronic acid, chondroitin sulfate, and heparin sulfate have been shown to induce photosensitivity in zooplankton (Forward and Rittschof 1999, 2000), though only chondroitin sulfate and hyaluronic acid have been identified as a component of fish mucus (van de Winkel et al. 1986; Karamanos et al. 1991). Mucus molecules from different species of marine fish and even a ctenophore are similarly effective in inducing defensive photobehavior (McKelvey and Forward 1995).

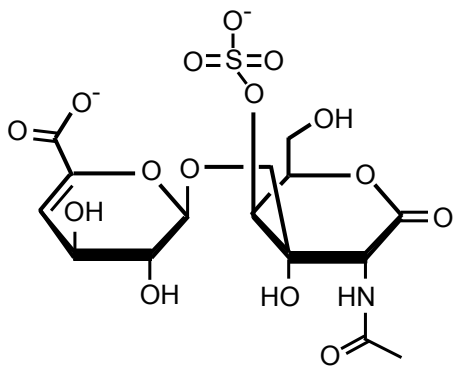

Figure 1.1: Chondroitin sulfate A disaccharide, one of the amino sugars known to induce behavioral changes in marine zooplankton. The molecule is shown as it would be charged in seawater.

Several laboratory studies have shown that kairomones from fish mucus and purified GAG mimics induce photosensitivity in marine zooplankton and a zooplankton from hypersaline, endorheic lakes (Forward and Hettler 1992; McKelvey

and Forward 1995; Forward and Rittschof 1999, 2000; Cohen and Forward 2003, 2005; Charpentier and Cohen 2015). However, further work is required to validate that previous laboratory studies used ecologically relevant mucus concentrations. In addition, we generally lack an understanding of relevant kairomone concentrations in the field, especially in marine environments.

1.3 The Current State of Affairs

The study of kairomone-induced defenses (including DVM) is, by no means, unchartered territory. Further, the adaptive significance of DVM as a predator avoidance strategy was hypothesized decades ago (Zaret and Suffern 1976), and entire books have been published about inducible defenses (e.g. Tollrian and Harvell 1999). Despite being well established, interest in inducible defenses has not curbed. More recently, reviews and syntheses discuss the proximate/ultimate mechanisms, cost, and chemical ecology of these defenses (e.g. Cohen and Forward 2009; Ferrari et al. 2010; Ringelberg 2010; Williamson et al. 2011; Riessen 2012; Gilbert 2013). In *Daphnia*, for example, the specific proximate mechanisms that mediate inducible defenses have been investigated, down to the location of kairomone receptors and the interconnecting roles of nervous and endocrine system pathways (Weiss et al. 2012, 2015a,b). In addition, mathematical models have been adapted to describe how predator-prey interactions during migration impact trophic ecology (Samanta et al. 2013).

Vertical migration, in particular, is of great interest to oceanographers, because zooplankton migrations significantly impact biogeochemical cycles (Steinberg et al. 2002; Stukel et al. 2013), and migration amplitude is intimately tied to the environment. For example, Bianchi et al. (2008) found that oxygen concentration is

the best single predictor of migration depth on a global scale. However, we are only just beginning to understand how DVM and other ecologically important behaviors will adjust to our rapidly changing climate. Due to anthropogenic CO_2 emissions, scientists have observed ocean warming, acidification, and de-oxygenation on a global scale (Levitus et al. 2000; Doney et al. 2009; Gilly et al. 2013), and recent estimates indicate a continuation of these effects. For example, ocean pH is predicted to increase by 0.14–0.43 before 2100 (IPCC 2014). Acidification of this magnitude can alter sensation and behavior in marine animals (Clements and Hunt 2015), including defensive behavior (Bibby et al. 2007; Ferrari et al. 2011), chemosensation (Dixson et al. 2010), and vision (Chung et al. 2014). These changes may profoundly impact ecology. After exposure to pH levels expected before 2100, larval reef fish were either attracted to or could not discriminate predator odor, which increased their mortality due to predation (Dixson et al. 2010; Munday et al. 2010).

Nilsson et al. (2012) proposed that these acidification effects are due to a disruption of neural function during acid-base regulation, specifically by action of the ubiquitous, inhibitory neurotransmitter γ-aminobutyric acid (GABA). Briefly, when GABA binds to its ionotropic $GABA_A$ receptor, the receptor opens, and anions (namely chloride, Cl^-) enter the neuron, resulting in hyperpolarization. Following an acid disturbance, many marine fish and crustaceans avoid acidosis by accumulating extracellular bicarbonate while removing/exchanging Cl^- to the external environment (Brauner and Baker 2009; Henry et al. 2012). Decreases in extracellular Cl^-, relative to intracellular concentrations, alter the electrochemical gradient, after which Cl^- exits the neuron through $GABA_A$ receptors, causing depolarization and ultimately loss of original function. In support of this hypothesis, exposure to gabazine, a $GABA_A$

antagonist, eliminates acidification effects on behavior in both fishes and a mollusk (Nilsson et al. 2012; Hamilton et al. 2014; Watson et al. 2014). Surprisingly, most studies testing this GABA hypothesis do not provide direct measurements of extracellular Cl^-, with few exceptions (Damsgaard et al. 2015).

Kairomone-induced defenses require chemosensation, and often the integration of other sensory systems (e.g. vision in DVM). Hence, I would expect acidification to impact zooplankton behavior and ecology. As described above, prior study has focused on deleterious pH effects in the context of future global ocean acidification. However, many zooplankton species inhabit shallow coastal environments, where present-day diel and tidal fluctuations in pH are common and often greater than near-future predictions for global declines in pH (Baumann et al. 2014). An understanding of how these animals function in present-day acidification cycles will provide insight to adaptive variation and response to future change.

1.4 Dissertation Objectives and Structure

Nearly five years ago, I was provided with the fortunate opportunity to expand what was once a concise research objective (described in Chapter 2) into a PhD dissertation that fit my research interests and personality (for better or for worse). As such, this dissertation is a compilation of thoughtfully scattered ideas, which generally fall under the topics of predator-induced defenses, chemical ecology, and zooplankton physiology. Using crustacean zooplankton and their fish predators as a model, my principle objectives were to (1) determine the mechanism by which kairomones alter photobehavior in marine zooplankton, (2) compare this marine mechanism to a zooplankter that behaves similarly but resides in endorheic, saltwater lakes, (3) assess whether diel pH cycles might impact kairomone-induced photobehavior and test

Nilsson et al.'s GABA hypothesis, (4) investigate the possibility of inducible morphological defenses in marine crustacean zooplankton, and (5) quantify fish kairomones in a marine ecosystem and assess how these concentrations compare to those used in previous laboratory studies.

The crustacean zooplankton used in behavioral and physiological analyses were two species of marine crab larvae, *Rhithropanopeus harrisii* (estuarine) and *Hemigrapsus sanguineus* (coastal), as well as the brine shrimp, *Artemia* spp. from an endorheic, saltwater lake. These models were chosen because kairomones amplify photobehavioral responses in larval *R. harrisii* (Forward and Rittschof 2000; Cohen and Forward 2003) and in naupliar *Artemia* spp. (Forward and Rittschof 1999). Further, the three selected species provide interesting ecological and evolutionary comparisons, described below.

Crab larvae, also known as *zoeae*, provide a fitting model to assess kairomone-induced photosensitivity, as they predictably maintain a depth in the water column near the isolume of their threshold for light detection (Forward 1985; Sulkin 1984). In addition, coastal species vary in their location of larval development, and thereby in their exposure to predators through ontogeny. For example, *R. harrisii* spends its entire life history within the estuary, including planktonic zoeal stages (Cronin, 1982). However, most estuarine crab larvae, including *H. sanguineus*, migrate into coastal waters during these early planktonic stages (Park et al. 2005; Epifanio 2013; Cohen et al., 2015). This migration is thought to decrease vulnerability to the high predator concentrations found in estuaries (Christy 2011). Hence, by comparing *R. harrisii* and *H. sanguineus*, I can assess whether the kairomone effect is similar between zooplankters with differences in larval ecology. Also, *H. sanguineus* are invasive to

the West Atlantic (Epifanio 2013), and hence could be less or differentially attuned to chemical cues derived from local predators than the native *R. harrisii*. In addition, crab larvae offer a suitable model for assessing kairomone-induced morphological defenses. Zoeae have spines protruding from the carapace. Compared to most species (including *H. sanguineus*), *R. harrisii* larvae have uniquely large spines. Morgan (1989) determined that *R. harrisii* spines effectively deter planktivorous fish. However, it is unknown if crab larvae display plasticity in spine morphology upon exposure to predator kairomones.

The third model species, *Artemia* spp., is a branchiopod crustacean that inhabits hypersaline endorheic waters, which are physiologically intolerable to most animals, including fish (Persoone and Sorgeloos 1980; Belovsky et al. 2011). Although they generally lack exposure to fish, naupliar *Artemia* exhibit increases in photobehavior after exposure to kairomones from marine and estuarine fish, similar to larval *R. harrisii* (Forward and Hettler 1992, Forward and Rittschof 1999). Further, I used preserved cysts of *Artemia* spp, which can be hatched and used in experiments year-round. Hence, *Artemia* spp provide an accessible behavioral model that opens an interesting evolutionary comparison with marine malacostracan crustaceans, e.g. crab larvae.

Overall, this dissertation is composed of two published manuscripts (Chapter 2 [Charpentier and Cohen 2015] and Chapter 4 [Charpentier and Cohen 2016]), one manuscript currently under review (Chapter 5), and two manuscripts in preparation (Chapters 3 and 6). Chapters 2 and 3 discuss physiological mechanisms for kairomone-induced photobehavior in two crustacean lineages, crab larvae and adult brine shrimp, respectively. Chapter 4 examines the role of acidification and

GABAergic signaling in kairomone-induced photobehavior of marine crab larvae. Moving to a different defense strategy, Chapter 5 describes how kairomones impact the morphology and predation of marine crab larvae. Finally, Chapter 6 tests a methodology for quantifying fish kairomones in a marine ecosystem and investigates whether previous laboratory studies used ecologically relevant kairomone concentrations.

REFERENCES

Baumann, H., Wallace, R. B., Tagliaferri, T., and Gobler, C. J. (2014). Large natural pH, CO_2 and O_2 fluctuations in a temperate tidal salt marsh on diel, seasonal, and interannual time scales. *Estuar. Coast.* 38, 220–231.

Belovsky, G. E., Stephens, D., Perschon, C., Birdsey, P., Paul, D., Naftz, D., … Allen, D. V. (2011). The Great Salt Lake ecosystem (Utah, USA): long term data and a structural equation approach. *Ecosphere* 2, 1–40.

Bianchi, D., Galbraith, E. D., Carozza, D. A., Mislan, K. A. S., and Stock, C. A. (2013). Intensification of open-ocean oxygen depletion by vertically migrating animals. *Nat. Geosci.* 6, 545–548.

Bibby, R., Cleall-Harding, P., Rundle, S., Widdicombe, S., and Spicer, J. (2007). Ocean acidification disrupts induced defences in the intertidal gastropod *Littorina littorea*. *Biol. Lett.* 3, 699–701.

Bjærke, O., Andersen, T., and Titelman, J. (2014). Predator chemical cues increase growth and alter development in nauplii of a marine copepod. *Mar. Ecol. Prog. Ser.* 510, 15–24.

Brauner, C. J. and Barker, D. W. (2009). Patterns of acid-base regulation during exposure to hypercarbia in fishes. In *Cardio-Respiratory Control in Vertebrates* (eds. M. L. Glass and S. C. Wood), pp. 43–63. Berlin: Springer.

Brönmark, C. and Hansson, L. -A. 2012. Chemical ecology in aquatic systems-an introduction. In *Chemical Ecology in Aquatic Systems* (eds. C. Brönmark and L. -A. Hansson), pp. 1-19. New York: Oxford University Press.

Charpentier, C. L. and Cohen, J. H. (2015). Chemical cues from fish heighten visual sensitivity in larval crabs through changes in photoreceptor structure and function. *J. Exp. Biol.* 218, 3381–3390.

Charpentier, C. L. and Cohen, J. H. (2016). Acidification and γ -aminobutyric acid independently alter behaviour. *R. Soc. Open Sci.* 3, 160311.

Christy, J. H. (2011). Timing of hatching and release of larvae by brachyuran crabs: patterns, adaptive significance and control. *Integr. Comp. Biol.* 51, 62–72.

Chung, W.-S., Marshall, N. J., Watson, S. -A., Munday, P. L., and Nilsson, G. E. (2014). Ocean acidification slows retinal function in a damselfish through interference with $GABA_A$ receptors. *J. Exp. Biol.* 217, 323–326.

Clements, J. C. and Hunt, H. L. (2015). Marine animal behaviour in a high CO_2 ocean. *Mar. Ecol. Prog. Ser.* 536, 259–279.

Cohen, J. H. and Forward Jr., R. B. (2003). Ctenophore kairomones and modified aminosugar disaccharides alter the shadow response in a larval crab. *J. Plankton Res.* 25, 203 – 214.

Cohen, J. H. and Forward, R. B. (2005). Photobehavior as an inducible defense in the marine copepod *Calanopia americana*. *Limnol. Oceanogr.* 50, 1269–1277.

Cohen, J. H. and Forward, R. B. (2009). Zooplankton diel vertical migration - A review of proximate control. *Oceanogr. Mar. Biol. Ann. Rev.* 47, 77–110.

Cohen, J. H., Hanson, C. K., Dittel, A. I., Miller, D. C., and Tilburg, C. E. (2015). The ontogeny of larval swimming behavior in the crab *Hemigrapsus sanguineus*: Implications for larval transport. *J. Exp. Mar. Biol. Ecol.* 462, 20–28.

Cronin, T. W. (1982). Estuarine retention of larvae of the crab *Rhithropanopeus harrisii*. *Estuar. Coast. Shelf Sci.* 15, 207–220.

Damsgaard, C., Gam, L. T. H., Dang, D. T., Van Thinh, P., Huong, D. T. T., Wang, T., and Bayley, M. (2015). High capacity for extracellular acid-base regulation in the air-breathing fish *Pangasianodon hypophthalmus*. *J. Exp. Biol.* 218, 1290–1294.

Diaz, H., Orihuela, B., Forward, R. B., and Rittschof, D. (2003). Orientation of juvenile blue crabs, *Callinectes sapidus* Rathbun, to currents, chemicals, and visual cues. *J. Crust. Biol.* 23, 15–22.

Dixson, D. L., Munday, P. L., and Jones, G. P. (2010). Ocean acidification disrupts the innate ability of fish to detect predator olfactory cues. *Ecol. Lett.* 13, 68–75.

Doney, S. C., Fabry, V. J., Feely, R. A, and Kleypas, J. A. (2009). Ocean acidification: The other CO_2 problem. *Ann. Rev. Mar. Sci*. 1, 169–192.

Epifanio, C. E. (2013). Invasion biology of the Asian shore crab *Hemigrapsus sanguineus*: A review. *J. Exp. Mar. Biol. Ecol.* 441, 33–49.

Epifanio, C. E. and Cohen, J. H. (2016). Behavioral adaptations in larvae of brachyuran crabs : A review. *J. Exp. Mar. Biol. Ecol.* 482, 85–105.

Ferrari, M. C. O., Wisenden, B. D., and Chivers, D. P. (2010). Chemical ecology of predator – prey interactions in aquatic ecosystems: a review and prospectus. *Can. J. Zool.* 724, 698–724.

Ferrari M. C. O., McCormick, M. I., Munday P. L., Meekan M. G., Dixson D. L., Lonnstedt Ö., and Chivers D. P. (2011). Putting prey and predator into the CO_2 equation—qualitative and quantitative effects of ocean acidification on predator-prey interactions. *Ecol. Lett.* 14, 1143–1148.

Forward, R. B. (1985). Behavioral responses of larvae of the crab *Rhithropanopeus harrisii* (Brachyura: Xanthidae) during diel vertical migration. *Mar. Biol.* 90, 9–18.

Forward, R. B. and Hettler, W. F. (1992). Effects of feeding and predator exposure on photoresponses during diel vertical migration of brine shrimp larvae. *Limnol. Oceanogr.* 37, 1261–1270.

Forward, R. B. and Rittschof, D. (1999). Brine shrimp larval photoresponses involved in diel vertical migration: Activation by fish mucus and modified amino sugars. *Limnol. Oceanogr.* 44, 1904–1916.

Forward, R. B. and Rittschof, D. (2000). Alteration of photoresponses involved in diel vertical migration of a crab larva by fish mucus and degradation products of mucopolysaccharides. *J. Exp. Mar. Biol. Ecol.* 245, 277–292.

Gilbert, J. J. (2013). The cost of predator-induced morphological defense in rotifers: experimental studies and synthesis. *J. Plankton Res.* 35, 461–472.

Gilly, W. F., Beman, J. M., Litvin, S. Y., and Robison, B. H. (2013). Oceanographic and biological effects of shoaling of the oxygen minimum zone. *Ann. Rev. Mar. Sci.* 5, 393–420.

Hamilton, T. J., Holcombe, A., and Tresguerres, M. (2014). CO_2-induced ocean acidification increases anxiety in Rockfish via alteration of $GABA_A$ receptor functioning CO_2-induced ocean acidification increases anxiety in Rockfish via alteration of $GABA_A$ receptor functioning. *Proc. R. Soc. B* 281, 20132509.

Hay, M. E. (2009). Marine chemical ecology: Chemical signals and cues structure marine populations, communities, and ecosystems. *Ann. Rev. Mar. Sci.* 1, 193–212.

Hays, G. C. (2003). A review of the adaptive significance and ecosystem consequences of zooplankton diel vertical migrations. *Hydrobiologia* 503, 163–170.

Hazlett, B. A. (2000). Responses to single and multiple sources of chemical cues by New Zealand crustacean. *Mar. Freshwater Behav. Physiol.* 34, 1–20.

Henry, R. P., Lucu, C., Onken, H., and Weihrauch, D. (2012). Multiple functions of the crustacean gill: osmotic/ionic regulation, acid-base balance, ammonia excretion, and bioaccumulation of toxic metals. *Front. Physiol.* 3, 431.

IPCC. (2014). The ocean. Climate Change 2014: impacts, adaptation, and vulnerability. Part B: regional aspects. In Contribution of working group II to the fifth assessment report of the intergovernmental panel on climate change (ed. V. R. Barros et al.), pp. 1655–1731. Cambridge: Cambridge University Press.

Karamanos, N. K., Manouras, A., Politou, A. D., Gritsoni, P., and Tsegendidis, T. (1991). Isolation and high-performance liquid chromatographic analysis of ray (*Raja clavata*) skin glycosaminoglycans. *Comp. Biochem. Physiol. B* 100, 827–832.

Kuhlmann, H. W., Kusch, J., and Heckmann, K. (1999). Predator-induced defenses in ciliated protozoa. In *The Ecology and Evolution of Inducible Defenses* (eds. R. Tollrian and C.D. Harvell), pp. 142–159. Princeton: Princeton University Press.

Lass, S. and Spaak, P. (2003). Chemically induced anti-predator defences in plankton: a review. *Hydrobiologia* 491, 221–239.

Levitus, S., Antonov, J. I., Boyer, T. P., and Stephens, C. (2000). Warming of the world ocean. *Science* 287, 2225–2229.

Mckelvey, L. M. and Forward, R. B. (1995). Activation of brine shrimp nauplii photoresponses involved in diel vertical migration by chemical cues from visual and non-visual planktivores. *J. Plankton Res.* 17, 2191–2206.

Morgan, S. G. (1989). Adaptive signficance of spination in estuarine crab zoeae. *Ecol.* 70, 464–482.

Munday, P. L., Dixson, D. L., McCormick, M. I., Meekan, M., Ferrari, M. C. O., and Chivers, D. P. (2010). Replenishment of fish populations is threatened by ocean acidification. *PNAS*, 107, 12930–12934.

Nilsson, G. E., Dixson, D. L., Domenici, P., McCormick, M. I., Sørensen, C., Watson, S.-A., and Munday, P. L. (2012). Near-future carbon dioxide levels alter fish behaviour by interfering with neurotransmitter function. *Nat. Clim. Change* 2, 201–204.

Park, S., Epifanio, C. E., and Iglay, R. B. (2005). Patterns of larval release by the Asian shore crab *Hemigrapsus sanguineus* (De Haan): Periodicity at diel and tidal frequencies. *J. Shellfish Res.* 24, 591–595.

Persoone, G. and Sorgeloos, P. (1980). General aspectis of the ecology and biogeography of *Artemia*. In *The Brine Shrimp Artemia* (eds. G. Persoone, P. Sorgeloos, O. Roels, and E. Jaspers), pp. 3–24). Wettere: Universa Press.

Pohnert, G., Steinke, M., and Tollrian, R. (2007). Chemical cues, defence metabolites and the shaping of pelagic interspecific interactions. *Trends Ecol. Evol.* 22, 198–204.

Riessen, H. P. (1999). Predator-induced life history shifts in *Daphnia*: a synthesis of studies using meta-analysis. *Can. J. Fish. Aquat. Sci.* 56, 2487–2494.

Riessen, H. P. (2012). Costs of predator-induced morphological defences in *Daphnia*. *Freshwater Biol.* 57, 1422–1433.

Ringelberg, J. (2010). Diel Vertical Migration of Zooplankton in Lakes and Oceans. Dordrecht: Springer.

Ringelberg, J. and Van Gool, E. (1998). Do bacteria, not fish, produce "fish kairomone"? *J. Plankton Res.* 20, 1847–1852.

Rittschof, D. and Cohen, J. H. (2004). Crustacean peptide and peptide-like pheromones and kairomones. *Peptides* 25, 1503–1516.

Samanta, S., Chowdhury, T., and Chattopadhyay, J. (2013). Mathematical modeling of cascading migration in a tri-trophic food-chain system. *J. Biol. Phys*. *39*, 469–87.

Shephard, K. L. (1994). Functions for fish mucus. *Rev. Fish Biol. Fish*. 4, 401–429.

Steinberg, D. K., Goldthwait, S. A., and Hansell, D. A. (2002). Zooplankton vertical migration and the active transport of dissolved organic and inorganic nitrogen in the Sargasso Sea. *Deep-Sea Res.* 49, 1445–1461.

Stukel, M., Ohman, M., Benitez-Nelson, C., and Landry, M. (2013). Contributions of mesozooplankton to vertical carbon export in a coastal upwelling system. *Mar. Ecol. Prog. Ser.* 491, 47–65.

Sulkin, S. (1984). Behavioral basis of depth regulation in the larvae of brachyuran crabs. *Mar. Ecol. Prog. Ser.* 15, 181–205.

Tollrian, R. and Dodson, S. I. (1999). Inducible defenses in Cladocera: constraints, costs, and multipredator environments. In *The Ecology and Evolution of Inducible Defenses* (eds. R. Tollrian and C.D. Harvell), pp. 177– 202. Princeton: Princeton University Press.

Van De Winkel, J. G. J., Toin, H. M. S., Van Kupevelt, M., Janssen, H. M., and Lock, R. A. (1986). Glycosaminoglycans in the skin of rainbow trout (*Salmo gairdneri*). *Comp. Biochem. Physiol.* 85B, 473–475.

Vaughn, D. (2007). Predator-induced morphological defenses in marine zooplankton: a larval case study. *Ecol.* 88, 1030–1039.

Vaughn, D., and Strathmann, R. R. (2008). Predators induce cloning in echinoderm larvae. *Science* 319, 1503.

Von Elert, E. (2012). Information conveyed by chemical cues. In *Chemical Ecology in Aquatic Systems* (eds. C Brönmark and L. -A. Hansson), pp. 19-38. New York: Oxford University Press.

Von Elert, E. and Pohnert, G. (2000). Predator specificity of kairomones in diel vertical migration of *Daphnia*: a chemical approach. *Oikos* 88, 119–128.

Watson, S. -A., Lefevre, S., McCormick, M. I., Domenici, P., Nilsson, G. E., and Munday, P. L. (2014). Marine mollusc predator-escape behaviour altered by near-future carbon dioxide levels. *Proc. R. Soc. B* 281, 1–8.

Weiss, L. C., Kruppert, S., Laforsch, C., and Tollrian, R. (2012). *Chaoborus* and *Gasterosteus* anti-predator responses in *Daphnia pulex* are mediated by independent cholinergic and gabaergic neuronal signals. *PloS One* 7, e36879.

Weiss, L. C., Leimann, J., and Tollrian, R. (2015). Predator-induced defences in *Daphnia longicephala*: location of kairomone receptors and timeline of sensitive phases to trait formation. *J. Exp. Biol.* 218, 2918–26.

Weiss, L. C., Leese, F., Laforsch, C., and Tollrian, R. (2015). Dopamine is a key regulator in the signalling pathway underlying predator- induced defences in *Daphnia*. *Proc. R. Soc. B* 282, 20151440.

Williamson, C. E., Fischer, J. M., Bollens, S. M., Overholt, E. P., and Breckenridge, J. K. (2011). Towards a more comprehensive theory of zooplankton diel vertical migration: Integrating ultraviolet radiation and water transparency into the biotic paradigm. *Limnol. Oceanogr.* 56, 1603–1623.

Zaret, T. M. and Suffern, S. (1973). Vertical migration in zooplankton. *Limnol. Oceanogr.* 21, 804 – 812.

Chapter 2

FISH KAIROMONES HEIGHTEN VISUAL SENSITIVITY IN LARVAL CRABS THROUGH CHANGES IN PHOTORECEPTOR STRUCTURE AND FUNCTION

Several predator avoidance strategies in zooplankton rely on the use of light to control vertical position in the water column. Although light is the primary cue for such photobehavior, predator chemical cues or kairomones increase swimming responses to light. We currently lack a mechanistic understanding for how zooplankton integrate visual and chemical cues to mediate phenotypic plasticity in defensive photobehavior. In marine and estuarine systems, kairomones are thought to be amino sugar degradation products of fish body mucus. Here, I demonstrate that increasing concentrations of fish kairomones heightened sensitivity of light-mediated swimming behaviors for two larval crab species (*Rhithropanopeus harrisii* and *Hemigrapsus sanguineus*). Consistent with these behavioral results, I report increased visual sensitivity at the retinal level in larval crab eyes directly following acute (1 – 3 h) kairomone exposure, as evidenced electrophysiologically from V – log I curves and morphologically from wider, shorter rhabdoms. The observed increases in visual sensitivity do not correspond with a decline in temporal resolution, as latency in electrophysiological responses actually increased after kairomone exposure. Collectively, these data suggest that phenotypic plasticity in larval crab photobehavior is achieved, at least in part, through rapid changes in photoreceptor structure and function.

2.1 Introduction

Many zooplankton exhibit phenotypically plastic defense strategies following detection of predator chemical cues. These chemical cues are defined as *kairomones*, because they are interspecific signal molecules that benefit the receiver (Brönmark and Hansson 2012). Predator kairomones have been shown to induce phenotypically plastic changes in defensive behaviors of zooplankton. For instance, exposure to kairomones has been shown to alter photobehavior that is important to predator avoidance, including descent responses with rapid decreases in downwelling light (i.e., shadow responses; Cohen and Forward 2003). Many zooplankton species also descend with small increases in downwelling light, and these responses are thought to contribute to depth regulation behavior, such as diel vertical migration (Cohen and Forward 2009; Ringelberg 2010; Williamson et al. 2011). Thought to be the greatest migration of biomass on earth, diel vertical migration generally describes a habitual nighttime ascent to food-abundant surface waters and a daytime descent to darker waters (Hays 2003). This daytime descent has long been proposed as a strategy to avoid visual predators (Stich and Lampert 1981). More recent work supports diel vertical migration as a predator evasion strategy, as kairomones increase swimming responses to light in marine and freshwater zooplankton (Cohen and Forward 2005; Forward and Rittschof 2000; Van Gool and Ringelberg 2002). Kairomones affect defensive photobehavior after exposure times ranging from 5 minutes to several hours (Forward and Rittschof 1993; Forward and Rittschof 2000), and these changes are reversible after the removal of predator cues in several species (Bollens and Frost 1989; Forward and Hettler 1992).

Although light is the primary cue for these defensive photobehaviors and kairomone exposure can increase such responses, other exogenous cues influence

photobehavior and depth regulation in zooplankton, including temperature, salinity, and food availability (Williamson et al. 2011). Temperature gradients or thermoclines often act as a barrier during depth regulation (Haney 1993; Kessler 2004; Cooke et al. 2008), and tidal cues, such as salinity, can influence vertical distribution and phototaxis in estuarine and coastal zooplankton species that regulate estuarine export or retention during different phases of their life history (Latz and Forward 1977; Cronin and Forward 1986; Welch and Forward 2001). In addition, laboratory studies indicate that starvation affects phototaxis, such that animals activate an ascent response following decreases in downwelling light or maintain shallower daytime depths (Forward and Hettler 1992; Haney 1993). In marine systems, kairomones involved in defensive photobehavior are thought to be degradation products of external body mucus sloughed from fish and ctenophores, and likely contain disaccharide glycosaminoglycans (Rittschof and Cohen 2004).

Although previous work has demonstrated that zooplankton respond behaviorally to light stimuli at lower intensities in the presence of predator kairomones (Forward and Rittschof 2000; Cohen and Forward 2005), we currently lack a mechanism for these observed increases in photobehavioral responses, which are important to predator avoidance. Larval crabs offer a fitting model for better understanding kairomone-induced changes to defensive photobehavior, because zoea larvae predictably maintain a depth near the isolume of their threshold for light detection (Forward 1985; Sulkin 1984), and kairomones exaggerate photobehavior important to predator evasion in larvae of at least one crab species, *Rhithropanopeus harrisii* (Cohen and Forward 2003; Forward and Rittschof 2000). The estuarine mud crab *R. harrisii* spends its entire life history within the estuary, including four

planktonic zoeal stages (Cronin 1982). However, most estuarine crab larvae migrate into coastal waters during their early planktonic stages. Since peak abundance of planktivorous estuarine fish coincides with seasonal crab spawning on the Atlantic coast of the United States (Hagan and Able 2003; Forward 2009; Epifanio 2013), this migration likely decreases vulnerability to estuarine predators (Christy 2011). Such an 'export-and-return' pattern of larval development and recruitment has been proposed for the rocky intertidal crab *Hemigrapsus sanguineus* (Cohen et al. 2015; Epifanio 2013; Park et al. 2005). Thus, a comparison among crab species of kairomone-mediated changes to photosensitivity may yield differences related to predation pressures experienced during larval development.

The main objective of this study was to deduce whether kairomones affect photobehavior by increasing visual sensitivity at the retinal level in two larval crab species, *R. harrisii* and *H. sanguineus*. As previously described, light is thought to be the primary cue for defensive photobehavior in zooplankton with other factors, such as kairomones, modifying the behavioral response to light (Cohen and Forward 2009). Hence, a likely mechanism for how kairomones affect photobehavior, important to predator avoidance via depth regulation, is by increasing visual sensitivity, where zooplankton exposed to kairomones exhibit behavioral and physiological responses to dimmer changes in light than they would otherwise. In a vertical migration scenario, for instance, this might place zooplankton at overall deeper depths in the water column throughout the diel cycle (Forward 1985). Visual sensitivity may be controlled by structural and/or physiological mechanisms, as both play important roles mediating diel changes in visual sensitivity in crustaceans (Meyer-Rochow 1999, 2001) and other arthropods (Battelle 2002, Warrant et al. 2014). Here, electroretinogram (ERG)

recordings and histological methods are employed to investigate kairomone-induced changes to retinal physiology and eye structure that could increase visual sensitivity and thereby result in kairomone-induced increases in photobehavior.

A second objective of this study was to compare defense photobehavior of decapod larvae that utilize two different early life history strategies: estuarine retention in *R. harrisii* and export-and-return in *H. sanguineus*. The presence or magnitude of predator kairomone-induced changes to photobehavior may vary between species that experience different levels of predation pressure during larval development, such as *R. harrisii* and *H. sanguineus*.

2.2 Methods

2.2.1 Experimental solutions

Seawater used in all experiments was collected from Indian River Inlet (~ 32 psu, Delaware, USA). Biologically active molecules were removed by ultrafiltration (100 kDa; GE Life Sciences UFP-100-C-5A) and aging in darkness for at least 1 week (Forward and Rittschof 1999). This water served as control seawater for rearing and all experiments. I produced kairomone solutions with diluted mucus, isolated from *Fundulus heteroclitus*. I isolated fish mucus with a previously described body wipe method (Forward and Rittschof 1999) and diluted it with control seawater to produce uniform concentrations of 0.1, 0.01, or 0.001 g wet weight mucus L^{-1} seawater. Aliquots of concentrated mucus were stored at -80 °C but were thawed and diluted immediately before using in experiments. Mucus from *F. heteroclitus* at similar concentrations has been shown to elicit strong behavioral responses in zooplankton (Forward and Rittschof 1999, 2000; Cohen and Forward 2005). However, it is

unlikely that responses to kairomones are specific to predator species, as similar behavioral effects have been observed in animals exposed to kairomones from multiple fish and gelatinous invertebrate species (McKelvey and Forward 1995).

2.2.2 Crab collection and rearing

During summer (May – September) of 2013, I collected ovigerous female crabs from either Broadkill River, DE, USA (*R. harrisii*) or Roosevelt Inlet, DE, USA (*H. sanguineus*). I maintained females in the laboratory under a 14:10 h light:dark cycle at ~ 23 °C in control seawater (20 psu for *R. harrisii* and 30 psu for *H. sanguineus*). On the day of hatching, larvae from single female broods were placed into new control seawater, and water changes were conducted three times per week. I fed larvae newly hatched brine shrimp (*Artemia* spp.) nauplii *ad libitum*.

2.2.3 Behavioral experiments

I conducted behavioral experiments in an apparatus that mimics the underwater angular light distribution, similar to that used by Forward et al. (1984). Within a light-tight enclosure, I placed groups of zoeae (n ≈ 30) in a transparent acrylic chamber (5 × 5 × 5 cm), enclosed within a larger black acrylic water bath (40 × 40 × 15 cm; ~ 23°C). Experimental light was produced by an Oriel 300 W Xe Arc Lamp (Newport Corp., Irvine, CA, USA), and filtered to 488 nm with an interference filter (10 FWHM, Melles Griot 03FIL002, Irvine, CA, USA). I chose this wavelength, because it is near peak spectral sensitivity in *R. harrisii* and *H. sanguineus* (Cohen et al. 2015; Forward and Costlow 1974). Fixed neutral density filters (Melles Griot, Irvine, CA, USA) allowed us to control the intensity of light stimuli, which passed horizontally through a collimating lens, electromagnetic shutter (Newport Corp., Irvine, CA, USA),

wavelength and intensity filters, and then reflected off a mirror inside the light-tight enclosure to pass vertically through a white acrylic diffuser that covered the water bath. The described light assembly produces a relatively diffuse downwelling light source, entering a dark larval chamber. Prior to experiments, I measured downwelling irradiance at the larval chamber with an optometer and calibrated radiometric probe (models S471 and 247; Gamma Scientific, Baltimore, MD, USA) to select an appropriate range and resolution of light stimuli.

I recorded swimming behavior through two narrow transparent sections in the black water bath with a digital camera (scA750-60gm; Basler AG Electronics, Ahrensburg, Germany) with a 16 mm varifocal lens (HF16HA-1B; Fujinon Corp, Edison, NJ, USA), backlit by an infrared LED array (880 nm; Advanced Illumination, Edmund Optics, Barrington, NJ, USA). Camera optics were set such that the field-of-view and depth-of-field could resolve all swimming individuals within the chamber, regardless of their position in the three-dimensional chamber. I used a custom program in LabVIEW (National Instruments, Austin, TX, USA) to coordinate timing of shutter opening and closing as well as capture video recordings.

Behavioral experiments were conducted on stage 4 *R. harrisii* and stage 3 *H. sanguineus* zoeae, because larvae at these stages are active swimmers that exhibit strong phototactic responses (Forward and Rittscof, 2000; Cohen et al., 2015). In addition, exposure to fish kairomones resulted in enhanced photoresponses in stage 4 *R. harrisii* zoeae from the Neuse River estuary, North Carolina, USA (Forward and Rittschof 2000). I conducted similar behavioral experiments in this study, because no such evidence exists for either larval *H. sanguineus* or *R. harrisii* populations in Delaware Bay, USA. Prior to behavioral experiments, animals were exposed to either

control seawater or kairomone solutions of three concentrations (0.1, 0.01, and 0.001 g mucus L^{-1} seawater) for 1 – 3 h and acclimated to the dark for at least 1 h, 15 minutes of which were in the experimental chamber. After the acclimation period, experimental animals experienced a series of six 3 s light stimuli increasing in intensity from approximately 5×10^{11} to 5×10^{13} photons m^{-2} s^{-1} in *R. harrisii* and 1×10^{11} to 1×10^{13} photons m^{-2} s^{-1} in *H. sanguineus*. During these experiments, four minutes of dark acclimation time separated each stimulus. I recorded swimming behavior 3 s prior ("dark") and after each light stimulus. Behavioral experiments were replicated five times for both species, and each replicate represents a brood from a single mother to account for potential maternal effects.

I determined start and end XY-coordinates of swimming individuals in each 3 s video recording using a PC-based motion analysis system (CellTrak software, Motion Analysis Corp., Santa Rosa, CA, USA). An individual was considered to be descending if the line between its start and end XY-coordinates were within nadir ± 60°. I then calculated percent descending for each group (replicate × treatment) before (dark) and after each light stimulus. Within each treatment, I compared percent descending in the dark to percent descending after each of the given light stimuli with one-way repeated measures (RM) ANOVAs. If RM ANOVAs detected significant differences ($P < 0.05$), Holm-Sidak *post-hoc* tests determined which specific light stimuli evoked a significant descent response relative to swimming behavior in the dark. The light stimulus of the lowest intensity that induced a descent response was deemed the 'behavioral threshold'. One-way ANOVAs within treatments suggested that percent descending of animals swimming in the dark did not differ significantly between replicates ($P > 0.05$). Hence, I used mean percent descending before each

light stimulus as “percent descending in the dark” in the RM ANOVA analyses described above. All statistical analyses were conducted in SigmaPlot 12.0 (Systat Software, San Jose, CA).

2.2.4 Electrophysiology

I measured extracellular electroretinograms (ERGs) on stage 4 *R. harrisii* and stage 3 *H. sanguineus* zoeae. Prior to experiments, animals were exposed to either control seawater or kairomones at 0.1 g mucus L^{-1} seawater for at least 1 h. This kairomone concentration was chosen, because it induced strong behavioral responses in both species (Fig. 2.1). In ERG experiments, zoeae were attached by their dorsal carapace to the plastic head of a pin with cyanoacrylate gel adhesive (Loctite, Rocky Hill, CT, USA) and then suspended in a 19 °C water bath of their respective treatment by a plexiglass support. I then placed the recording electrode, a tungsten microelectrode (127 μm tip, A-M Systems, Sequim, WA, USA), subcorneally in the eye and a second differential electrode with the same specifications in the water bath. Differential AC signals were amplified (Ext-02 B, NPI Electronic Instruments, Germany), digitized, and stored in LabChart 7 (AD Instruments) for analysis of peak-to-peak response height and response time.

Light stimuli were produced by a quartz halogen lamp (DC-150, Dolan-Jenner Industries, Boxborough, MA) and delivered to the eye with a 4 mm diameter liquid light guide. Wavelength was set by a blue/green broadband pass filter (BG-18, Schott, Elmsford, NY, USA) and light intensity controlled with fixed neutral density filters (Melles Griot, Irvine, CA, USA). Again, I chose this wavelength, because it is near peak spectral sensitivity for *R. harrisii* and *H. sanguineus* (Cohen et al. 2015; Forward 2009). An electromagnetic shutter and shutter driver (LS6S2T0-100, VCM-D1,

Uniblitz/Vincent Associates, Rochester, NY, USA) under computer control mediated stimulus onset and duration. Sensitivity may differ between night and day in crustaceans (Meyer-Rochow 1999, 2001), so I conducted all experiments during the day between 9:00 and 16:00. Prior to experiments, irradiance was measured with a spectroradiometer (USB4000; Ocean Optics, Dunedin, FL, USA) to determine the range and resolution of light stimuli.

Response-intensity (V – log I) curves were generated from ERG recordings, where response magnitude (peak-to-peak height) increased with intensity until reaching some maximum response (V_{max}). I acclimated animals in the dark prior to experiments and did not give an experimental flash until the ERG response to a dim test flash consistently yielded a consistent response magnitude. Experimental flashes (100 ms) were given in order of increasing irradiance, ranging from 10^{11} – 10^{16} photons $m^{-2}s^{-1}$. Between experimental flashes, animals acclimated in the dark for at least two minutes, but total acclimation time was determined with intermittent test flashes during experiments.

To generate V – log I curves, I plotted peak-to-peak response height across the intensity range of given light stimuli. I normalized individual curves to the maximum response (V_{max}) and modeled the response-intensity relationship with the Zettler modification of the Naka-Rushton equation to determine the curve's half saturation point (log K), V_{max}, slope, and dynamic range or log range from 5 to 95% of V_{max} (Frank 2003). Here, log K was defined as a measure of physiological sensitivity. As such, lower values indicate greater sensitivity. In this analysis, I only included curves that had a measured V_{max} value at least 80% of the model's estimated V_{max}. I assessed differences in log K, slope, and dynamic range with t-tests, comparing individuals

exposed to control seawater (n = 5) and kairomones (n = 5) in *R. harrisii* and *H. sanguineus*. I conducted statistical analyses in SigmaPlot 12.0, and differences were considered significant if $P < 0.05$. As in behavioral experiments, replicates were taken from a brood from a single mother to avoid possible maternal effects

In addition, I investigated the kinetics of ERG responses at each irradiance for the generated V – log I curves (n = 5 for each treatment), specifically the time from the light stimulus onset to the response start (response latency) and to the response peak (peak latency). Response start was defined as the point at which the ERG signal begins to decrease in magnitude above background noise. I assessed the effect of treatment and irradiance on response and peak latency with two-way ANOVAs. Again, I conducted all statistical analyses in SigmaPlot 12.0, and accepted significant differences at $P < 0.05$.

2.2.5 Histology: Eye structure

I applied histological techniques to observe possible kairomone-induced changes in eye structure that could increase visual sensitivity over a 3-h time interval. I exposed stage 4 *R. harrisii* and stage 3 *H. sanguineus* zoeae to kairomones from 0.1 g mucus L^{-1} seawater for a period of 0 (control seawater), 0.5, 1, or 3 h (n = 10 at each time interval). Following exposure, I removed and fixed heads in 2.5% glutaraldehyde in 0.4 *M* Millonig's buffer solution for 3.25 h between 8:00 and 13:00 under fluorescent room light (~ 10^{18} photons m^{-2} s^{-1} white light). Larvae were dehydrated in a graded ethanol series, gradually transferred into medium grade acrylic resin (London White Company, London, UK), and embedded in resin by hot curing at 60 ± 2 °C for 20 – 24 h in an Isotemp oven (Fisher Scientific, Waltham, MA, USA). I then cut semi-thin (0.2 μm) sections with a Sorvall MT-2B Ultramicrotome (Du Pont Company,

Tuscon, AZ, USA) and stained these sections with a mixture of Toludine Blue O and Basic Fuchsin (Electron Microscopy Sciences, Hatfield, PA, USA) before mounting on slides.

From the slides, I measured several characteristics of eye structure with an ocular reticle on a compound microscope (CX31, Olympus Corp., Tokyo, Japan). These included rhabdom diameter, rhabdom length, aperture diameter, and length of crystalline cone (Fig. 2.4A). Here, I measured rhabdom diameter at the distal end of the rhabdom and estimated aperture diameter as the distance between distal accessory pigments surrounding the crystalline cone. All measurements were from longitudinally sectioned ommatidia in the anterior/dorsal quadrant of the eye, and measurements were only used if all the above-mentioned characteristics were present. To ensure that the structural characteristics did not vary with ommatidia location, I divided the anterior/dorsal quadrant of the eye into three portions: anterior, intermediate, and lateral. These were 0 – 25°, 25 – 65°, and 65 – 90° from the anteriormost ommatidium, respectively, ranging dorsally from the frontal to the sagittal plane. Since the chosen characteristics of eye structure did not vary between these three locations in control animals (one-way ANOVA), all measurements taken from the anterior/dorsal quandrant of the eye were used in analysis. In addition, structural parameters were measured blindly, i.e. treatment was not identified until after all measurements were completed. I calculated the grand mean of all measurements taken from an individual zoea, and this grand mean was considered a replicate. Since I only used measurements from ommatidia that contained all structural characteristics (Fig. 2.4A), the number of replicates decreased slightly from n = 10 to n = 8, 6, 5, and 7 in *R. harrisii* and n = 6, 6, 4, and 6 in *H. sanguineus* exposed to kairomones for 0

(control), 0.5, 1, or 3 h, respectively. I took digital images of each measured section with a digital camera (EOS Rebel T3i, Canon Inc., Japan), and qualitatively compared distribution of screening pigments.

Optical sensitivity of larval crab compound eyes, S (μm^2 Sr), was calculated according to Land (1981; Equation 2.1). I calculated optical sensitivity to compare control and kairomone treated animals and to determine whether changes in eye structure resulted in optical sensitivity differences.

$$S = \left(\frac{\pi}{4}\right)^2 A^2 \left(\frac{d}{f}\right)^2 \left(\frac{\mathrm{kl}}{2.3+kl}\right). \qquad \text{Equation 2.1}$$

Structural characteristics in the sensitivity equation include aperture diameter (A), rhabdom diameter (d), focal length (f), the absorption coefficient (k), and rhabdom length (l). Since focal length of an apposition compound eye is typically the distance from the nodal point of the corneal lens to the distal tip of the rhabdom, I estimated focal length to be the length of the crystalline cone. This estimation began at the distal tip of the crystalline cone rather than the nodal point of the corneal lens, because the corneal lens was separated from its corresponding crystalline cone in some sections. Further, the thickness of the corneal lens was approximately 2 – 3 μm in both *R. harrisii* and *H. sanguineus*, and the nodal point within would be less than this total distance. Since the crystalline cone extends from just beneath the corneal lens to the distal tip of the rhabdom in all sections, with length ranging from 23 – 30 μm, ignoring the distance between the nodal point of the corneal lens and the distal tip of the crystalline cone in my estimation of focal length should introduce little error. I used an absorption coefficient of 0.008 μm^{-1} (Cronin and Forward 1988).

I also calculated acceptance angle using several structural characteristics (Equation 2.2; Snyder 1979), including facet diameter (D), rhabdom diameter (d), and

focal length (*f*). Facet diameter (D) was measured after initial analysis of eye structure, but these diameters were consistent between control and kairomone treated animals; mean values of 20 and 19 μm were used for *R. harrisii* and *H. sanguineus*, respectively. Again, focal length was estimated to be the length of the crystalline cone. A wavelength (λ) of 500 nm was used to represent peak spectral sensitivity in *R. harrisii* and *H. sanguineus* (Cohen et al. 2015; Forward and Costlow 1974).

$$\Delta\rho = \sqrt{\left(\frac{\lambda}{D}\right)^2 + \left(\frac{d}{f}\right)^2}. \qquad \text{Equation 2.2}$$

To assess whether kairomone exposure affected eye structure, optical sensitivity, and/or acceptance angle, I conducted a one-way ANOVA for each parameter, comparing animals exposed to kairomones for 0 (control), 0.5, 1, and 3 h. I then used a Holm-Sidak *post-hoc* test to make multiple comparisons of all kairomone treatments (0.5, 1, 3 h) versus the control. Values of optical sensitivity and acceptance angle were log transformed for analysis. I conducted all statistical analyses in SigmaPlot 12.0, and accepted significant differences at $P < 0.05$. All individuals used in experiments came from a single female in both *R. harrisii* and *H. sanguineus*.

2.2.6 Estimated changes to depth

I compared downwelling irradiance with depth at two times of day to the behavioral thresholds in *R. harrisii* with and without kairomone exposure in order to assess the magnitude of depth change expected with kairomone exposure. At a site in Delaware Bay where larval *R. harrisii* are abundant (38° 57.862’ N, 75° 16.093’ W), I measured spectral irradiance just below the surface to a depth of 3.25 m at midday in August 2014 (Hydro-Rad-3, HOBI Labs, Bellevue, WA, USA). Spectral irradiance at each depth interval was weighted by the spectral sensitivity of *R. harrisii* larvae

determined electrophysiologically (Forward et al. 2014), and then integrated to yield light intensity as 'crab utilized photons'. These integrated values were used to determine a diffuse attenuation coefficient (K_d) of 1.4 m^{-1} by linear regression and used in the Lambert-Beer equation as a simplified model of light attenuation with depth (e.g. Gallegos 2001) to determine irradiance (crab utilized photons) over the water column. A similar irradiance profile was modeled for twilight using the same K_d value, but assuming irradiance just below the surface to be two orders of magnitude less than that at midday, based on previous observations (Cohen and Forward 2005). With these two depth profiles of irradiance as crab utilized photons, I calculated the expected change in depth of *R. harrisii* based on my observed behavioral thresholds from behavioral experiments with and without kairomone exposure.

2.3 Results

2.3.1 Defensive photobehavior

I conducted behavioral experiments in an apparatus that mimics the underwater angular light distribution, characterized by a relatively bright, diffuse light from above entering a dark chamber. In experiments, I exposed crab larvae to an intensity range of downwelling light stimuli and measured their swimming responses. The behavioral threshold was quantified and used as a proxy for defensive photobehavior; this threshold was defined here as the lowest light intensity to evoke a descent swimming response in a group of larvae when compared to swimming direction of pre-stimulus behavior in darkness. I exposed larvae to control seawater or kairomones from fish mucus at three concentrations (0.1, 0.01, 0.001 g mucus L^{-1} seawater) for 1 – 3 hours (h) before they were used in experiments. The percentage of larvae descending while

swimming in darkness between successive light stimuli did not differ throughout each experiment, and mean percent descending of animals in the dark ranged from 19 – 24% in *R. harrisii* and 10 – 22% in *H. sanguineus*. In both species, percent descending differed before and after light stimulation in all treatments ($P < 0.001$; One-way repeated-measures ANOVAs).

Kairomone exposure decreased behavioral thresholds for light-evoked descents (Fig. 2.1; Table 2.1). In stage 4 *R. harrisii* zoeae, the behavioral threshold was 1.10×10^{13} photons m^{-2} s^{-1} in animals exposed to control seawater. Relative to the control, animals exposed to the two lowest kairomone concentrations (0.01 and 0.001 g mucus L^{-1} seawater) had behavioral thresholds that were half that of the control at 4.77×10^{12} photons m^{-2} s^{-1}, and thresholds in animals exposed to the highest kairomone concentration (0.1 g mucus L^{-1} seawater) were a third of the control threshold at 3.48×10^{12} photons m^{-2} s^{-1} (Fig. 2.1A).

In stage 3 *H. sanguineus* zoeae, the behavioral threshold was 4.77×10^{12} photons m^{-2} s^{-1} in the control. Thresholds decreased to about a third of the control at 1.51×10^{12} photons m^{-2} s^{-1} after exposure to kairomones at all three concentrations (Fig. 2.1B). The behavioral threshold shift in kairomone-exposed animals was similar in *R. harrisii* and *H. sanguineus*. However, behavioral thresholds were lower in *H. sanguineus* overall, i.e. *H. sanguineus* in the control had a behavioral threshold that was half that of *R. harrisii*.

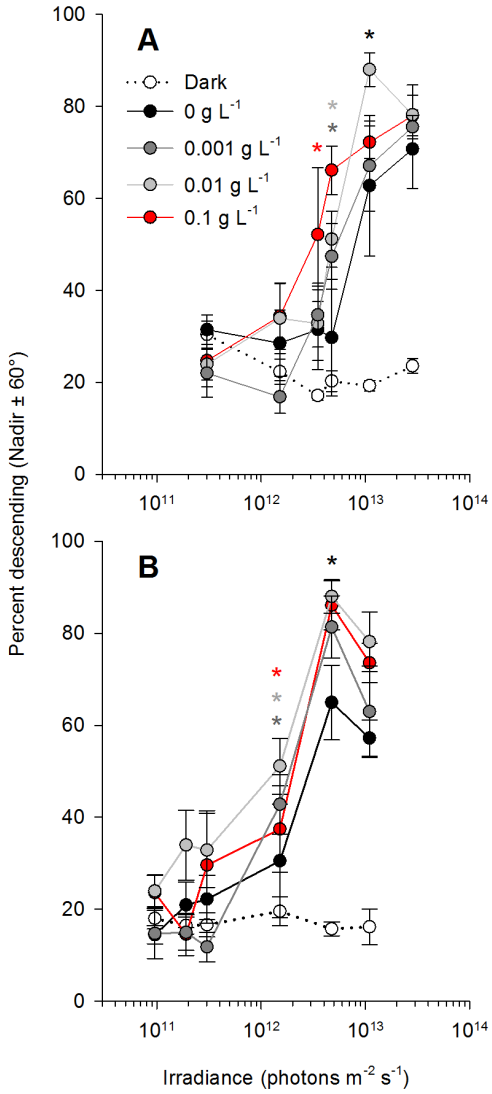

Figure 2.1: Behavioral thresholds of photobehavior. Mean ± s.e.m. percent descending (± 60°) of (A) stage 4 *Rhithropanopeus harrisii* and (B) stage 3 *Hemigrapsus sanguineus* zoeae before (swimming in the dark) and after light stimulation. Animals (~30 individuals) in each replicate (n = 5) were exposed to either control seawater (0 g L^{-1}) or kairomones from *Fundulus heteroclitus* mucus at 0.1, 0.01, or 0.001 g mucus L^{-1} seawater. Behavioral thresholds, or significant differences in percent descending before and after light stimulation, were determined by one-way repeated measures ANOVAs with Holm-Sidak *post-hoc* tests and accepted at $P < 0.05$. These thresholds are represented by asterisks of respective treatment symbol colors. Data shown here for animals swimming in the dark are the combined mean ± s.e.m. of all four treatments.

Table 2.1: Behavioral threshold, physiological sensitivity, and optical sensitivity in *Rhithropanopeus harrisii* and *Hemigrapsus sanguineus* exposed to control seawater (C) or kairomones (K) from *Fundulus heteroclitus* mucus (0.1 g L^{-1})

		Behavioral threshold (log photons m^{-2} s^{-1})		Physiological sensitivity (log photons m^{-2} s^{-1})		Optical sensitivity (μm^2 Sr)	
R. harrisii	C	13.0	*	14.37 ± 0.57		0.009 ± 0.003	*
	K	12.5		13.53 ± 0.10		0.034 ± 0.009	
H. sanguineus	C	12.7	*	14.23 ± 0.22	*	0.015 ± 0.006	
	K	12.2		13.50 ± 0.21		0.022 ± 0.007	

Behavioral thresholds (log photons m^{-2} s^{-1}) were determined in analysis of photobehavior experiments (Fig. 2.1). Physiological sensitivity (mean ± se) was defined as the log K value (log photons m^{-2} s^{-1}) of V – log I curves (Fig. 2.2; n = 5); lower values indicate greater sensitivity. Optical sensitivity (μm^2 Sr) was calculated from structural characteristics using the Land equation (Equation 2.1), and values shown (mean ± se) are from animals that were exposed to kairomones for 0 h (control; n = 8, 6) or 1 h (kairomones; n = 6, 4) in *R. harrisii* and *H. sanguineus*, respectively. Significant differences ($P < 0.05$) are represented by an asterisk and were determined using repeated-measures ANOVAs with Holm-Sidak *post-hoc* tests for behavioral thresholds, t-tests for physiological sensitivity, and one-way ANOVAs with Holm-Sidak *post-hoc* tests for optical sensitivity.

2.3.2 Electrophysiology

I generated response-intensity (V – log I) curves from extracellular electroretinograms (ERGs) to investigate whether kairomones alter retinal physiology to increase visual sensitivity and therefore influence changes to photobehavior observed in previous experiments. Prior to electrophysiological experiments, animals were exposed to either control seawater or kairomones at 0.1 g mucus L^{-1} seawater for 1 – 3 h. Kairomone exposure resulted in a shift of V – log I curves to lower intensities in both *R. harrisii* and *H. sanguineus* (Fig. 2.2), consistent with increased visual sensitivity. Further, physiological sensitivity was defined here as the half-saturation (log K) of V – log I curves, and log K values were lower in kairomone-exposed than in control animals, also suggesting increased visual sensitivity (Fig. 2.2; Table 2.1).

However, this difference was only significant in *H. sanguineus* ($P = 0.04$; t-test). In addition, I observed decreases in V_{max} following kairomone exposure (Table 2.2), with significant differences between control and kairomone treatments in *H. sanguineus.* No significant differences were detected in the slope or dynamic range of V – log I curves (Table 2.2).

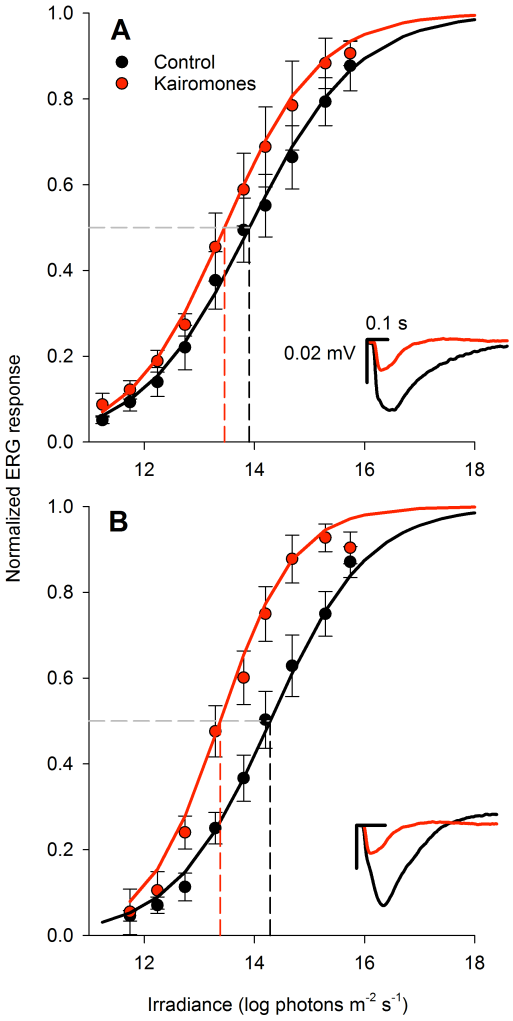

Figure 2.2: Response-intensity (V – log I) curves. Mean ± s.e.m. normalized ERG responses across a log range of irradiances (photons m^{-2} s^{-1}), in (A) stage 4 *Rhithropanopeus harrisii* and (B) stage 3 *Hemigrapsus sanguineus* zoeae exposed to control seawater (n = 5) or kairomones from *Fundulus heteroclitus* mucus at 0.1 g mucus L^{-1} seawater (n = 5). Curves were modeled using the Zettler modification of the Naka-Rushton equation, and log k of each curve is indicated by a dotted line of its respective treatment color. Inset with each V – log I curve, are representative ERG response waveforms at log K of control (black) and kairomone-treated animals (red), with length of light stimulus (0.1 s) and response magnitude indicated by scale bars. The timescale of insets is positioned at the onset of the light stimulus.

Table 2.2: Response-intensity curve parameters in *Rhithropanopeus harrisii* and *Hemigrapsus sanguineus* exposed to control seawater (C) or kairomones (K) from *Fundulus heteroclitus* mucus (0.1 g L^{-1})

		V_{max} (mV)		Slope	Dynamic range (log photons m^{-2} s^{-1})
R. harrisii	C	1. 41± 0.37		0.48 ± 0.02	5.41 ± 0.26
	K	0.47 ± 0.47		0.53 ± 0.07	4.69 ± 0.34
H. sanguineus	C	0.80 ± 0.16	*	0.59 ± 0.04	4.27 ± 0.37
	K	0.36 ± 0.06		0.70 ± 0.07	3.89 ± 0.55

Values (mean ± s.e.m.) of V_{max}, slope, and dynamic range were derived from the Zettler modification of the Naka-Rushton model (n = 5). Significant differences between control and kairomone treatments were accepted at $P <$ 0.05 (t-test) and represented by an asterisk.

I also assessed temporal resolution by measuring latency of the ERG response relative to the stimulus flash at each irradiance of V – log I curves. Specifically, I compared the time from light stimulus onset to response start (response latency) and to response maximum (peak latency) between control and kairomone-treated animals. Further, the response start was defined as the point at which the ERG signal begins to decrease in magnitude above background noise. Response waveform varied between control and kairomone treatments, and response tended to be of smaller magnitude and

reach the response maximum more quickly in kairomone-exposed animals than in the control (Fig. 2.2). In *R. harrisii*, response and peak latency decreased with increasing irradiance ($P < 0.009$) and after kairomone exposure ($P < 0.001$; Fig. 2.3A,B; two-way ANOVAs). In *H. sanguineus*, response latency decreased with increasing irradiance ($P < 0.001$; Fig. 2.3C), and peak latency was shorter after kairomone exposure ($P < 0.001$; Fig. 2.3D). The interaction between treatment and irradiance was not significant in either species.

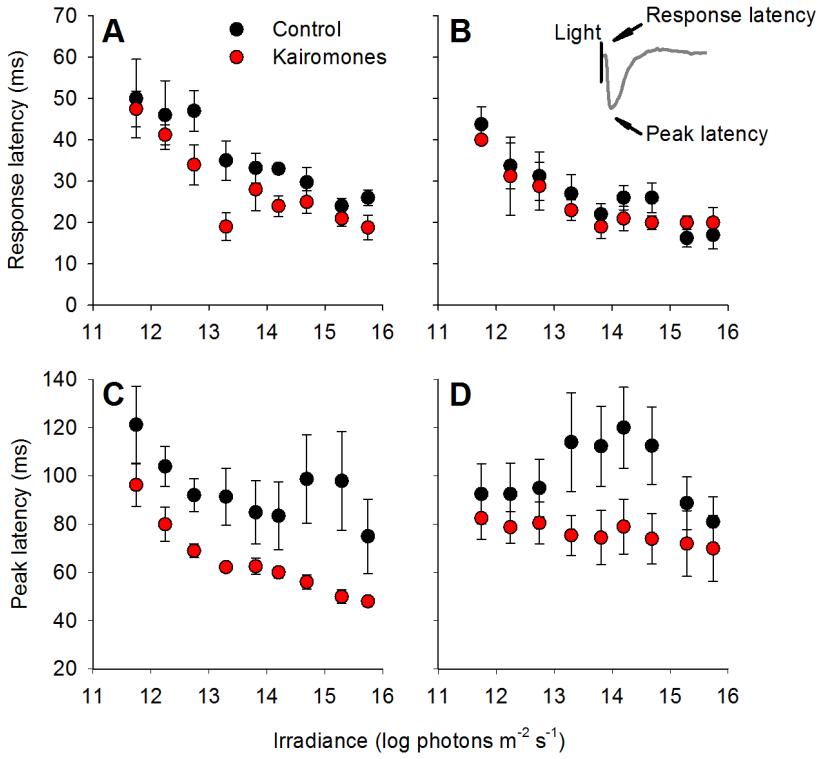

Figure 2.3: Latency in ERG responses. Mean ± s.e.m. response latency (ms) in (A) stage 4 *Rhithropanopeus harrisii* and (B) stage 3 *Hemigrapsus sanguineus* zoeae as well as mean ± s.e.m. peak latency (ms) in the same stage *R. harrisii* (C) and *H. sanguineus* (D) across a log range of irradiances (photons m^{-2} s^{-1}). Animals were exposed to either control seawater (n = 5) or kairomones from *Fundulus heteroclitus* mucus at 0.1 g mucus L^{-1} seawater (n = 5). As indicated by the inset, response latency was defined as the time from the light stimulus onset to the response start, and peak latency as the time from the light stimulus onset to the response peak.

2.3.3 Eye structure

Using light microscopy of semi-thin sections, I compared several characteristics of eye structure (Fig. 2.4A) in control and kairomone-exposed zoeae. Further, rhabdom diameter was measured at the distal tip of the rhabdom, and aperture diameter was defined as the distance between distal accessory pigments at the base of the crystalline cone in longitudinal sections. Prior to fixation and embedding, animals were exposed to kairomones at a concentration of 0.1 g mucus L^{-1} seawater for durations of 0 (control), 0.5, 1, or 3 h. Kairomone-induced changes to photobehavior in crustacean larvae are evoked over this timeframe (Forward and Rittschof 1993, 2000). In *R. harrisii*, rhabdom diameter and length differed between kairomone-exposed and control animals (P = 0.04 and 0.03, respectively; One-way ANOVA). Specifically, rhabdom diameter was significantly wider in *R. harrisii* exposed to kairomones for 1 and 3 h, relative to control animals (Fig. 2.4B). In addition, rhabdom length was shorter in *R. harrisii* exposed to kairomones for 3 h, compared to the control (Fig. 2.4D). In *H. sanguineus*, rhabdom diameter also differed after kairomone exposure (P = 0.05; One-way ANOVA). Rhabdoms widened after 3 h of kairomone exposure relative to control animals (Fig. 2.4C). However, differences in rhabdom length were not statistically significant between the kairomone treatment and control

in *H. sanguineus* (Fig. 2.4D). Cone length and aperture diameter did not vary across the 3-h kairomone exposure time in either species, and I did not observe changes in screening pigment quantity or position.

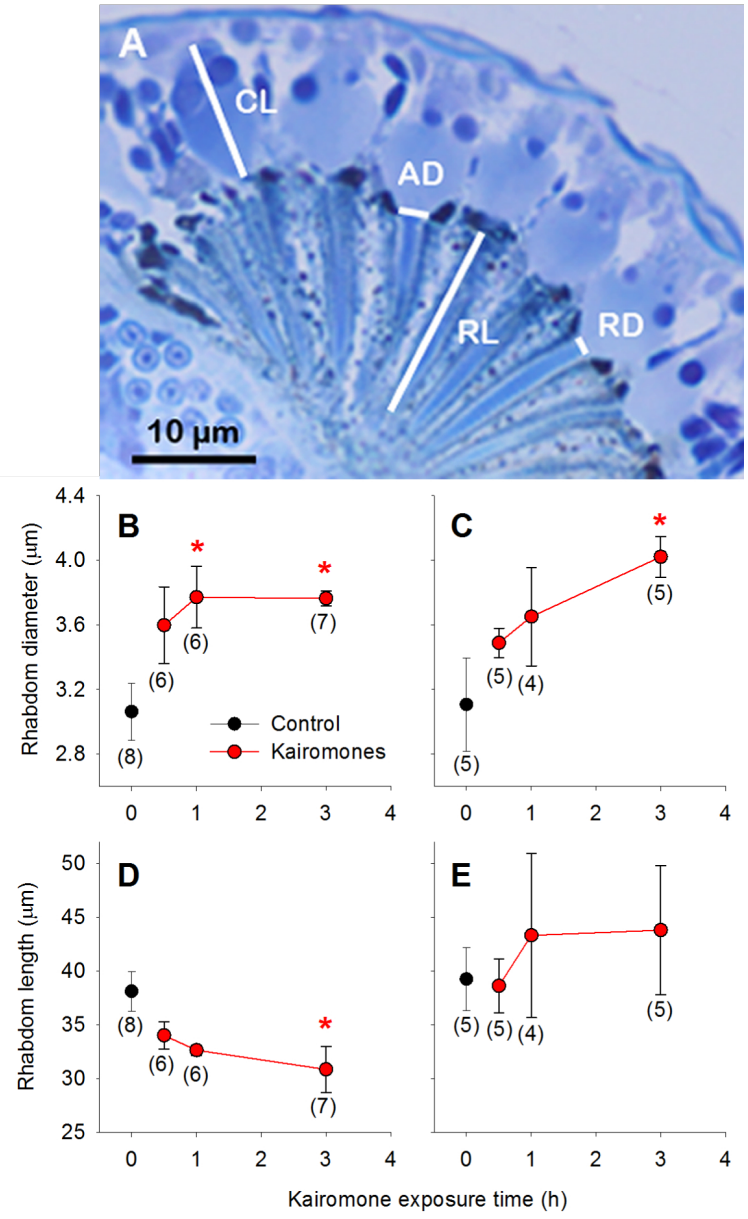

Figure 2.4: Characteristics of eye structure. (A) Semi-thin (0.2 μm) longitudinal section from a stage 4 *Rhithropanopeus harrisii* zoeae compound eye. Structural characteristics used in analysis are highlighted in white and include cone length (CL), aperture diameter (AD), rhabdom length (RL), and rhabdom diameter at the distal tip (RD). Mean ± s.e.m. rhabdom diameter (μm) in (B) stage 4 *Rhithropanopeus harrisii* and (C) stage 3 *Hemigrapsus sanguineus* zoeae, as well as mean ± s.e.m. rhabdom length (μm) in the same stage (D) *R. harrisii* and (E) *H. sanguineus*. Zoeae were exposed to kairomones from *Fundulus heteroclitus* mucus at a concentration of 0.1 g L^{-1} for 0 (control), 0.5, 1, or 3 h, and sample size at each exposure time is noted in parentheses. Significant differences in rhabdom size between control and kairomone-exposed animals (0.5, 1, 3 h) were determined by one-way ANOVAs with Holm Sidak *post-hoc* tests, accepted if $P < 0.05$, and represented by asterisks.

In addition, I used characteristics of eye structure to calculate optical sensitivity (Equation 1; Land 1981) and acceptance angle (Equation 2; Snyder, 1979). Mean optical sensitivity and acceptance angle increased after 1 h of kairomone exposure in both species (Table 2.1, 2.3). However, differences between the control and kairomone treatments were only significant in *R. harrisii* ($P = 0.03$; One-way ANOVAs). Specifically, optical sensitivity increased after 1 h of kairomone exposure (Table 2.1), and acceptance angle was larger in animals exposed to kairomones for 0.5 – 3 h, relative to the control (Table 2.3).

2.4 Discussion

In both *R. harrisii* and *H. sanguineus*, I observed changes to photobehavior that could impact predator-avoidance behavior, specifically decreases in the behavioral threshold, following kairomone exposure (Fig. 2.1; Table 2.1). These results were comparable to findings with a North Carolina (USA) population of *R. harrisii* (Forward and Rittschof 2000), and once established for my Delaware (USA)

R. harrisii study population and now *H. sanguineus*, I investigated whether kairomones mediate these behavioral changes by increasing visual sensitivity. Visual sensitivity can be regulated with physiological and/or structural mechanisms, e.g. changes to photoreceptor membrane potential and size (Meyer-Rochow 2001).

Table 2.3: Acceptance angle calculated from eye structure across kairomone exposure time in *Rhithropanopeus harrisii* and *Hemigrapsus sanguineus*

Kairomone exposure time (h)	*R. harrisii*			*H. sanguineus*	
	Δρ		n	Δρ	n
0	6.2 ± 0.5		6	7.2 ± 0.8	6
0.5	9.3 ± 1.4	*	6	6.8 ± 0.6	6
1	9.3 ± 0.9	*	5	7.8 ± 0.7	4
3	8.4 ± 0.7	*	7	8.1 ± 0.6	6

Data are calculated values (means ± s.e.m.) of acceptance angle (Δρ , °) and sample size (n). Method for angle calculation is given in Equation 2.2. Significant differences between control (0 h) and kairomone treatments (0.5, 1, 3 h) were accepted at $P < 0.05$ by one-way ANOVAs with Holm-Sidak *post hoc* tests and represented by an asterisk.

Extracellular recordings in the retina suggest greater visual sensitivity in zoeae exposed to fish kairomones (Fig. 2.2; Table 2.1). Similar ERG methods have been used to assess light/dark adaptation and cyclic diel changes to sensitivity in crustaceans, where sensitivity increases during nighttime hours (Aréchiga and Rodriguez-Sosa 1998; Hariyama et al. 2001; Meyer-Rochow and Tiang 1984; Yang et al. 1986), as well as at night in adult *H. sanguineus* with intracellular photoreceptor recordings (Arikawa et al. 1987). The observed pattern of increase in sensitivity of crab larvae following kairomone exposure matched these light/dark and diel changes in sensitivity of adult crustaceans, though were smaller in magnitude by about 25%

(Hariyama et al. 2001). Hence, larval crabs exposed to kairomones may use similar physiological mechanisms at the retinal level to mediate phenotypic plasticity in defensive photobehavior, e.g. descent to darker waters during daytime when fish are abundant. Further work using intracellular recording could be employed to determine the effect of kairomones on individual photoreceptors, as has been done to demonstrate higher nighttime signal-to-noise ratios in photoreceptor cells of *Limulus* (Kaplan and Barlow 1980).

Increases in visual sensitivity often come at the cost of temporal resolution (Warrant 1999, 2008; Warrant et al. 2014). For example, higher sensitivity is associated with decreases in temporal resolution in mesopelagic and deep-sea crustaceans (Frank 1999, 2000; Frank et al. 2012), and log K values are often negatively correlated with response latency in these animals (Frank 2003). Here, I tested whether increases in visual sensitivity of kairomone-exposed animals resulted in a loss of temporal resolution by measuring latency in response onset and peak. Surprisingly, I found no indication of longer latency times in kairomone-exposed animals with heightened photoreceptor sensitivity; latency actually decreased after kairomone exposure (Fig. 2.3). Hence, kairomones do not increase sensitivity at the cost of temporal resolution in these larval crabs. Moreover, observed decreases in response amplitude and V_{max} after kairomone exposure (Fig. 2.2; Table 2.2) may allow for increases in visual sensitivity in conjunction with greater temporal resolution.

I also found changes to eye structure in kairomone-exposed animals. Rhabdoms were wider and shorter after 1 – 3 h of kairomone exposure in *R. harrisii* and were wider after 3 h of exposure in *H. sanguineus* (Fig. 2.4). This change in rhabdom diameter likely drove the observed increases in optical sensitivity in *R.*

harrisii exposed to kairomones for 1 h, relative to those in the control (Table 2.1), though similar increases were not found in *H. sanguineus.* I would expect sensitivity changes to occur over this timeframe as crustacean larvae show behavioral responses to kairomones within 1 h, as demonstrated here and elsewhere (e.g. Forward and Rittschof 1993; McKelvey and Forward 1995). Chamberlain and Barlow (1987) similarly observed wider, shorter rhabdoms in *Limulus* at night when animals are known to be most visually sensitive. Furthermore, rhabdom size increased in adult *H. sanguineus* and several other adult crab species during the nocturnal phase of the diel cycle (Nässel and Waterman 1978; Stowe 1980; Toh and Waterman 1981; Arikawa et al. 1987), and several studies have similarly reported greater rhabdom width or volume in more sensitive dark-adapted eyes (Meyer-Rochow and Tiang 1984) or at night in other crustaceans (Hariyama et al. 2001; Matsuda and Wilder 2014; Yuan et al. 1997).

Spatial summation is common in animals that need to resolve fast moving objects as well as improve sensitivity (Warrant 1999). Some crustaceans demonstrate spatial summation by increasing their visual acceptance angle (Bryceson and McIntyre 1983; Hariyama et al. 2001), and other arthropod groups neurally pool information by laterally spreading and coupling the interneurons responsible for photoreceptor analysis (Greiner et al. 2004; Greiner et al. 2005; Warrant et al. 2014). Here, I used characteristics of eye structure to determine visual acceptance angle. Since acceptance angle did increase after 0.5, 1, and 3 h of kairomone exposure in *R. harrisii* (Table 2.3), observed increases in sensitivity may be achieved through spatial summation. Hence, heightened sensitivity following kairomone exposure may be at the expense of

spatial resolution, but zoeae maintain the ability to detect fast moving objects such as predatory fish.

In this study, I observed kairomone-induced changes to rhabdom shape that may increase visual sensitivity. However, several structural characteristics, not observed here, also mediate sensitivity changes in compound eyes. For instance, I did not find evidence of screening pigment migration within ommatidia between control or kairomone treatments, but distribution of screening pigments often mediates change in visual sensitivity, e.g. those seen over the diel cycle (Meyer-Rochow 2001). In dark-adapted eyes or during the nocturnal phase of the diel cycle, screening pigments frequently migrate distally from the rhabdom or become more dispersed in crustacean compound eyes, including adult *H. sanguineus* (Arikawa et al. 1987; Cellier et al. 1998; Hariyama et al. 2001; Meyer-Rochow and Tiang 1984). Although less commonly observed, Nilsson and Odselius (1981) found changes to the dioptric apparatus, including cone shortening and lens elongation, in dark-adapted, nighttime eyes of *Artemia*. The authors concluded that these changes, along with additional differences in rhabdom shape, might increase sensitivity while maintaining spatial resolution by decreasing focal length and widening the area that can be used for light capture. However, I did not observe a similar result in crystalline cones of crab larvae.

I observed several physiological and structural differences in the retina that could lead to increased visual sensitivity, including higher physiological sensitivity, i.e. lower log K values, namely in *H. sanguineus*, and changes to rhabdom shape and optical sensitivity, which were most distinct in *R. harrisii*. However, some differences were too small to detect a kairomone effect, e.g. physiological sensitivity in *R. harrisii*, suggesting that factors other than increases in sensitivity directly at the retinal

level may be involved in the observed shift in behavioral thresholds. For instance, neural amplification or changes to photochemical processes could be contributing to the observed kairomone-induced changes to defensive photobehavior. Neural summation strategies, temporal or spatial, are often employed to increase visual sensitivity. This is done by neurally increasing gain, e.g. summing input from neighboring visual channels (Warrant 1999). Specific neural inputs that mediate sensitivity changes are rarely reported. However, intracellular electrophysiological recordings in *Limulus* suggest that efferent input from the optic nerve plays an important role in increasing response gain in photoreceptor cells and that octopamine likely acts as the neurotransmitter for these optic nerve pulses (Barlow et al. 1987; Battelle 2002; Kaplan and Barlow 1980). Alternatively, Blest and Stowe (1997) found that inhibition of phospholipase, an enzyme important to phototransduction, prevented the diurnal decreases in rhabdom diameter that occur during the diel cycle of an adult crab. This finding suggests potential photochemical control on rhabdom size. However, phospholipase enzymes are important to processes aside from phototransduction, and changes to other biological pathways could be contributing to this result. In addition, Oberwinkler and Stavenga (2000) used calcium imaging to examine intracellular calcium levels in the rhabdomeres of blowflies and found that reduced sensitivity caused by light adaptation resulted in a decrease in the duration of calcium transients in the rhabdomere. In the case of larval crab sensitivity increases with kairomones, similar mechanisms warrant investigation.

In addition to investigating the mechanism by which kairomones increase defensive photobehavior, I also aimed to identify potential differences in the phenotypic plasticity of behavior and visual sensitivity between two crab species with

different early life history strategies: estuarine retention (*R. harrisii*) and offshore transport (*H. sanguineus*). More drastic increases in photobehavior might be expected in *R. harrisii*, because these crabs spend their entire life history within the estuary (Forward 2009) and likely experience higher predation pressure than *H. sanguineus*, which is exported offshore during larval development before recruiting back to the coast (Christy 2011; Epifanio 2013; Hagan and Able 2003). Conversely, the kairomone effect on behavior was similar in *R. harrisii* and *H. sanguineus* after exposure to the highest mucus concentration, and behavioral thresholds were lower in *H. sanguineus* than in *R. harrisii* overall, regardless of kairomone exposure or concentration (Fig. 2.1). Furthermore, a larger kairomone effect in *R. harrisii* was not clearly demonstrated in my electrophysiological and histological investigation of visual sensitivity. In fact, V – log I curves suggest a greater kairomone-induced sensitivity increase in *H. sanguineus* (Fig. 2.2; Table 2.1), while changes to eye structure that would increase visual sensitivity, namely rhabdom shape, were more distinct in *R. harrisii* (Fig. 2.4; Table 2.1). Overall, the observed physiological and structural changes likely play a similar role in mediating kairomone-induced increases in photobehavior in both species.

Here, I present evidence that kairomones affect photobehavior, specifically by lowering the behavioral threshold. Given that crab larvae maintain depth near the isolume of their threshold for light detection (Forward 1985; Sulkin 1984), I estimated how the observed physiological and behavioral changes after kairomone exposure would influence depth selection in the estuarine water column by modeling downwelling irradiance with depth at two times of day at a site in Delaware Bay where larval *R. harrisii* are abundant. Depth change in *R. harrisii* was estimated with

and without kairomone exposure from the behavioral thresholds determined in behavioral experiments. With kairomone exposure, *R. harrisii* would reside approximately 1 m deeper than animals without kairomone exposure at both midday and twilight (Fig. 2.5). Assuming that kairomone production is positively related to predator abundance (Shephard 1994; Van Gool and Ringelberg 2002), such a descent to deeper, darker waters could limit feeding ability in visual predators. Indeed, Grecay and Targett (1996) demonstrated light-limited feeding in a common zooplanktivorous predator from this habitat, juvenile weakfish *Cynoscion regalis*.

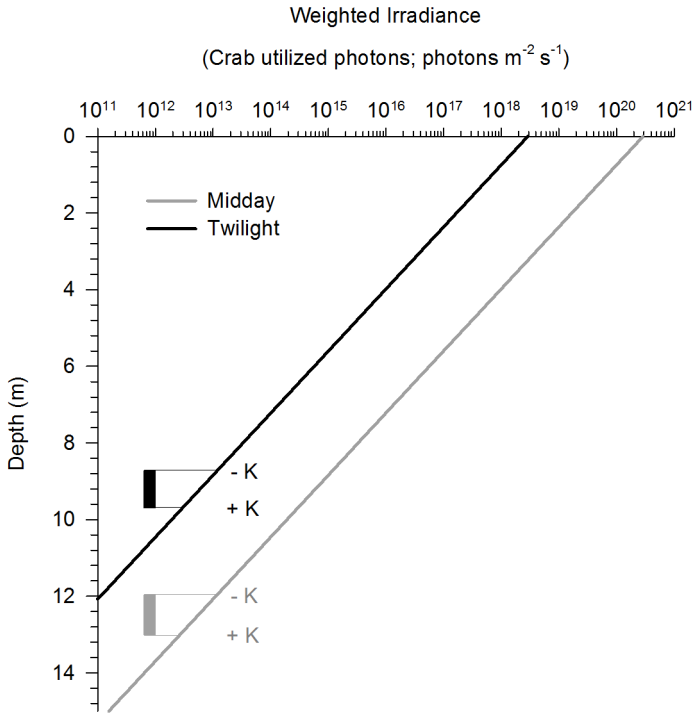

Figure 2.5: Estuarine water column depth at the larval crab behavioral threshold. Solid lines are downwelling irradiance weighted by the spectral sensitivity of *Rhithropanopeus harrisii* larvae, thereby representing the light utilized by the larval crab eye at a given depth (Crab utilized photons). Light at depth is calculated from surface irradiance of 2.9×10^{20} photons m^{-2} s^{-1} (midday; grey line) and 2.9×10^{18} photons m^{-2} s^{-1} (twilight; black line), using a diffuse attenuation coefficient (K_d) of 1.4 m^{-1}. For each time of day, the depth difference for *R. harrisii* behavioral threshold with (+ K) and without kairomones (- K) is shown as an inset thickened vertical line, with horizontal lines indicating the light level at these behavioral thresholds.

2.5 Conclusion

Behavioral strategies for predator avoidance are phenotypically plastic in several zooplankton species, where predator kairomones induce increases in swimming responses to light (Cohen and Forward 2009; Ringelberg 2010; Williamson et al. 2011). Here, I extend previously observed kairomone-induced changes to defensive photobehavior to another crab species, and more importantly report evidence that increases in visual sensitivity at the physiological and structural level in the eyes of both crab species are consistent with these behavioral changes. The kairomone effect on the observed behavioral and physiological responses was similar in the estuarine-retained *R. harrisii* and the offshore-transported *H. sanguineus*. Latency in electrophysiological responses decreased after kairomone exposure. Hence, it is unlikely that visual sensitivity increased at the expense of temporal resolution, though I present some evidence for spatial summation. In addition, I estimated changes in zooplankton depth with the observed decreases in the behavioral threshold of larval *R. harrisii* exposed to kairomones, and my model suggests that depth of these larval crabs would increase about 1 m with kairomone exposure. Overall, this study offers a potential mechanism to explain previous observations of phenotypic plasticity

in photobehavior important to predator avoidance and vertical migrations in zooplankton.

REFERENCES

Aréchiga, H. and Rodriguez-Sosa, L. (1998). Circadian clock function in isolated eyestalk tissue of crayfish. *Proc. R. Soc. Lond. B* 265, 1819–1823.

Arikawa, K., Kawamata, K., Suzuki, T., and Eguchi, E. (1987). Daily changes of structure, function and rhodopsin content in the compound eye of the crab *Hemigrapsus sanguineus*. *J. Comp. Physiol. A.* 161, 161–174.

Barlow, R. B., Kaplan, E., Renninger, G. H., and Saito, T. (1987). Circadian rhythms in *Limulus* photoreceptors. I. Intracellular studies. *J. Gen. Physiol.* 89, 353–378.

Battelle, B. A. (2002). Circadian efferent input to *Limulus* eyes: anatomy, circuitry, and impact. *Microsc. Res. Techniq.* 58, 345–355.

Blest, A. D. and Stowe, S. (1997). A phospholipase inhibitor, manoalide, and a G-protein activator, Mas-7, both affect the turnover of phototransductive membranes by crab retinas in darkness. *J. Comp. Physiol. A* 810, 347–355.

Bollens, S. and Frost, B. (1989). Zooplanktivorous fish and variable diel vertical migration in the marine planktonic copepod *Calanus pacificus*. *Limnol. Oceanogr.* 34, 1072–1083.

Brönmark, C. and Hansson, L.-A. (2012). Chemical ecology in aquatic systems-an introduction. In *Chemical Ecology in Aquatic Systems* (eds. by C. Brönmark and L.-A. Hansson), pp 1–19. New York: Oxford University Press.

Bryceson, K. P. and McIntyre, P. (1983). Image quality and acceptance angle in a reflecting superposition. *J. Comp. Physiol. A* 151, 367–380.

Cellier, S. and Buisson, B. (1998). The role of the eye in the migratory rhythms of *Daphnia magna* and *Daphnia longispina* (Cladocera). *Annls. Limnol.* 34, 159–164.

Chamberlain, S. C. and Barlow, R. B. (1987). Control of structural rhythms in the lateral eye of *Limulus*: interactions of natural lighting and circadian efferent activity. *J. Neurosci.* 7, 2135–2144.

Christy, J. H. (2011). Timing of hatching and release of larvae by brachyuran crabs: patterns, adaptive significance and control. *Integr. Comp. Biol.* **51**, 62–72.

Cohen, J. H. and Forward, R. B. (2003). Ctenophore kairomones and modified aminosugar disaccharides alter the shadow response in a larval crab. *J. Plankton Res.* 25, 203–214.

Cohen, J. H. and Forward, R. B. (2005). Photobehavior as an inducible defense in the marine copepod *Calanopia americana*. *Limnol. Oceanogr.* 50, 1269–1277.

Cohen, J. H. and Forward, R. B. (2009). Zooplankton diel vertical migration - A review of proximate control. *Oceanogr. Mar. Biol.* 47, 77–110.

Cohen, J. H., Hanson, C. K., Dittel, A. I., Miller, D. C., and Tilburg, C. E. (2015). The ontogeny of larval swimming behavior in the crab *Hemigrapsus sanguineus*: Implications for larval transport. *J. Exp. Mar. Biol. Ecol.* 462, 20–28.

Cooke, S. L., Williamson, C. E., Leech, D. M., Boeing, W. J., and Torres, L. (2008). Effects of temperature and ultraviolet radiation on diel vertical migration of freshwater crustacean zooplankton. *Can. J. Fish. Aquat. Sci.* 65, 1144–1152.

Cronin, T. W. (1982). Estuarine retention of larvae of the crab *Rhithropanopeus harrisii*. *Estuar. Coast. Shelf S.* 15, 207–220.

Cronin, T. W. and Forward, R. B. (1986). Vertical migration cycles of crab larvae and their role in larval dispersal. *Bull. Mar. Sci.* 39, 192–201.

Cronin, T. W. and Forward, R. B. (1988). The visual pigments of crabs. I: Spectral characteristics. *J. Comp. Physiol. A* 162, 463–478.

Epifanio, C. E. (2013). Invasion biology of the Asian shore crab *Hemigrapsus sanguineus*: A review. *J. Exp. Mar. Biol. Ecol.* 441, 33–49.

Forward, R. B. (1985). Behavioral responses of larvae of the crab *Rhithropanopeus harrisii* (Brachyura: Xanthidae) during diel vertical migration. *Mar. Biol.* 90, 9–18.

Forward, R. B. (2009). Larval biology of the crab *Rhithropanopeus harrisii* (Gould): a synthesis. *Biol. Bull.* 216, 243–256.

Forward, R. B. and Costlow, J. D. **(**1974). The ontogeny of phototaxis by larvae of the crab *Rhithropanopeus harrisii*. *Mar. Biol.* 26, 27–33.

Forward, R. B., Cronin, T. W., and Stearns, D. E. (1984). Control of diel vertical migration : Photoresponses of a larval crustacean. *Limnol. Oceanogr.* 29, 146–154.

Forward, R. B. and Hettler, W. F. (1992). Effects of feeding and predator exposure on photoresponses during diel vertical migration of brine shrimp larvae. *Limnol. Oceanogr.* 37, 1261–1270.

Forward, R. B., Moeller, B. P., and Cohen, J. H. (2014). Circadian rhythm in larval release by the crab *Rhithropanopeus harrisii*: Entrainment model. *Biol. Bull.* 226, 92–101.

Forward, R. B. and Rittschof, D. (1993). Activation of photoresponses of brine shrimp nauplii involved in diel vertical migration by chemical cues from fish. *J. Plankton Res.* 15, 693–701.

Forward, R. B. and Rittschof, D. (1999). Brine shrimp larval photoresponses involved in diel vertical migration: Activation by fish mucus and modified amino sugars. *Limnol. Oceanogr.* 44, 1904–1916.

Forward, R.B. and Rittschof, D. (2000). Alteration of photoresponses involved in diel vertical migration of a crab larva by fish mucus and degradation products of mucopolysaccharides. *J. Exp. Mar. Biol. Ecol.* 245, 277–292.

Frank, T. M. (1999). Comparative study of temporal resolution in the visual systems of mesopelagic crustaceans. *Biol. Bull.* 196, 137–144.

Frank, T. M. (2000). Temporal resolution in mesopelagic crustaceans. *Philos. T. Roy. Soc.* 355, 1195–1198.

Frank, T. M. (2003). Effects of light adaptation on the temporal resolution of deep-sea crustaceans. *Integr. Comp. Biol.* 43, 559-570.

Frank, T. M., Johnsen, S., and Cronin, T. W. (2012). Light and vision in the deep-sea benthos: II. Vision in deep-sea crustaceans. *J. Exp. Biol.* 215, 3344–3353.

Gallegos, C.L. (2001) Calculating optical water quality targets to restore and protect submersed aquatic vegeatation: overcoming problems in partitioning the diffuse attenuation coefficient for photosynthetically active radiation. *Estuaries* 24, 381–397.

Grecay, P. A. and Targett, T. E. (1996). Effects of turbidity, light level and prey concentration on feeding of juvenile weakfish *Cynoscion regalis*. *Mar. Ecol. Prog. Ser.* 131, 11–16.

Greiner, B., Ribi, W. A., Wcislo, W. T., and Warrant, E. J. (2004). Neural organisation in the first optic ganglion of the nocturnal bee *Megalopta genalis*. *Cell Tissue Res.* 318, 429–437.

Greiner, B., Ribi, W. A, and Warrant, E. J. (2005). A neural network to improve dim-light vision? Dendritic fields of first-order interneurons in the nocturnal bee *Megalopta genalis*. *Cell Tissue Res.* 322, 313–320.

Hagan, S. M. and Able, K. W. (2003). Seasonal changes of the pelagic fish assemblage in a temperate estuary. *Estuar. Coast. Shelf Sci*. 56, 15–29.

Haney, J. F. (1993). Environmental control of diel vertical migration behavior. *Arch. Hydrobiol. Beih. Ergebn. Limnol.* 39, 1–17.

Hariyama, T., Meyer-rochow, V. B., Kawauchi, T., Takaku, Y., and Tsukahara, Y. (2001). Diurnal changes in retinula cell sensitivities and receptive fields (two-dimensional angular sensitivity functions) in the apposition eyes of *Ligia exotica* (Crustacea, Isopoda). *J. Exp. Biol.* 248, 239– 248.

Hays, G. C. (2003). A review of the adaptive significance and ecosystem consequences of zooplankton diel vertical migrations. *Hydrobiol*. 503, 163–170.

Kaplan, E. and Barlow, R. B. (1980). Circadian clock in *Limulus* brain increases response and decreases noise of retinal photoreceptors. *Nature* 286, 393–395.

Kessler, K. (2004). Distribution of *Daphnia* in a trade-off between food and temperature: individual habitat choice and time allocation. *Freshwater Biol.* 49, 1220–1229.

Land, M. F. (1981). Optics and vision in invertebrates. In *Handbook of sensory physiology,* Vol. VII/6B (ed. H. Autrum), pp 471-592. Berlin: Springer.

Latz, M. I. and Forward, R. B. (1977). The effect of salinity upon phototaxis and geotaxis in a larval crustacean. *Biol. Bull.* 153, 163–179.

Matsuda, K. and Wilder, M. N. (2014). Eye structure and function in the giant freshwater prawn *Macrobrachium rosenbergii*. *Fish. Sci.* 80, 531–541.

Mckelvey, L. M. and Forward, R. B. (1995). Activation of brine shrimp nauplii photoresponses involved in diel vertical migration by chemical cues from visual and non-visual planktivores. *J Plankton Res.* 17, 2191–2206.

Meyer-Rochow V. B. (1999). Compound eye: circadian rhythmicity, illumination, and obscurity. In *Atlas of Arthropod Sensory Receptors* (eds. E. Eguchi and Y. Tominaga), pp 97–124. New York: Springer.

Meyer-rochow, V. B. (2001). The crustacean eye: dark/light adaptation, polarization sensitivity , flicker fusion frequency , and photoreceptor damage. *Zool. Sci.* 1197, 1175–1197.

Meyer-Rochow V. B. and Tiang, K. M. (1984). The eye of *Jasus edwardsii* (Crustacea, Decapoda): electrophysiology, histology, and behaviour. *Zoologica* 45, 1–61.

Nässel, D. and Waterman, T. (1979). Massive diurnally modulated photoreceptor membrane turnover in crab light and dark adaptation. *J. Comp. Physiol. A*. 131, 205–216.

Nilsson, D. and Odselius, R. (1981). A new mechanism for light-dark adaptation in the *Artemia* compound eye (Anostraca, Crustacea). *J. Comp. Physiol. A*. 143, 389–399.

Oberwinkler, J., and Stavenga, D. G. (2000). Calcium transients in the rhabdomeres of dark- and light-adapted fly photoreceptor cells. *J. Neurosci.* 20, 1701–1709.

Park, S., Epifanio, C. E., and Iglay, R. B. (2005). Patterns of larval release by the Asian shore crab *Hemigrapsus sanguineus* (De Haan): Periodocity at diel and tidal frequencies. *J. Shellfish Res.* 24, 591–595.

Ringelberg, J. (2010). *Diel Vertical Migration of Zooplankton in Lakes and Oceans*. Dordrecht: Springer.

Rittschof, D. and Cohen, J. H. (2004). Crustacean peptide and peptide-like pheromones and kairomones. *Peptides* 25, 1503–1516.

Shephard, K. L. (1994). Functions for fish mucus. *Rev. Fish Biol. and Fisher.* 4, 401–429.

Snyder, A. W. (1979). Physics of vision in compound eyes. In *Handbook of sensory physiology,* Vol. VII/6A (ed. by H. Autrum), pp. 225–313. Berlin : Springer.

Stich, H. B. and Lampert, W. (1981). Predator evasion as an explanation of diurnal vertical migration by zooplankton. *Nature* 293, 396–398.

Stowe, S. (1980). Rapid synthesis of photoreceptor membrane and assembly of new microvilli in a crab at dusk. *Cell Tissue Res.* 211, 419–440.

Sulkin, S. (1984). Behavioral basis of depth regulation in the larvae of brachyuran crabs. *Mar. Ecol. Prog. Ser.* 15, 181–205.

Toh, Y. and Watermn, T. H. (1982). Diurnal changes in compound eye fine structure in the blue crab *Callinectes*. *J. Ultrastruct. Res.* 78, 40–59.

Van Gool, E. and Ringelberg, J. (2002). Relationship between fish kairomone concentration in a lake and phototactic swimming by *Daphnia*. *J. Plankton Res.* 24, 713–721.

Warrant, E. J. (1999). Seeing better at night: life style, eye design and the optimum strategy of spatial and temporal summation. *Vision Research* 39, 1611–1630.

Warrant, E. J. (2008). Seeing in the dark: vision and visual behaviour in nocturnal bees and wasps. *J. Exp. Biol.* 211, 1737–1746.

Warrant, B. E., Oskarsson, M., and Malm, H. (2014). The remarkable visual abilities of nocturnal insects: Neural Principles and bioinspired night-vision algorithms. *Proc. IEEE.* 102, 1411–1426

Welch, J. M. and Forward, R. B. (2001). Flood tide transport of blue crab, *Callinectes sapidus*, postlarvae: behavioral responses to salinity and turbulence. *Mar. Biol.* 139, 911–918.

Williamson, C. E., Fischer, J. M., Bollens, S. M., Overholt, E. P., and Breckenridge, J. K. (2011). Towards a more comprehensive theory of zooplankton diel vertical migration: Integrating ultraviolet radiation and water transparency into the biotic paradigm. *Limnol. Oceanogr.* 56, 1603–1623.

Yang, X. G. (1986). Circadian-rhythms of the ERG of the crab *Scylla serrata*. *Acta Zoologica Sinica* 32, 122–129.

Yuan, W. J. (1997). Ultrastructure changes of the photoreceptor in the crab, *Eriocheir sinensis* by diurnal photoperiodism. *Acta Zoologica Sinica* 43, 344-352.

Chapter 3

KAIROMONES FROM MARINE FISH INCREASE VISUAL SENSITIVITY IN BRINE SHRIMP FROM GREAT SALT LAKE, UTAH, USA

Chemical cues from fish, or kairomones, often impact the behavior of zooplankton. These behavioral changes are thought to improve predator avoidance. For example, marine and estuarine crustacean zooplankton become more sensitive to light after kairomone exposure, which likely deepens their vertical distrubtion into darker waters and thereby reduces their visibility to fish predators. Here, I show that kairomones from marine fish induce similar behavioral responses in adult brine shrimp (*Artemia* spp.) from an endorheic, hypersaline lake, Great Salt Lake, Utah, USA. Given downwelling light stimuli, kairomone-exposed *Artemia* spp. induce a descent response upon dimmer light flashes than they do in the absence of kairomones. Using extracellular electroretinogram (ERG) recordings, I also find that kairomones induce physiological changes in the retina that may lead to increased visual sensitivity, suggesting that kairomone-induced changes to photobehavior are mediated at the photoreceptor level. However, the observed increases in visual sensitivity were not a result of kairomone-induced changes to eye structure as observed for crab larvae (Chapter 2). Although *Artemia* spp. inhabit endorheic environments that are intolerable to most fish, kairomones from marine fish amplify photobehavior in these branchiopod crustaceans, and the mechanism for this behavioral change is both similar

to and diverges from that described in marine malacostracan crustaceans. Hence, I also relate my findings to the evolution of nervous systems.

3.1 Introduction

In marine and freshwater zooplankton, chemical cues from fish predators, known as *kairomones*, induce behaviors that are known to aid in predator avoidance (reviewed in Cohen and Forward 2009; Ringelberg 2010). The initiation and production of these phenotypically plastic changes likely involves integration of multiple sensory modalities. For example, kairomones induce greater sensitivity to light in several zooplankton species, as evidenced from descent responses to dimmer changes in downwelling light after kairomone exposure (Cohen and Forward 2009). Such changes would impact predator avoidance behavior, including diel vertical migration (DVM). Kairomone-induced changes to photobehavior have been observed in several species of marine crustacean zooplankton, including copepods (Cohen and Forward 2005) and larval crabs (Forward and Rittschof 2000; Cohen and Forward 2003; Charpentier and Cohen 2015 [Chapter 2]). In marine systems, kairomone molecules that induce changes to photobehavior are degradation products of fish body mucus, namely disaccharide amino sugars (reviewed in Rittschof and Cohen 2004).

Brine shrimp (*Artemia* spp.) inhabit hypersaline ponds and lakes, which are intolerable to most animals (Persoone and Sorgeloos 1980). Hence, these saltwater habitats generally have low species diversity and simple trophic structures (Lenz and Browne 1991). In Great Salt Lake, Utah, USA, for example, *Artemia* spp. constitute a significant component of the total faunal biomass, where they are usually spatially separated from fish predators, and primarily consumed by migrating waterfowl and the corixid insect, *Trichocorixa veticalis* (Belovsky et al. 2011). However, *Artemia* spp.

populations in other lakes do experience predation from fish that can tolerate relatively high salinities (< 120), e.g. mullet, milkfish, killifish, and *Tilapia* (Griffith 1974; Persoone and Sorgeloos 1980; Giddings and Stephens 1999), and increased freshwater input in the spring causes dilution in parts of Great Salt Lake (Price 1985), which could seasonally expand fish habitat.

Similar to marine crustacean zooplankton, *Artemia* nauplii from Great Salt Lake become more sensitive to downwelling light after exposure to mucus from estuarine and marine fish and to relevant amino sugar molecules (Forward and Hettler 1992; Forward and Rittschof 1999). Further, Lenz (1980) observed adult *Artemia* conducting DVM in the field, which could be attributed to similar control of photobehavior between marine zooplankton and these hypersaline crustaceans. Accordingly, *Artemia* spp. from Great Salt Lake have either retained a mechanism for integrating chemical and visual information into migration behavior from an earlier period when they were exposed to fish predators, or this sensory integration presently serves another purpose.

In the larvae of two crab species, Charpentier and Cohen (2015) found that kairomone-induced changes to photobehavior were mediated, at least in part, by increases in visual sensitivity at the photoreceptor level (Chapter 2). Given that marine fish kairomones induce photosensitivity in both *Artemia* nauplii and marine crustacean zooplankton, I hypothesize that similar physiological mechanisms mediate altered photobehavior in *Artemia*. In addition, the compound eye of adult *Artemia* is analogous in structure to that of crab larvae (Cronin 1986). Alternatively, the neural organization of visual and olfactory systems varies slightly between malacostracan crab larvae and branchiopod crustaceans (i.e. brine shrimp; Harzsch and Glötzner

2002; Wildt and Harzch 2002). Hence, it is also possible that integration of visual and chemical cues may differ between the two crustacean lineages.

In this study, I first assessed whether kairomones from marine fish altered the photobehavior of adult *Artemia* spp. from Great Salt Lake, similarly to nauplii (Forward and Hettler 1992; Forward and Rittschof 1999) and marine zooplankton (Cohen and Forward 2009). Second, I tested my hypothesis that the mechanism by which kairomones alter photobehavior is comparable to that described in marine and estuarine crab larvae (Charpentier and Cohen 2015 [Chapter 2]). Further, electroretinogram (ERG) recordings and histological methods were used to examine whether kairomones induce changes to retinal physiology and eye structure that would amplify visual sensitivity, and thereby result in increased photobehavior.

3.2 Methods

3.2.1 Experimental solutions

Seawater used in all experiments was collected from Indian River Inlet (~ 32 psu, Delaware, USA). Biologically active molecules were removed by ultrafiltration (100 kDa; GE Life Sciences UFP-100-C-5A) and aging in darkness for at least 1 week (Forward and Rittschof, 1999). This water served as control seawater for all experiments. I produced kairomone solutions with diluted mucus from the estuarine fish, *Fundulus heteroclitus*, where mucus was isolated with a previously described body wipe method (Forward and Rittschof, 1999) and diluted with control seawater to produce uniform concentrations of 0.001, 0.01, or 0.1 g wet weight mucus L^{-1} seawater. Aliquots of concentrated mucus were stored at -80 °C but were thawed and diluted immediately before using in experiments. Mucus from *F. heteroclitus* at

similar concentrations has been shown to elicit strong behavioral responses in zooplankton, including *Artemia* spp. nauplii (Forward and Rittschof 1999, 2000; Cohen and Forward 2005).

3.2.2 Animal rearing

Preserved cysts of *Artemia* spp. from Great Salt Lake, Utah, USA (Grade A; Brine Shrimp Direct, Ogden, Utah, USA) were hatched under incandescent light in a separator funnel with artificial seawater (Aquarium Sea Salt Mixture, Instant Ocean, Blacksburg, VA, USA) at a salinity of 30. Once hatched, animals were reared in a 38-L aquarium of artificial seawater under a 14:10 h light:dark cycle and fed *Nannochloropsis* algal paste (Brine Shrimp Direct, Ogden, Utah, USA), *ad libidum*. Only adult females with brood pouches were used in experiments.

3.2.3 Photobehavior

I conducted behavioral experiments in an apparatus that mimics the underwater angular light distribution, similar to that used by Forward et al. (1984). Within a light-tight enclosure, I placed groups of animals ($n \approx 20$) in a transparent acrylic chamber ($10 \times 10 \times 7.5$ cm), enclosed within a larger acrylic water bath painted flat black ($40 \times 40 \times 15$ cm; ~ 23°C). Experimental light was produced by an Oriel 300 W Xe Arc Lamp (Newport Corp., Irvine, CA, USA), and filtered to 488 nm with an interference filter (10 FWHM, Melles Griot, Irvine, CA, USA). I chose this wavelength, because it is near peak spectral sensitivity of *Artemia* (Bradley and Forward, 1984). Fixed neutral density filters (Melles Griot, Irvine, CA, USA) allowed us to control the intensity of light stimuli, which passed horizontally through a collimating lens, electromagnetic shutter (Newport Corp., Irvine, CA, USA), wavelength and intensity filters, and then

reflected off a mirror inside the light-tight enclosure to pass vertically through a white acrylic diffuser that covered the water bath. The described light assembly produces a relatively diffuse downwelling light source, entering a dark larval chamber. Prior to experiments, I measured downwelling irradiance at the larval chamber with an optometer and calibrated radiometric probe (models S471 and 247; Gamma Scientific, Baltimore, MD, USA) to select an appropriate range and resolution of light stimuli.

I recorded swimming behavior through two narrow transparent sections in the black water bath using a digital camera (scA750-60gm; Basler AG Electronics, Ahrensburg, Germany) with a 16 mm varifocal lens (HF16HA-1B; Fujinon Corp, Edison, NJ, USA), backlit by an infrared LED array (880 nm; Advanced Illumination, Edmund Optics, Barrington, NJ, USA). Camera optics were set such that the field-of-view and depth-of-field could resolve all swimming individuals regardless of their position in the three-dimensional chamber. I used a custom program in LabVIEW (National Instruments, Austin, TX, USA) to coordinate timing of shutter opening and closing as well as capture video recordings.

Prior to behavioral experiments, animals were exposed to either control seawater or kairomone solutions of three concentrations (0.001, 0.01, and 0.1 g mucus L^{-1} seawater) for 1 – 3 h and acclimated to the dark for at least 1 h, 15 minutes of which were in the experimental chamber. After the acclimation period, experimental animals experienced a series of seven 10 s light stimuli increasing in intensity from approximately 1×10^{12} to 5×10^{14} photons m^{-2} s^{-1}. During these experiments, each stimulus was separated by four minutes to allow time for dark acclimation. I recorded swimming behavior 10 s prior ("dark") and after each light stimulus. Behavioral

experiments were replicated five times for each solution with different groups of larvae.

I determined start and end XY-coordinates of swimming individuals in the last 9 s of each 10 s video recording using a PC-based motion analysis system (CellTrak software, Motion Analysis Corp., Santa Rosa, CA, USA). An individual was considered to be descending if the line between its start and end XY-coordinates was within the nadir ± 30°. I then calculated percent descending for each group (replicate × treatment) before (dark) and after each light stimulus. Within each treatment, I compared percent descending in the dark to percent descending after each of the given light stimuli with one-way repeated measures (RM) ANOVAs. If RM ANOVAs detected significant differences ($P < 0.05$), Holm-Šidák *post-hoc* tests determined which specific light stimuli evoked a significant descent response relative to swimming behavior in the dark. The light stimulus of the lowest intensity that induced a descent response was deemed the 'behavioral threshold'. A lower behavioral threshold indicates greater sensitivity to light. One-way ANOVAs within treatments suggested that percent descending of animals swimming in the dark did not differ significantly between replicates ($P > 0.05$). Hence, I used mean percent descending before each light stimulus as "percent descending in the dark" in the RM ANOVA analyses described above. For behavioral experiments, all statistical analyses were conducted in SigmaPlot 12.0 (Systat Software, San Jose, CA).

3.2.4 Electrophysiology

I used extracellular electroretinograms (ERGs) to assess visual physiology in adult female *Artemia* spp. Prior to experiments, animals were exposed to control seawater, kairomones at 0.001 and 0.01 g mucus L^{-1} seawater, or a negative control for

1 – 3 h. The negative control was a 0.1 g mucus L^{-1} seawater kairomone solution that was aged in the dark for > 24 h, a timeframe over which kairomones significantly degrade (McKelvey 1997). In ERG experiments, animals were attached by their dorsal carapace to the plastic head of a pin with cyanoacrylate gel adhesive (Loctite, Rocky Hill, CT, USA) and then suspended in an 18 °C water bath of their respective treatment by a plexiglass support. I then placed the recording electrode, a tungsten microelectrode (75 μm tip, FHC, Bowdoin, ME, USA), subcorneally in the eye and a second differential electrode with the same specifications in the water bath. Differential AC signals were amplified (Ext-02 B, NPI Electronic Instruments, Tamm, Germany), digitized, and stored in LabChart 7 (AD Instruments, Colorado Springs, CO, USA) for analysis of peak-to-peak response height and response time (see below).

Light stimuli were produced by a xenon arc lamp (ASB-XE-175, Spectral Products, Putnam, CT, USA) and delivered to the eye with a 4 mm diameter liquid light guide. Wavelength was set by a 532 nm interference filter (10 FWHM), and light intensity was controlled with fixed neutral density filters (Melles Griot). Again, I chose this wavelength, because it is near peak spectral sensitivity for *Artemia* (Bradley and Forward, 1984). An electromagnetic shutter and shutter driver (LS6S2T0-100, VCM-D1, Uniblitz/Vincent Associates, Rochester, NY, USA) under computer control mediated stimulus onset and duration. Sensitivity may differ between night and day in crustaceans (Meyer-Rochow 2001), so I conducted all experiments during the day between 9:00 and 16:00. Prior to experiments, irradiance was measured with a spectroradiometer (USB2000+; Ocean Optics, Dunedin, FL, USA) to determine the range and resolution of light stimuli.

Response-intensity (V – log I) curves were generated from ERG recordings, where response magnitude (peak-to-peak height) increased with stimulus intensity until reaching some maximum response (V_{max}). I acclimated animals in the dark prior to experiments and did not give an experimental flash until the ERG response to a dim test flash yielded a consistent response magnitude. Experimental flashes (0.1 s) were given in order of increasing irradiance, ranging from $10^{16} – 10^{19}$ photons $m^{-2}s^{-1}$. Between experimental flashes, animals were acclimated in the dark until their response to intermittent low intensity test flashes returned to its original magnitude (at least two minutes).

To generate V – log I curves, peak-to-peak response height was plotted across the intensity range of light stimuli. I modeled the response-intensity relationship with the Zettler modification of the Naka-Rushton equation to determine the curve's half saturation point (log K), maximum response (V_{max}), slope, and dynamic range or log range from 5 to 95% of V_{max} (Frank, 2003). Curves were then normalized to V_{max}. Here, log K was used as a measure of photophysiological sensitivity. As such, lower values indicate greater sensitivity. Modeled data were only included in this analysis if the measured V_{max} value was at least 60% of the modeled V_{max}. I used one-way ANOVAs to evaluate differences in log K, slope, dynamic range, and V_{max} between the four treatments, control seawater (n = 11), the aged kairomone negative control (n = 5), and kairomones at 0.1 g mucus L^{-1} seawater (n = 11) or 0.001 g mucus L^{-1} seawater (n = 5). If the results from my ANOVA analysis were not significant, I then directly assessed differences between animals given the control and kairomones at the highest concentration (0.1 g mucus L^{-1} seawater) using a Welch's t-test.

Using ERG responses from V – log I curves, I also investigated the temporal resolution of the extracellular responses. At each irradiance, I measured the time from the onset of the light stimulus to the response start (*response latency*) and to the response peak (*peak latency*). Response start was defined as the time at which the ERG signal begins to decrease in magnitude above background noise. I assessed the effect of kairomone treatment as well as log irradiance on response and peak latency with an ANCOVA. For electrophysiological experiments, I conducted all statistical analyses in R (R Core Team, 2016) using the car package (Fox and Weisberg 2011), and accepted significant differences at $P < 0.05$.

3.2.5 Eye structure

Using histological techniques, I assessed whether kairomones induce changes in eye structure over a 3-h time interval. First, adult female *Artemia* spp. were exposed to kairomones from 0.1 g mucus L^{-1} seawater for a period of 0 (control), 0.5, 1, or 3 h. Following exposure, I removed and fixed heads in 2.5% glutaraldehyde in 0.4 *M* Millonig's buffer solution for 3.25 h between 8:00 and 13:00. During and prior to kairomone exposure and fixation, animals were under fluorescent room light (~ 10^{18} photons m^{-2} s^{-1} white light). A follow-up experiment was conducted to assess differences in eye structure after light and dark acclimation. Light-acclimated animals were exposed to and fixed under fluorescent light, as in the above kairomone experiment. Dark-acclimated animals were kept in the dark overnight for approximately 12 h before fixation in darkness the following morning. Both light- and dark-acclimated animals were fixed at approximately 10:00. For both experiments, animals were fixed on two separate occasions, about one month apart.

After fixation, animals were dehydrated in a graded ethanol series, gradually transferred into medium grade acrylic resin (London White Company, London, UK), and embedded in resin by hot curing at 60 ± 2 °C for 20 – 24 h in an Isotemp oven (Fisher Scientific, Waltham, MA, USA). I then cut 0.2 μm sections with a Sorvall MT-2B Ultramicrotome (Du Pont Company, Tuscon, AZ, USA) and stained these sections with a mixture of Toludine Blue O and Basic Fuchsin (prepared tissue stain; Electron Microscopy Sciences, Hatfield, PA, USA) before mounting on slides.

From the prepared slides, several characteristics of eye structure were measured with an ocular reticle on a compound microscope (CX31, Olympus Corp., Tokyo, Japan), including rhabdom diameter, rhabdom length, aperture diameter, length and width of crystalline cone, as well as length and width of the glycogen body (Fig. 3.1). I measured rhabdom diameter at the distal end of the rhabdom and aperture diameter at the proximal end of the crystalline cone, where it attaches to the rhabdom. All measurements were made from longitudinally sectioned ommatidia, and conducted blindly, where the measurer was not aware of the corresponding treatment. Ommatidia structure varies with location in *Artemia*, so all of my measurements were made within the acute zone of the eye, as described by Nilsson and Odselius (1981) and labeled in Fig. 3.1. I calculated the grand mean of all measurements taken from an individual ($n \approx 6$), and this grand mean was considered a replicate. Measurements were only taken from ommatidia that contained all structural characteristics (Fig. 3.1), resulting in 10, 8, 9, and 11 replicates in animals exposed to kairomones for 0 (control), 0.5, 1, or 3 h, as well as 12 and 10 replicates for those acclimated to the light and dark, respectively. I captured images of each measured section with a digital camera (EOS Rebel T3i, Canon Inc., Japan).

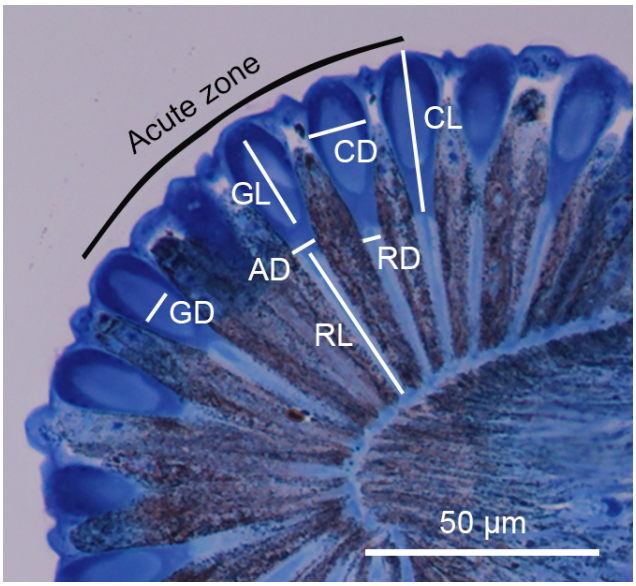

Figure 3.1: Semi-thin (0.2 um) longitudinal cross-section of the *Artemia* spp. compound eye stained with Toludine Blue O and Basic Fuchsin. Each of the characteristics measured in the structural analysis are highlighted in white, including glycogen body diameter (GD), glycogen body length (GL), aperture diameter (AD), rhabdom length (RL), rhabdom diameter (RD), cone diameter (CD), and cone length (CL). All measured ommatidia were within the acute zone, described by Nilsson and Odselius (1981).

Using the measured structural characteristics, I calculated optical sensitivity of *Artemia* spp. compound eyes, S (μm^2 Sr), according to Land (1981; Equation 2.1). I also calculated acceptance angle using several structural characteristics (Equation 2.2; Snyder, 1979). Here, focal length was estimated to be 65% that of the crystalline cone. This estimation was based on measurements made in the acute zone after both light and dark acclimation in *Artemia* (Nilsson and Odselius 1981). In addition, I used an absorption coefficient of 0.008 μm^{-1} (Cronin and Forward, 1988), and a wavelength of 520 nm was used to represent peak spectral sensitivity in *Artemia* (Bradley and Forward, 1984).

I assessed whether kairomone exposure and light/dark-acclimation affected eye structure, optical sensitivity, and/or acceptance angle using mixed models with likelihood ratio tests (Bolker et al. 2008). For each model, direct effects were either the length of kairomone exposure (0, 0.5, 1, 3 h) or light/dark conditions. The date of fixation was included as a random effect to account for potential differences in my culture over the one-month time gap between the two sample fixation times (described above). Significant differences were accepted at $P < 0.05$, and mixed model analyses were conducted in R (R Core Team 2016), using the lme4 and lsmeans packages (Bates et al. 2015, Lenth 2016, respectively).

3.3 Results

3.3.1 Photobehavior

For all treatments, the percentage of animals descending differed before and after light stimulation ($F_{6,27} > 3.4$, $P < 0.01$; one-way RM ANOVA). Further, the behavioral threshold, or lowest light intensity to induce a descent response, decreased after kairomone exposure (Fig. 3.2). Specifically, animals exposed to the highest kairomone concentration (0.1 g mucus L^{-1} seawater) had a behavioral threshold that was approximately 4% that of the control, at 3.14×10^{12} photons m^{-2} s^{-1} ($P = 0.048$) and 7.40×10^{13} photons m^{-2} s^{-1} ($P = 0.01$; Holm-Šidák *post hoc* test), respectively. This kairomone effect was concentration dependent, where the two lower concentrations (0.001, 0.01 g mucus L^{-1} seawater) both had a behavioral threshold between that of the control and the highest kairomone concentration (1.10×10^{13} photons m^{-2} s^{-1}; $P < 0.01$).

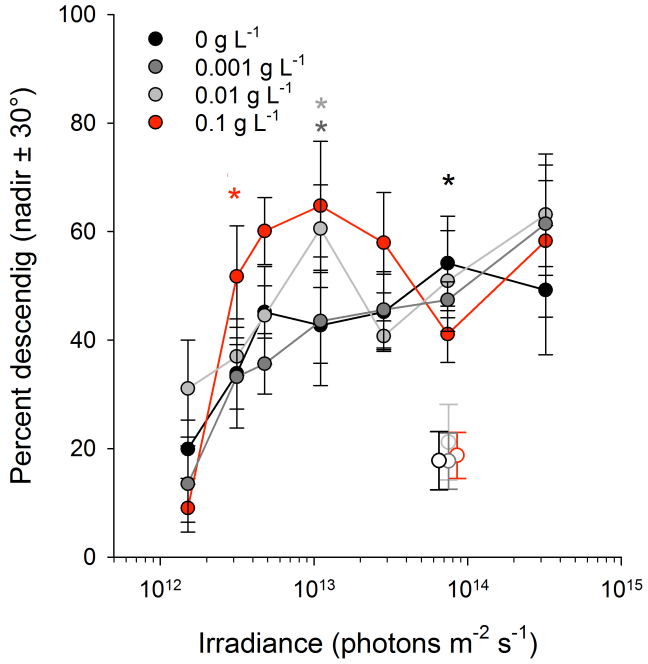

Figure 3.2: Kairomones alter photobehavior. Mean ± se percentage descending (nadir ± 30°) of *Artemia* spp. before (swimming in the dark, unfilled symbols) and after light stimulation (filled symbols). Prior to experiments, animals (≈ 20) from each replicate (n = 5) were exposed to control seawater (0 g L^{-1}) or kairomones from *Fundulus heteroclitus* mucus, across a concentration gradient (0.001 – 0.1 g mucus L^{-1} seawater). The behavioral threshold of each treatment, or lowest light intensity to induce a descent response, was determined using one-way repeated measures ANOVAs with Holm-Šidák *post hoc* analyses, where significant differences were accepted at $P < 0.05$. Asterisks represent these thresholds, with each given its respective treatment color.

3.3.2 Electrophysiology

From response-intensity (V – log I) curves, I first assessed whether kairomone exposure impacted visual sensitivity. Across the examined light intensity range, curve position appears to depend on kairomone treatment, where those of animals exposed to kairomones (0.001, 0.1 g mucus L^{-1} seawater) are shifted to the left of the control and negative control (aged 0.1 g mucus L^{-1} seawater) (Fig. 3.3). Regardless, the calculated

curve parameters (log K, slope, dynamic range, V_{max}) did not vary between the four treatments (Table 3.1) ($F_{3,26} < 1.9$, $P > 0.16$; one-way ANOVA). However, when comparing only the control and the highest kairomone concentration (Welch's t-test), I found that log K values were lower in kairomone-exposed animals ($t_{15} = 2.3$; $P = 0.04$), consistent with the left-shifted curve (Fig. 3.3). In addition, curves had a greater slope and smaller dynamic range in kairomone-exposed animals, relative to the control ($t_{18} > 2.1$; $P < 0.04$). However, I found no difference in V_{max} between these two treatments ($t_{18} = 1.2$, $P = 0.27$).

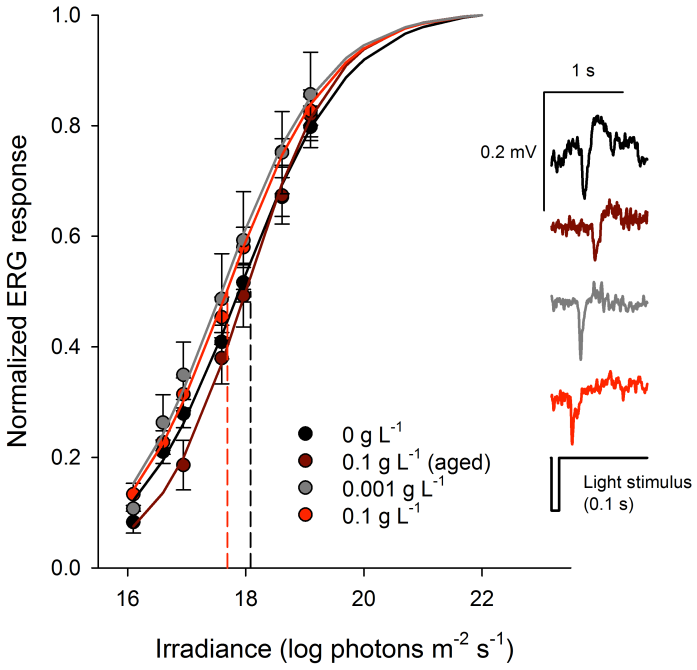

Figure 3.3: Response-intensity curves. Mean ± se normalized ERG responses across a log range of irradiance stimulations in *Artemia* spp.. Prior to experiments, individuals were given control seawater (0 g L^{-1}, n = 11), a negative control (aged 0.1 g mucus L^{-1} seawater, n = 5), or two concentrations of kairomones from *Fundulus heteroclitus* mucus (0.001, 0.1 g mucus L^{-1} seawater; n = 5 and 11, respectively). Curves were modeled using the Zettler modification of the Naka-Rushton equation, and log K of the control and highest kairomone concentration (0.1 mucus g seawater L^{-1}) are highlighted with dotted lines of their respective treatment colors. Insets (right) show a representative ERG response waveform at log K for each treatment as well as the length and timing of a light stimulus (0.1 s). Scale bar (top) indicates the time and magnitude of ERG responses.

Table 3.1: Response-intensity curve parameters in *Artemia* spp. exposed to the control, negative control (aged mucus), or kairomones ("kairo.") from *Fundulus heteroclitus* mucus (0.001 and 0.1 g mucus L^{-1} seawater)

Treatment	log K	m	DR	V_{max}
Control	18.1 ± 0.2	0.45 ± 0.04	5.6 ± 0.4	0.93 ± 0.25
Negative control	18.0 ± 0.2	0.54 ± 0.05	4.8 ± 0.5	1.45 ± 1.02
Kairo. (0.001 g L^{-1})	17.8 ± 0.3	0.58 ± 0.05	4.6 ± 0.3	0.71 ± 0.29
Kairo. (0.1 g L^{-1})	17.6 ± 0.1	0.49 ± 0.04	5.1 ± 0.5	0.98 ± 0.33

Values (mean ± se) of log K (log photons m^{-2} s^{-1}), slope (m), dynamic range (DR, log photons m^{-2} s^{-1}), and V_{max} (mV) were derived from the Zettler modification of the Naka-Rushton model. Sample sizes were 11, 5, 5, and 11 in the control, negative control, 0.001 and 0.1 g L^{-1} kairomone treatments, respectively.

Second, I evaluated kairomone-induced changes to temporal resolution using individual ERG responses, which were recorded during generation of V – log I curves. Namely, I compared response and peak latency between all four kairomone treatments, while also accounting for light intensity (Fig. 3.4) (ANCOVA). In both response and peak latency, models were significant ($F_{4,168} > 7.7$, $P < 0.001$), where latency was negatively related to light intensity ($P < 0.001$). Relative to the control, response latency was lower in animals exposed to the highest kairomone concentration ($P < 0.009$), but not those in the negative control, or lowest kairomone concentration

($P > 0.07$). Peak latency did not vary significantly between the four treatments ($P = 0.2$).

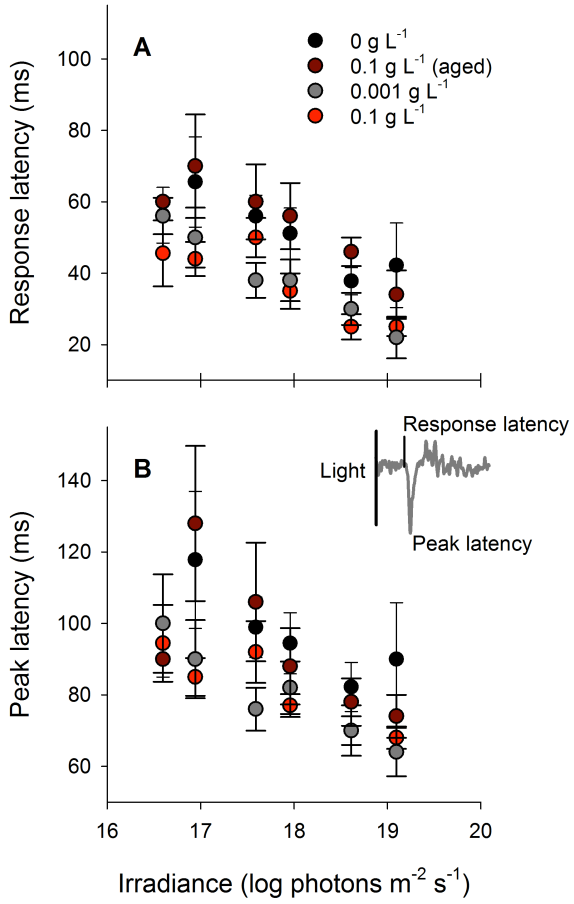

Figure 3.4: Effect of light and kairomones to temporal resolution. Mean ± se (A) response and (B) peak latency of *Artemia* spp. exposed to a log range of irradiance stimulations. Prior to experiments, individuals were given control seawater (0 g L^{-1}, n = 11), a negative control (aged 0.1 g mucus L^{-1} seawater, n = 5), or two concentrations of kairomones from *Fundulus heteroclitus* mucus (0.001, 0.1 g mucus L^{-1} seawater; n = 5 and 11, respectively). The inset at the top of panel B indicates the time of the light stimulus, response start ("response latency"), and response peak ("peak latency") in a representative response.

3.3.3 Eye structure

I compared eye structure of *Artemia* spp. after exposure to kairomones (0.1 g mucus L^{-1} seawater) for 0, 0.5, 1, and 3 h to evaluate whether kairomones induce morphological changes that would result in increased visual sensitivity (mixed models). Over the chosen timescale, however, I found no kairomone effect to eye structure, optical sensitivity, or acceptance angle (Table 3.2) ($\chi^2(1) < 2.9$, $P > 0.08$).

To validate my methodology, I evaluated whether eye structure changed between light- and dark-acclimated animals (mixed models), as described previously (Nilsson and Odselius 1981). Rhabdom diameter was approximately 25% larger in dark-acclimated animals (Table 3.3). However, there were no other significant differences in eye structure or calculated parameters between light and dark-acclimated *Artemia* spp. ($\chi^2(1) < 3.6$, $P > 0.06$).

Table 3.2: Characteristics of eye structure as well as optical sensitivity and acceptance angle in *Artemia* spp. after exposure to kairomones from *Fundulus heteroclitus* mucus (0.1 g mucus L^{-1} seawater) for 0, 0.5, 1, and 3 h.

	Kairomone exposure time (h)			
	0	0.5	1	3
Rhabdom diameter	4.52 ± 0.40	4.39 ± 0.24	4.46 ± 0.18	4.22 ± 0.18
Aperture diameter	4.68 ± 0.34	4.28 ± 0.24	4.48 ± 0.18	4.22 ± 0.18
Rhabdom length	45.9 ± 1.18	42.6 ± 1.92	42.8 ± 2.21	40.0 ± 3.93
Cone length	34.1 ± 0.43	36.4 ± 1.72	31.6 ± 0.90	33.83 ± 0.58
Cone diameter	14.8 ± 0.51	14.4 ± 0.82	15.0 ± 0.70	17.4 ± 1.75
Glycogen body length	24.5 ± 0.89	23.8 ± 0.70	22.0 ± 0.77	23.5 ± 0.62
Glycogen body diameter	12.2 ± 0.41	12.1 ± 0.83	12.0 ± 0.35	12.1 ± 0.71
S	0.11 ± 0.03	0.07 ± 0.02	0.09 ± 0.01	0.07 ± 0.01
Δρ	11.8 ± 0.96	11.0 ± 0.79	12.6 ± 0.75	11.4 ± 0.56

Values are mean ± se of eye structure parameters (μm), optical sensitivity (*S*, μm^2 Sr), and acceptance angle (Δρ, °). Sensitivity and acceptance angle were calculated with equations 2.1 and 2.2, respectively. Samples sizes for animals exposed to kairomones for 0, 0.5, 1, and 3 h were 10, 8, 9, and 11, respectively.

Table 3.3: Characteristics of eye structure as well as optical sensitivity and acceptance angle in *Artemia* spp. after light and dark acclimation

	Light acclimation	Dark acclimation
Rhabdom diameter *	3.33 ± 0.18	4.13 ± 0.29
Aperture diameter	3.49 ± 0.18	4.20 ± 0.31
Rhabdom length	41.3 ± 2.16	43.2 ± 1.87
Cone length	35.6 ± 1.69	35.0 ± 1.76
Cone diameter	15.2 ± 0.62	15.2 ± 0.41
Glycogen body length	24.2 ± 1.12	23.2 ± 0.65
Glycogen body diameter	12.5 ± 0.53	11.6 ± 0.32
S	0.03 ± 0.01	0.09 ± 0.03
Δρ	8.62 ± 0.56	11.1 ± 1.31

Values are mean ± se of eye structure parameters (μm), optical sensitivity (*S*, μm^2 Sr), and acceptance angle (Δρ, °). Sensitivity and acceptance angle were calculated with equations 2.1 and 2.2, respectively. I tested for differences between light- and dark-acclimated animals with a mixed model, and significant differences ($P < 0.05$) are indicated by an asterisk. Sample sizes were 12 and 10 in light- and dark-acclimated animals, respectively.

3.4 Discussion

In adult *Artemia* spp., exposure to fish kairomones lowered the behavioral threshold, where animals became more sensitive to light as kairomone concentration increased (Fig. 3.2). A similar kairomone effect has been observed in *Artemia* nauplii (Forward and Hettler 1992; Forward and Rittschof 1999) as well as several species of marine crustacean zooplankton (Cohen and Forward 2009). Further, kairomone exposure resulted in left-shifted V – log I curves with lower log K values as well as wider, shorter rhabdoms in the larvae of two marine crab species (Charpentier and Cohen 2015). Both of which indicate increased visual sensitivity in other arthropods (Chamberlain and Barlow 1987; Meyer-Rochow 2001). Below, I compare my electrophysiological and structural results with adult *Artemia* spp. to other crustaceans (namely crab larvae) and discuss how my findings relate to the evolution of nervous systems.

In this study, I measured electrophysiological responses in the retina to assess how kairomones affect visual sensitivity. Previous studies have used similar techniques to compare visual sensitivity across depths, between light- and dark-acclimation, as well as throughout diel cycles, where sensitivity increases during nighttime hours (Meyer-Rochow and Tiang; Aréchiga and Rodriguez-Sosa 1998; Frank 2003). More sensitive eyes produce V – log I curves that are shifted to the left with lower log K values. In support of my original hypothesis, I find some evidence from ERG recordings that kairomones increase visual sensitivity at the photoreceptor level. Specifically, V – log I curves were shifted to the left after exposure to kairomones, regardless of concentration (Fig. 3.3). In addition, log K values were lower in kairomone-exposed animals, likely due a greater slope and shorter dynamic range (Table 3.1). I recognize that these relationships were only significant when limiting my comparison to the control and highest kairomone concentration. Still, my data are consistent with kairomone-induced changes to retinal physiology contributing to amplified photobehavior in adult *Artemia* spp. The observed physiological change is similar to that described in kairomone-exposed crab larvae (Charpentier and Cohen 2015) but significantly smaller than differences reported over diel cycles (e.g. two log units of irradiance; Meyer-Rochow 2001).

Increases in visual sensitivity often come at the cost of temporal resolution (Warrant 1999). When comparing mesopelagic crustaceans, for example, log K values tend to decrease as response latency increases (Frank 2003). Here, however, I find that both visual sensitivity and temporal resolution (i.e. shortened response latency, Fig. 3.4A) increase after kairomone exposure. Both of these changes could be beneficial in predator avoidance, where increased visual sensitivity would result in a greater

daytime depth during DVM and increased temporal resolution would aid in perceiving fast-moving predators, e.g. fish. In crab larvae, peak latency decreased after kairomone exposure (Charpentier and Cohen 2015), possibly due to smaller ERG response magnitude and thereby faster succession to response peak. In contrast, response magnitude was similar between treatments in *Artemia* spp. (Fig. 3.3). Simultaneous increases in visual sensitivity and temporal resolution may be compensated for by decreased spatial resolution (Warrant 1999), although I did not assess this electrophysiologically.

Unlike retinal physiology, kairomone exposure did not impact eye structure, optical sensitivity, or acceptance angle in *Artemia* spp. (Table 3.2). This differs from the previously described findings in crab larvae, suggesting that the mechanism for kairomone-induced photosensitivity diverges slightly between these two crustacean lineages. To validate my results, I compared eye structure after light and dark acclimation, because *Artemia* are known to exhibit structural changes that would increase sensitivity during dark acclimation at nighttime, including widening at the distal tip of the rhabdom, shorter crystalline cones, and elongation of the glycogen body lens (Nilsson and Odselius 1981). Here, I observed similar increases in rhabdom diameter after dark acclimation, but no other structural changes (Table 3.3). Variation between my results and those of previous work are likely due to the time of fixation for dark-acclimated animals, i.e. nighttime (Nilsson and Odselius 1981) versus daytime (this study). Diel changes in eye structure are well documented in marine arthropods (Stowe 1980; Meyer-Rochow 2001; Battelle 2002). In addition, I used females with brood pouches, whereas Nilsson and Odselius used male *Artemia* for their experiments. Regardless, I observed a structural change consistent with previous

work that would increase visual sensitivity in dark-acclimated animals. Hence, I feel confident that my methods were adequate, and conclude that kairomones do not significantly impact eye structure in *Artemia* spp.

As previously mentioned, spatial summation may compensate for increases in visual sensitivity and/or temporal resolution (Warrant 1999). Arthropods accomplish spatial summation by widening acceptance angle (Bryceson and McIntyre 1983; Hariyama et al. 2001) or by neurally pooling visual information (Greiner et al. 2004, 2005; Warrant et al. 2014). My data suggest that kairomones increase both visual sensitivity and temporal resolution in *Artemia* spp. However, acceptance angle did not vary after kairomone exposure (Table 3.2). Hence, further work is needed to determine whether the observed changes are at the cost of spatial resolution and if these crustaceans use similar summation methods as those described in insects (Warrant et al. 2014).

Overall, adult *Artemia* spp. and marine crustacean zooplankton exhibit amplified photobehavior in response to kairomones from marine fish (Cohen and Forward 2009). Here, I observed physiological changes in the retina of *Artemia* spp. that are similar to changes previously described in crab larvae (Charpentier and Cohen 2015 [Chapter 2]). It is possible that similar signaling pathways may contribute to a comparable mechanism for behavioral adjustment in these two crustacean groups, i.e. branchiopods and malacostracans. For example, the inhibitory neurotransmitter, γ-aminobutyric acid (GABA), is required for the onset of fish predator-induced defenses in a freshwater branchiopod (*Daphnia*; Weiss et al. 2012) and for the detection/processing of fish kairomones in a larval malacostracan (*Hemigrapsus sanguineus*, Charpentier and Cohen 2016 [Chapter 4]). However, crab larvae also

exhibited changes in eye structure after kairomone exposure, which were absent in *Artemia* spp. Slight variation in the mechanism by which kairomones induce photosensitivity may be due to differences in neural organization. For example, in malacostracans, chemoreceptor nerve endings are organized into glomeruli within the olfactory lobe of the deutocerebrum (Sandeman et al. 1992; Schmidt 2007). However, these glomeruli appear to be absent in the deutocerebrum of *Artemia* (Harzsch and Glötzner 2002). In addition, brine shrimp lack a third visual neuropil (i.e. medulla interna) and optic chiasmata (Wildt and Harzsch 2002), both of which are present in malacostracans (Strausfeld 1998). A difference in medulla organization is particularly interesting, as the terminal medullae are centers for higher integration of visual and olfactory input in the malacostracan brain (Sandeman et al. 2014). Hence, the integration of visual and chemical cues may vary between malacostracan and branchiopod crustaceans, which could thereby result in a slightly different physiological response to kairomones.

The animals used in this study were hatched from cysts originally collected in Great Salt Lake, Utah, USA. Generally, fish are only found adjacent to a river outlet due to the high salinity of this lake, and are therefore spatially separated from locations of high brine shrimp density (Belovsky et al. 2011). In spring, however, increased freshwater input causes dilution of the lake (i.e. decreased salinity; Price 1985), which could expand the habitat range of fish into locations of high brine shrimp abundance. Notably, this spring diulution also coincides with increased hatching of *Artemia* spp. nauplii (Belovsky et al. 2011). Hence, it is possible that brine shrimp benefit from the described response to fish kairomones in the spring, in both adults (here) and nauplii (Forward and Rittschof 1993). Alternatively, the behavioral

response to amino sugars may serve some, not yet described, purpose, and further work is necessary to describe fish kairomone molecules in endorheic lakes.

Kairomones from fish mucus and/or mimic amino sugar molecules have been shown to increase photosensitivity in crustacean zooplankton from marine and estuarine environments (Forward and Rittschof 2000; Cohen and Forward 2005; Charpentier and Cohen 2015 [Chapter 2]) and endorheic saltwater environments (here; Forward and Rittschof 1999), as well as burrow emergence behavior of a marine polychaete (Schaum et al. 2013). Similar to the observed kairomone-induced photosensitivity, light and amino sugars impact cnidae discharge in cnidarians (Watson and Hessinger 1989a,b; Plachetzki et al. 2012). Hence, even amoungst diverse phyla (e.g. arthropods, annelids, cnidarians), similar cues persist in mediating behaviors that are important to foraging and defense, i.e. diel vertical migration, burrow emergence, and cnidae discharge (Hays 2003; Greenwood 2009). Therefore, defensive behavioral responses to amino sugars reach far beyond crustacean phylogeny. Further study of the characteristics and locations of kairomone receptors (e.g. Weiss et al. 2015) will provide further insight into the evolution of nervous systems.

REFERENCES

Aréchiga, H. and Rodriguez-Sosa, L. (1998). Circadian clock function in isolated eyestalk tissue of crayfish. *Proc. R. Soc. B* 265, 1819–1823.

Bates, D., M. Maechler, B. Bolker, and S. Walker. (2015). Fitting linear mixed-effects models using lme4. J. Stat. Softw. 67, 1–48.

Battelle, B.-A. (2002). Circadian efferent input to Limulus eyes: anatomy, circuitry, and impact. *Microsc. Res. Tech.* 58, 345–55.

Belovsky, G. E., Stephens, D., Perschon, C., Birdsey, P., Paul, D., Naftz, D., Baskin, R., Larson, C., Mellison, C., Luft, J., Mosley, R., Mahon, H., Van Leeuwen, J. and Allen, D. V. (2011). The Great Salt Lake Ecosystem (Utah, USA): long term data and a structural equation approach. *Ecosphere* 2, 33.

Bolker, B.M., M.E. Brooks, C.J. Clark, S.W. Geange, J.R. Poulsen, M.H.H. Stevens, and J-S.S. White. (2008). Generalized linear mixed models: a practical guide for ecology and evolution. *Trends Ecol. Evol.* 24, 127–135.

Bradley, D. J. and Forward, R. B. (1984). Phototaxis of adult brine shrimp, *Artemia salina*. *Can. J. Zool.* 62, 2357–2359.

Bryceson, K. P. and McIntyre, P. (1983). Image quality and acceptance angle in a reflecting superposition. *J. Comp. Physiol. A* 151, 367–380.

Chamberlain, S. C. and Barlow, R. B. (1987). Control of structural rhythms in the lateral eye of Limulus: interactions of natural lighting and circadian efferent activity. *J. Neurosci.* 7, 2135–2144.

Charpentier, C. L. and Cohen, J. H. (2015). Chemical cues from fish heighten visual sensitivity in larval crabs through changes in photoreceptor structure and function. *J. Exp. Biol.* 218, 3381–3390.

Charpentier, C. L. and Cohen, J. H. (2016). Acidification and γ -aminobutyric acid independently alter behaviour. *R. Soc. Open Sci.* 3, 160311.

Cohen, J. H. and Forward, R. B. (2003). Ctenophore kairomones and modified aminosugar disaccharides alter the shadow response in a larval crab. *J. Plankton Res.* 25, 203 – 214.

Cohen, J. H. and Forward, R. B. (2005). Photobehavior as an inducible defense in the marine copepod *Calanopia americana*. *Limnol. Oceanogr.* 50, 1269–1277.

Cohen, J. H. and Forward, R. B. (2009). Zooplankton diel vertical migration - A review of proximate control. *Oceanogr. Mar. Biol. Ann. Rev.* 47, 77–110.

Cronin, T. W. (1986). Optical design and evolutionary adaptation in crustacean compound eyes. *J. Crust. Biol.* 6, 1–23.

Cronin, T. W. and Forward, R. B. (1988). The visual pigments of crabs I. Spectral characteristics. *J. Comp. Physiol. A* 162, 463 –478.

Forward, R. B. and Hettler, W. F. (1992). Effects of feeding and predator exposure on photoresponses during diel vertical migration of brine shrimp larvae. *Limnol. Oceanogr.* 37, 1261–1270.

Forward, R. B. and Rittschof, D. (1993). Activation of photoresponses of brine shrimp nauplii involved in diel vertical migration by chemical cues from fish. *J. Plankton Res.* 15, 693–701.

Forward, R. B. and Rittschof, D. (1999). Brine shrimp larval photoresponses involved in diel vertical migration: Activation by fish mucus and modified amino sugars. *Limnol. Oceanogr.* 44, 1904–1916.

Forward, R.B. and Rittschof, D. (2000). Alteration of photoresponses involved in diel vertical migration of a crab larva by fish mucus and degradation products of mucopolysaccharides. *J. Exp. Mar. Biol. Ecol.* 245, 277–292.

Fox, J. and S. Weisberg. (2011). An R Companion to Applied Regression. Thousand Oaks: Sage.

Frank, T. M. (2003). Effects of Light Adaptation on the Temporal Resolution of Deep-sea Crustaceans. *Integr. Comp. Biol.* 43, 559–70.

Greenwood, P. G. (2009). Acquisition and use of nematocysts by cnidarian predators. *Toxicon* 54, 1065–1070.

Greiner, B., Ribi, W. A, and Warrant, E. J. (2004). Retinal and optical adaptations for nocturnal vision in the halictid bee *Megalopta genalis*. *Cell Tiss. Res.* 316, 377–390.

Greiner, B., Ribi, W. A, and Warrant, E. J. (2005). A neural network to improve dim-light vision? Dendritic fields of first-order interneurons in the nocturnal bee *Megalopta genalis*. *Cell Tiss. Res.* 322, 313–20.

Giddings, E. M. P. and Stephens, D. W. (1999). Selected aquatic biological investigations in the Great Salt Lake basins, 1875-1998, National Water-Quality Assessment Program. *Water-Resources Investigations Report*. Salt Lake City, UT.

Griffith, R. W. (1974). Environment and salinity tolerance in the genus *Fundulus*. *Copeia* 1974, 319–331.

Hader, D.-P. and Tevini, M. (1987). Halobacterium. *In* General Photobiology (pp. 103). Oxford: Pergamon Press.

Hariyama, T., Meyer-rochow, V. B., Kawauchi, T., Takaku, Y., and Tsukahara, Y. (2001). Diurnal changes in retinula cell sensitivities and receptive fields (two-dimensional angular sensitivity functions) in the apposition eyes of *Ligia exotica* (Crustacea, Isopoda). *J. Exp. Biol.* 248, 239–248.

Harzsch, S. and Glötzner, J. (2002). An immunohistochemical study of structure and development of the nervous system in the brine shrimp *Artemia salina* Linnaeus, 1758 (Branchiopoda, Anostraca) with remarks on the evolution of the arthropod brain. *Arthropod Struct. Dev.* 30, 251–270.

Hays, G. C. (2003). A review of the adaptive significance and ecosystem consequences of zooplankton diel vertical migrations. *Hydrobiologia* 503, 163–170.

Land, M. F. (1981). Optics and vision in invertebrates. In *Handbook of Sensory Physiology* Vol. VII/6B (ed. H. Autrum), pp. 471-592. Berlin: Springer.

Lenth, R.V. (2016). Least-squares means: The R package lsmeans. J. Stat. Softw. 69, 1–33.

Lenz, P.H. (1980). Ecology of an alkali adapted variety of *Artemia* from Mono Lake, California, U.S.A., p. 79–96. In *The Brine Shrimp Artemia* (eds. R.A. Browne, P. Sorgeloss, and C.N.A. Trotman), V. 3. Wettere: Universa Press.

Lenz, P. H. and R. A. Browne. (1991). Ecology of *Artemia*. In *Artemia Biology* (eds. R.A. Browne, P. Sorgeloss, and C.N.A. Trotman). Coca Raton: CRC Press.

McKelvey, L.M. (1997). Predator chemical cues mediate zooplankton diel vertical migration. Ph.D. Dissertation, Duke University, Beaufort, NC, USA.

Meyer-Rochow, V. B. and Tiang, K. M. (1984). The eye of *Jasus edwardsii* (Crustacea, Decapod): electrophysiology, histology, and behaviour. *Zoologica* 45, 1–61.

Meyer-Rochow, V. B. (2001). The crustacean eye: Dark/light adaptation, polarization sensitivity, flicker fusion frequency, and photoreceptor damage. *Zool. Sci.* 1197, 1175–1197.

Nilsson, D. and Odselius, R. (1981). A new mechanism for light-dark adaptation in the *Artemia* compound eye (Anostraca, Crustacea). *J. Comp. Physiol. A*, 143, 389–399.

Persoone, G. and Sorgeloos, P. (1980). General aspects of the ecology and biogeography of *Artemia*. In *The Brine Shrimp Artemia* (eds. G. Persoone, P. Sorgeloos, O. Roels, and E. Jaspers), pp. 3–24. Wettere: Universa Press.

Plachetzki, D. C., Fong, C. R., and Oakley, T. H. (2012). Cnidocyte discharge is regulated by light and opsin-mediated phototransduction. *BMC Biol.* 10, 17.

Price, D. (1985). Ground water in Utah's densely populated Wasatch Front area; the challenge and the choices. *U.S. Geological Survey Water Supply Paper* No. 2232.

R Core Team. (2016). R: A language and environment for statistical computing. R Foundation for Statistical Computing, Vienna, Austria. URL http://www.R-project.org/.

Ringelberg, J. (2010). Diel Vertical Migration of Zooplankton in Lakes and Oceans. Dordrecht: Springer.

Rittschof, D., and Cohen, J. H. (2004). Crustacean peptide and peptide-like pheromones and kairomones. *Peptides* 25, 1503–1516.

Sandeman, D. C., Kenning, M., and Harzsch, S. (2014). Adaptive trends in malacostracan brain form and function related to behavior. In *Nervous Systems & Control of Behavior. The Natural History of the Crustacea. 3rd edition.* (eds. C. Derby and M. Thiel), pp. 11–48. Oxford: Oxford University Press.

Sandeman, D., Sandeman, R., Derby, C., and Schmidt, M. (1992). Morphology of the brain of crayfish, crabs, and spiny lobsters: A common nomenclature for homologous structures. *Biol. Bull.* 183, 304–326.

Schaum, C. E., Batty, R., and Last, K. S. (2013). Smelling danger - alarm cue responses in the polychaete *Nereis (Hediste) diversicolor* (Müller, 1776) to potential fish predation. *PloS One* 8, e77431.

Schmidt, M. (2007). The olfactory pathway of decapod crustaceans--an invertebrate model for life-long neurogenesis. *Chem. Senses* 32, 365–84.

Stowe, S. (1980). Effects of illumination changes on rhabdom synthesis in a crab. *J. Comp. Physiol. A* 142, 19–25.

Strausfeld, N. J. (1998). Crustacean-insect relationships: the use of brain characters to derive phylogeny amongst segmented invertebrates. *Brain Behav. Evol.* 52, 186–206.

Warrant, E. J. (1999). Seeing better at night: life style: eye design and the optimum strategy of spatial and temporal summation. *Vis. Res.* 39, 1611–1630.

Warrant, B. E., Oskarsson, M., and Malm, H. (2014). The remarkable visual abilities of nocturnal insects: Neural principles and bioinspired night-vision algorithms. *Proc. IEE* 102, 1411–1426.

Watson, G. M. and Hessinger, D. A. (1989)a. Cnidocytes and adjacent supporting cells form receptor-effector complexes in anemone tentacles. Tissue & Cell *21*: 17–24.

Watson, G. M. and Hessinger, D. A. (1989)b. Cnidocyte mechanoreceptors are tuned to the movements of swimming prey by chemoreceptors. *Science* 243, 1589–1591.

Weiss, L. C., Kruppert, S., Laforsch, C., and Tollrian, R. (2012). *Chaoborus* and *gasterosteus* anti-predator responses in *Daphnia pulex* are mediated by independent cholinergic and gabaergic neuronal signals. *PloS One* 7, e36879.

Weiss, L. C., Leimann, J., and Tollrian, R. (2015). Predator-induced defences in *Daphnia longicephala*: location of kairomone receptors and timeline of sensitive phases to trait formation. *J. Exp. Biol.* 218, 2918–2926.

Wildt, M., and Harzsch, S. (2002). A new look at an old visual system: structure and development of the compound eyes and optic ganglia of the brine shrimp *Artemia salina* Linnaeus, 1758 (Branchiopoda, anostraca). *J. Neurobiol.* 52, 117–132.

Chapter 4

ACIDIFICATION AND γ-AMINOBUTYRIC ACID ALTER KAIROMONE-INDUCED BEHAVIOR IN A LARVAL CRAB

Exposure to high pCO_2 or low pH alters sensation and behavior in many marine animals. I show that crab larvae lose their ability to detect and/or process predator kairomones after exposure to low pH over a timescale relevant to diel pH cycles in coastal environments. Previous work suggests that acidification affects sensation and behavior through altered neural function, specifically the action of γ-aminobutyric acid (GABA), because a GABA antagonist, gabazine, restores the original behavior. Here, however, gabazine resulted in a loss of kairomone detection/processing, regardless of pH. My results also suggest that GABAergic signalling is necessary for kairomone identification in these larvae. Hence, the mechanism for the observed pH effect varies from the original GABA hypothesis. Further, I suggest that this pH effect is adaptive under diel cycling pH.

4.1 Introduction

Anthropogenic CO_2 emissions to the atmosphere are predicted to lower ocean pH by 0.14-0.43 before 2100 (IPCC 2014), as a result of elevated oceanic CO_2 and subsequent changes to the marine carbonate system. Changes of this magnitude can alter sensation and behavior in marine animals. In fact, there has been an outpouring

of literature on this topic over the last several years (Clements and Hunt 2015). To name a few, these elevated CO_2 conditions can inhibit or alter olfaction (Munday et al. 2009; Dixson et al. 2010; Munday et al. 2010; de la Haye et al. 2012), vision (Chung et al. 2014), auditory function (Simpson et al. 2011), lateralization (Domenici et al. 2012; Jutfelt et al. 2013), anti-predator behavior (Bibby et al. 2007; Ferrari et al. 2011), visual risk assessment (Ferrari et al. 2012b), foraging behavior (Cripps et al. 2011; Nowicki et al. 2012; Dodd et al. 2015), shell assessment/homing or settlement ability (de la Haye et al. 2011; Devine et al. 2012a,b), and learning (Ferrari et al. 2012a), in marine fish, crustaceans, and mollusks from both tropical and temperate environments. Such changes may have profound ecological consequences (Nagelkerken et al. 2016). For example, larval reef fish were either attracted to or unable to detect predator odors after exposure to pH levels expected before 2100 (Dixson et al. 2010). Further, mortality due to predation was higher in fish exposed to acidified seawater (Munday et al. 2010).

Nilsson et al. (2012) proposed a neural mechanism to describe pH/CO_2-induced behavioral disruption. Briefly, γ-aminobutyric acid (GABA) is a ubiquitous, inhibitory neurotransmitter. When GABA binds to its ionotropic $GABA_A$ receptor, the receptor opens, and anions (namely chloride, Cl^-) enter the neuron, resulting in hyperpolarization. Following decreases in environmental pH, many marine fish and crustaceans avoid acidosis by accumulating extracellular bicarbonate (HCO_3^-) while depleting/exchanging Cl^- to the external environment (Brauner and Baker 2009; Henry et al. 2012). Decreases in extracellular Cl^- may alter the electrochemical gradient, whereby Cl^- exits the neuron through $GABA_A$ receptors, causing depolarization. In support of this hypothesis, exposure to gabazine, a $GABA_A$ antagonist, eliminates

acidification effects on behavior in both vertebrates and invertebrates (e.g. Nilsson et al. 2012; Watson et al. 2014), though gabazine did not reverse increases in anxiety after exposure to acidified seawater in a juvenile rockfish (Hamilton et al. 2014).

Such changes to animal behavior are often studied in the context of future predictions for ocean acidification (Clements and Hunt 2015). However, present-day diel and tidal fluctuations in pH are common in shallow coastal environments, and are often greater than near-future predictions for global declines in pH (Baumann et al. 2014). Many species of crustacean zooplankton inhabit environments with diel-cycling pH and exhibit behaviors that require integration of multiple sensory modalities. For example, crab larvae maintain depth near an isolume of some lower threshold in light intensity, descending with increases in downwelling light and ascending in darkness due to negative geotaxis (Sulkin 1984). In addition, predator chemical cues or kairomones alter photobehaviors that are important to depth regulation (Cohen and Forward 2009). For instance, kairomones from fish decrease the light intensity needed to elicit descent responses in larvae of the Asian shore crab, *Hemigrapsus sanguineus*. This leads to deeper daytime distributions, and in turn avoidance of predatory fish (Charpentier and Cohen 2015).

Since *H. sanguineus* experience diel fluctuations in pH, these larvae provide an excellent model for assessing the effect of present-day pH changes on behaviors with multisensory integration. With larval *H. sanguineus*, I assessed (1) if decreases in pH (i.e. increases in pCO_2) alter the kairomone effect to photobehavior over a diel/tidal timescale using a behavioral assay with two pH treatments, (2) whether GABAergic signalling plays a role in the kairomone effect with a second assay assessing the dose-response relationship of gabazine to photobehavior, and (3) if my results support

Nilsson et al.'s GABA hypothesis with the above behavioral assays and a comparison of extracellular Cl^- concentrations.

4.2 Methods

4.2.1 Animal collection and rearing

In September of 2014 and 2015, ovigerous female *Hemigrapsus sanguineus* (De Haan 1853) were collected from Roosevelt Inlet, DE, USA. Water temperature ranged from 18 – 23 °C during this time. I kept these females in the laboratory under a 14 h:10 h light:dark cycle at ~ 22 °C in seawater at a salinity of 32 practical salinity units (psu). I used either artificial seawater or local, filtered seawater (described below), and all animals were reared at ambient pH (~ 8.1). On the day of hatching, I moved larvae into fresh seawater and water changes were conducted three times per week. Larvae were fed newly hatched brine shrimp (*Artemia* spp.) nauplii, *ad libitum*.

4.2.2 Behavioral experiments

Behavioral experiments were conducted on third stage *H. sanguineus* larvae in an apparatus that mimics the underwater angular light distribution, using the same setup, procedure, and analysis described in Charpentier and Cohen (2015; Chapter 2). Each experimental group (treatment-*x*-replicate) contained ~ 15 larvae. Animals were dark-acclimated within their respective treatments for 1 – 3 h. I then observed and recorded their responses to 3-s downwelling light stimuli across an intensity range (10^{11} – 10^{13} photons m^{-2} s^{-1}). All experiments were conducted at the same temperature in which animals were reared (22 °C). To compare differences in photosensitivity, I determined 'behavioral thresholds' for each treatment. These thresholds were defined as the lowest light intensity to elicit a descent response, where the percentage of

animals descending (nadir ± 60°) increased after light stimulation. A lower behavioral threshold indicates greater photosensitivity.

To determine behavioral thresholds, I first calculated the percentage descending for each group (replicate-*x*-treatment) before (dark) and after each light stimulus. Within each treatment, I compared this percentage before and after each light stimulus with one-way repeated measures (RM) ANOVAs. Given significant differences in the RM ANOVA ($P < 0.05$), Holm-Šidák *post hoc* tests were used to determine which specific light stimuli evoked a significant descent response, compared to swimming behavior in the dark ($P < 0.05$; *P*-values corrected for multiple comparisons). The light stimulus of the lowest intensity to induce a response was deemed the 'behavioral threshold'. Since two-way ANOVAs within treatments suggested that the percentage of animals descending did not vary between replicates or across light intensities, the mean percentage descending before each light stimulus was used as 'percentage descending in the dark' in the RM ANOVA analyses. All behavioral analyses were conducted in SigmaPlot 12.0 (Systat Software, San Jose, CA, USA).

4.2.2.1 The pH experiment

Using behavioral thresholds, I assessed whether pH affects kairomone-induced photosensitivity and if the mechanism for these effects supports the proposed GABA hypothesis (Nilsson et al. 2012). Prior to the behavioral assay, larvae were held in 4-L glass jars of ambient (8.1) or low (7.6) pH seawater overnight (12 h). This exposure represents the timescale over which diel/tidal pH cycles occur (Baumann et al. 2014). These containers were sealed to reduce exchange of gas or dust particles with the surrounding environment. Temperature and salinity did not change during this

exposure time. Though oxygen was not measured, potential changes to dissolved oxygen would have been minimal (see Appendix A.1.1).

To choose an appropriate pH range, I measured pH at the site of *H. sanguineus* collection, Roosevelt Inlet, Lewes, DE, and reviewed open access pH data from a relevant offshore environment. Further, on July 9th, 2015, I measured pH in Roosevelt Inlet, Lewes, DE at four time points throughout the day (6600-V2 sonde with 6589 Fast-Response pH sensor; YSI Incorporated, Yellow Springs, OH, USA) (Fig. 4.1). This potentiometric electrode measures pH on the NBS scale. I recognize that this method is not ideal for measurement of seawater pH (Dickson 1993; Riebesell et al. 2010). However, when comparing pH values during the behavioral experiment, the percent error between pH measured on the NBS scale and the total pH scale (pH_T; described in further detail below) was < 2%. The ambient treatment reflects daytime pH values found on the continental shelf of the mid-Atlantic (7.9-8.1; Barbero et al. 2016), where *H. sanguineus* spend much of their larval development (Epifanio et al. 2013). I chose a low pH of 7.6 to exemplify the minimum pH these animals may experience during embryonic development, transport, and diel changes in pH in this coastal environment at present day (Fig. 4.1; Barbero et al. 2016). However, *H. sanguineus* may be exposed to pH conditions below the current minimum under future ocean acidification (IPCC 2014). Seawater was regulated to pH 7.6 in a pH/CO_2 stat system, described below.

I randomly selected 10 individuals from each pH treatment and found no difference in heart rate before and after the 12 h pH exposure ($t(7) = 0.8$, $P = 0.4$; t-test), suggesting that there were no apparent differences in physiological condition between pH treatments prior to behavioral assays. After 12 h of exposure, larvae from

both pH treatments were additionally exposed to the control, kairomones, gabazine (10 µ*M;* SR-95531; Sigma-Aldrich, St. Louis, MO, USA), and kairomones with gabazine for 1 – 3 h before I conducted assays to determine behavioral thresholds for each treatment. This pH experiment was replicated five times. Throughout the experiment, larvae were maintained in their respective pH treatments, where the 'control' signifies no addition of kairomones or gabazine.

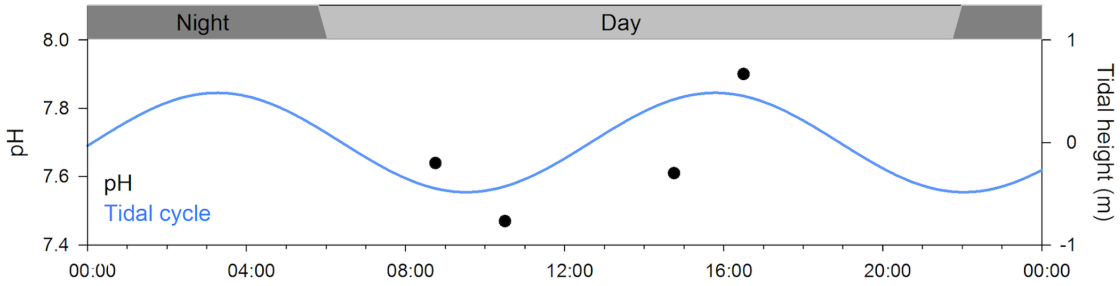

Figure 4.1: Tidal and diel pH cycles. Time series of pH (black), tidal height (m above mean lower low water, blue), and day (light grey) versus night (dark grey), measured on July 9th, 2015 in Roosevelt Inlet, DE, USA, adjacent to collection site, with a Sonde (6600-V2; YSI Incorporated, Yellow Springs, OH, USA).

Kairomone solutions were made with fish mucus, isolated from *Fundulus heteroclitus* as previously described (Forward and Rittschoff 1999) and diluted to 0.1 g mucus L^{-1} seawater. Preliminary experiments indicated that 10-µ*M* gabazine had no effect on heart rate or survival ($t(8) = 0.1$, $P = 0.9$; t-test), suggesting that gabazine at this concentration was not toxic to these crab larvae. Further, I chose to use gabazine to inhibit GABAergic signaling in this study, because (1) gabazine has effectively reversed the effects of acidification in both vertebrates and invertebrates (e.g. Nilsson et al. 2012; Watson et al. 2014) and (2) gabazine functions as a competitive antagonist

in other arthropods, e.g. fruitfly, *Drosophila* (Hosie and Sattelle 1996) and locust, *Locusta migratoria* (Janssen et al. 2010) and in an aquatic invertebrate, *Hydra vulgaris* (Concas et al. 1998; Pierobon et al. 2004).

4.2.2.2 The gabazine dose-response experiment

I conducted a kairomone/gabazine dose-response experiment to better determine the role of GABAergic signalling in the kairomone effect to photobehavior. Larvae in ambient pH were exposed to the control, kairomones, gabazine-only (10 μ*M*), or kairomones with gabazine at three concentrations (10, 1, 0.1 μ*M*) for 1 – 3 h. As before, I determined behavioral thresholds for each treatment, and this dose-response experiment was replicated five times.

4.2.3 Analysis of extracellular fluid

Following the pH experiment, individuals (n ~ 30) from ambient and low pH treatments were blotted dry and homogenized with a micropestle. I extracted extracellular fluid (ECF) with a syringe. These samples were diluted 1:5000 with eluent buffer (3.2-m*M* sodium carbonate, 1.0-m*M* sodium bicarbonate, 6.5% v/v acetone), filtered (0.2 μm), and stored at 4°C for subsequent analysis of ECF Cl^- by anion chromatography (Metrohm AG, Herisau, Switzerland). I compared Cl^- concentrations between animals exposed to ambient and low pH with a t-test, and results were deemed significant if $P < 0.05$. This analysis was conducted in R (R Core Team, 2015, Vienna, Austria).

To better understand the pH effect on electrochemical gradients, I also conducted a separate experiment with paired measurements of extracellular fluid (ECF) Cl^- and osmolality. At least one day post-hatching, stage 1 *H. sanguineus* larvae

were placed in artificial seawater with a salinity of 15, 30, or 40 psu at ambient pH or a salinity of 30 psu at low pH. After 24 h of exposure, ECF was exacted from groups of ~ 40 individuals in each treatment. After extraction, I measured ECF osmolality on a vapor pressure osmometer (Vapro 5600, ELITech Group, Puteaux, France) and chloride (Cl^-) with ion chromatography, as described above. This paired experiment was repeated twice. Samples were diluted prior to analysis, and I corrected for this dilution. Perhaps due to my method of extraction, values for both osmolality and Cl^- appeared lower than expected (Anger et al. 2008). Hence, I also multiplied all values by a common factor (1.99) to reach expected values, nearly isosmotic to seawater (Anger et al. 2008). These corrections had no effect on the outcome of my statistical comparisons (see Appendix A.1.2), and all samples were extracted, measured, and analyzed in the same fashion. Here, I report corrected values of osmolality and Cl^- for both the pH and paired experiment. Contrary to the behavioral experiments, I used first-stage zoeae in this chloride-osmolality analysis to increase the ECF sample volume, as some broods experience high mortality over larval development (e.g. due to maternal effects; Giménez and Anger 2003). Since zoeae are osmoconformers at both beginning and intermediate stages of development (Anger et al. 2008), the use of younger zoeae should not change my interpretation.

4.2.4 Seawater chemistry

In all experiments, I controlled for the presence of kairomones. Further, in the pH experiment, seawater for rearing and both pH treatments was artificial seawater (Instant Ocean, Spectrum Brands, Blacksburg, VA, USA). In the gabazine dose-response experiment, however, seawater for rearing and experiments was collected from Indian River Inlet, Delaware, USA. Biologically active molecules were removed

by ultrafiltration at 100 kDa (GE Life Sciences UFP- 100-C-5A) and ageing in darkness for > 1 week (Forward and Rittschof 1999). I chose to use artificial seawater for the pH experiment because I regulated pH in a laboratory setup that operates with artificial seawater exclusively.

In the pH experiment, the low pH treatment was regulated to pH 7.6 with a pH/CO_2 stat system, which consisted of a custom program in LabVIEW (National Instruments, Austin, TX, USA) that communicated to a relay board to activate flow of CO_2 and CO_2-scrubbed air, given feedback from a differential pH electrode (Hach Company, Loveland, CO, USA). Air bubbled directly into a sump, and water was retrieved from this sump for experiments. Due to spatial and temporal constraints, the ambient pH was not regulated with the described pH/CO_2 stat system. However, I used the same salinity and artificial seawater mix in both to obtain similar carbonate parameters. Before and after pH exposure, I made pH measurements with a combination electrode (Thermo Fisher Scientific, Inc, Beverly, MA, USA) using the NBS scale. Within the sealed containers, I found that pH increased slightly during exposure time in the low pH treatment (~ 0.1), but this increase was consistent across replicates. As stated previously, I understand that pH measurements with potentiometric electrodes on the NBS scale are not ideal for measuring seawater pH (Dickson 1993; Riebesell et al. 2010). Hence, I report the ambient and low pH treatments on the total pH scale (pH_T), calculated from measured values of dissolved inorganic carbon (DIC) and total alkalinity (TA), described below.

At the time of exposure, seawater samples were fixed with saturated mercury bichloride (Cai and Wang 1998; Jiang et al. 2008) and stored at 4 °C for future analysis. Total alkalinity (TA) was analysed by Gran titration (Gran 1952), using the

open-cell method with a semi-automatic titration system (Apollo Scitech, LLC, Newark, DE, USA; Cai et al. 2010; Huang et al. 2012). To determine the concentration of dissolved inorganic carbon (DIC), samples were acidified with phosphoric acid, and the quantity of extracted CO_2 gas was then measured with an infrared gas analyzer (Apollo Scitech, LLC). Both TA and DIC measurements were taken at a precision level of about 2 μmol kg^{-1} (Huang et al. 2012) and calibrated against a certified reference material (provided by A.G. Dickson, Scripps Institution of Oceanography). Values for pCO_2 (μatm) and pH_T were calculated with the Excel MACRO CO2Sys developed by Pierrot et al. (2006) with $[B]_T$ from Uppstrom (1974), k1, k2 from Mehrbach et al. (1973) and Dickson and Millero (1987), and Ks from Dickson (1990; Table 4.1). Though values of TA are higher than would be expected at a salinity of 32 in the ambient pH treatment (Table 4.1), my pH calculations and results should not be affected by this difference (details in Appendix A.1.3).

Table 4.1: Parameters of the carbonate system during experiments

	Ambient	Low
pH_T	8.1 ± 0.06	7.6 ± 0.01
pCO_2 (μatm)	461 ± 97	1380 ± 30
TA (μmol kg^{-1})	3021 ± 85	2546 ± 17
DIC (μmol kg^{-1})	2612 ± 86	2448 ± 13

Values are means ± s.e. Dissolved inorganic carbon and total alkalinity are represented by DIC and TA, respectively. Calculation of P_{CO_2} and pH_T was made using the Excel MACRO CO2Sys developed by Pierrot et al. (2006), with $[B]_T$ from Uppstrom (1974), k1, k2 from Mehrbach et al. (1973) and Dickson and Millero (1987), and Ks from Dickson (1990). Temperature and salinity were 22 °C and 32, respectively, in both pH treatments.

4.3 Results and Discussion

I assessed the effect of pH and the role of GABAergic signalling in kairomone-induced changes to photobehavior by comparing the behavioral threshold, i.e. the lowest light intensity to elicit a descent response, between pH and kairomone/gabazine treatments. For all treatments in the pH experiment, percentage descending was greater after light stimulation than in darkness ($F(6,7) = 2.6\text{-}11.2$, $P < 0.04$; one-way RM ANOVA). Under ambient pH conditions (~8.1), the behavioral threshold of kairomone-exposed larvae was 1.28×10^{12} photons m^{-2} s^{-1} ($P = 0.03$; Holm-Šidák *post hoc* test), nearly two times less than those not exposed to kairomones (2.55×10^{12} photons m^{-2} s^{-1}; $P = 0.006$; Fig. 4.2*a*). All those in low pH had the same threshold as the ambient control ($P < 0.01$; Fig. 4.2*b*). Hence, exposure to acidified seawater removed kairomone-induced photosensitivity in *H. sanguineus*. Past studies attribute similar changes in behavior and sensation to increases in CO_2, reviewed in Clements and Hunt (2015). Given differences in carbonate chemistry between pH treatments (Table 4.1), I cannot isolate which particular carbonate parameter(s) may be driving these changes. Further, addition of gabazine with and without kairomones also resulted in the same threshold as the control, regardless of pH ($P < 0.04$; Fig. 4.2*c*,*d*). Previous work suggests that such changes to behavior are due to disrupted function of GABAergic signalling, because gabazine restored the loss of behavioral function in both vertebrates and invertebrates (e.g. Nilsson et al. 2012; Watson et al. 2014). Here, however, inhibiting $GABA_A$ receptors at low pH did not restore the 'normal' kairomone effect, suggesting that the observed pH effect is mediated by a different mechanism. Hamilton et al. (2014) similarly found that gabazine did not reverse increases in anxiety after exposure to acidified seawater in a juvenile fish. However, a GABA agonist, muscimol, added to increases in anxiety at low pH. Since muscimol is

known to decrease anxiety (Rodgers and Dalvi 1997), changes to the 'normal' function of this agonist ultimately support Nilsson et al.'s hypothesis of reversed function of $GABA_A$ receptors in acidified conditions. Naturally, further work examining the effects of muscimol on behavior would offer greater certainty in confirming or contradicting Nilsson et al.'s hypothesis.

To better understand the role of GABAergic signalling in kairomone-induced photosensitivity, I assessed the effect of gabazine across a concentration gradient at ambient pH in a dose-response experiment. Again, percentage descending was greater after light stimulation than in darkness ($F(5,6) = 8.0\text{-}17.8$, $P < 0.001$, one-way RM ANOVA. Here, the behavioral threshold was lower in larvae exposed to kairomones ($P = 0.013$; Holm-Šidák *post hoc* test) and kairomones with gabazine at the lowest concentration (0.1 μ*M*; $P = 0.017$), compared to those exposed to the control, gabazine-only, and kairomones with gabazine at higher concentrations (10, 1 μ*M;* $P < 0.02$; Table 4.2). As in the pH experiment, gabazine resulted in a loss of kairomone-induced photosensitivity. In this dose-response experiment, I also find that the effect of gabazine decreased with concentration, suggesting that GABAergic signalling is required to induce the 'normal' kairomone effect. Since swimming behavior did not differ between control and gabazine treatments, GABAergic signalling likely plays a role in kairomone detection and/or processing. In the spiny lobster, *Panulirus argus*, opening of $GABA_A$ receptors induced presynaptic inhibition of olfactory receptor neurons that regulate input to the central nervous system (Wachowiak et al. 2002). Perhaps, *H. sanguineus* lose a similar regulatory step after exposure to gabazine or low pH.

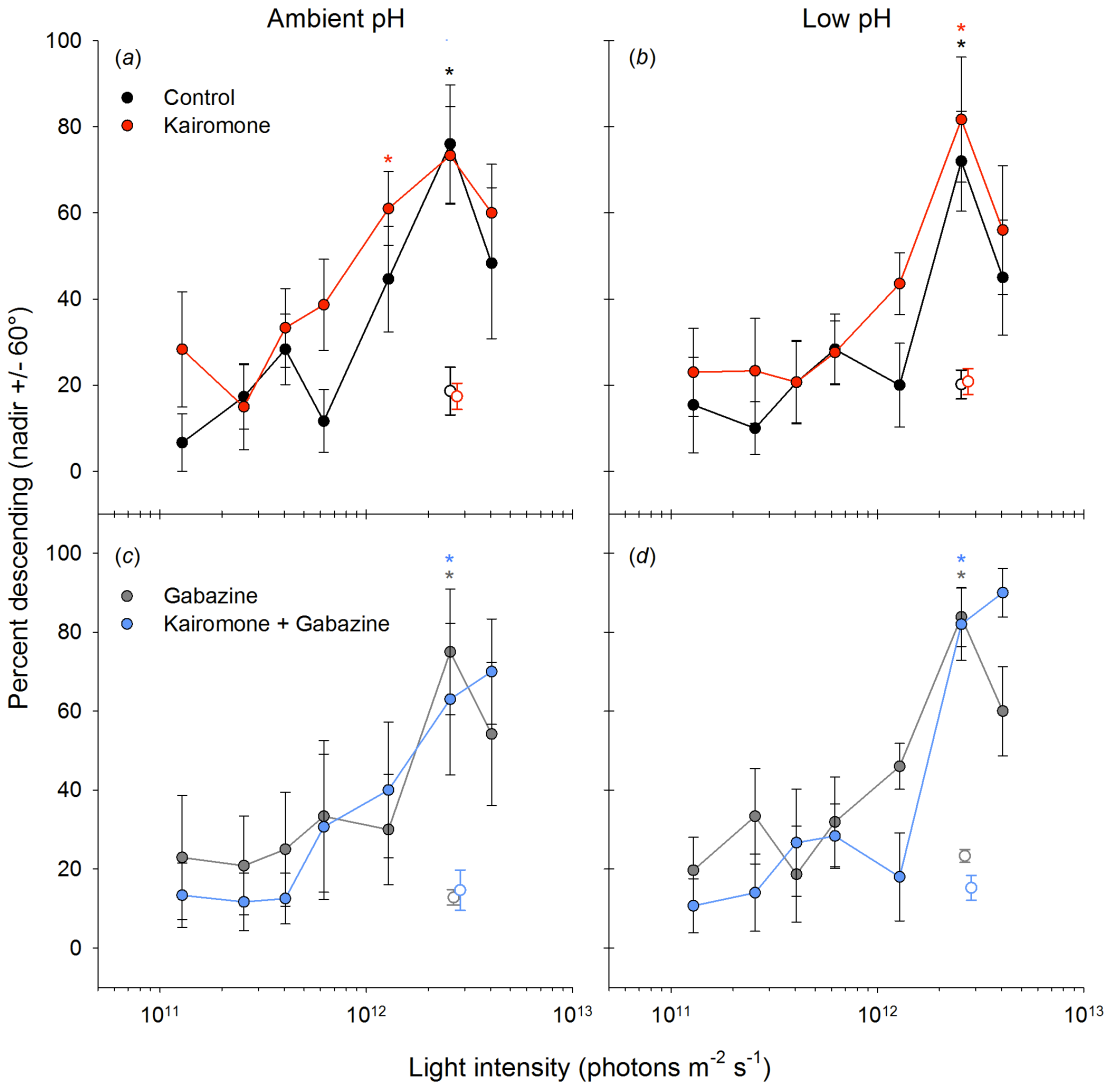

Figure 4.2: Effect of pH on kairomone-induced photosensitivity. Mean ± se percent descending of larval *Hemigrapsus sanguineus* in darkness (unfilled) and after exposure to downwelling light (filled). Before experiments, animals were exposed to (*a*,*c*) ambient pH or (*b*,*d*) low pH, and to control (black), gabazine-only (10 μ*M*, gray), kairomones (red), or kairomones with gabazine (blue). Behavioral thresholds, or light intensity that elicits a descent response, are indicated with asterisks and were determined by one-way RM ANOVAs with Holm-Šidák *post hoc* tests ($P < 0.05$; n = 5 replicates with ~ 15 larvae per replicate, except n = 4 replicates in ambient, gabazine-only treatment).

Table 4.2: Effect of gabazine on kairomone-induced photosensitivity of stage 3 *Hemigrapsus sanguineus* larvae

	Behavioral threshold (photons m^{-2} s^{-1})
Control	6.52×10^{11}
Kairomones	4.10×10^{11}
Gabazine (10 μ*M*)	6.52×10^{11}
Kairomones + Gababzine (10 μ*M*)	6.52×10^{11}
Kairomones + Gababzine (1 μ*M*)	6.52×10^{11}
Kairomones + Gababzine (0.1 μ*M*)	4.10×10^{11}

Behavioral thresholds were determined by one-way RM ANOVAs with Holm-Šidák *post hoc* tests, comparing percentage descending before and after exposure to a range of light intensities (n = 5 replicates, ~ 15 larvae per replicate), conducted at ambient pH (~8.1).

Nilsson et al. (2012) hypothesized that altered behavior and neural function at low pH is due to changes in the electrochemical gradient during an acid disturbance, namely accumulation of HCO_3^- that is compensated by reduced extracellular Cl^-. Contrary to this hypothesis, extracellular Cl^- did not vary between larvae exposed to ambient or low pH, with mean ± se concentrations of 292 ± 63 and 282 ± 94 m*M*, respectively (n = 5; t-test, t(8) = 0.08, *P* = 0.9). In an additional paired chloride-osmolality analysis, both Cl^- and osmolality increased with seawater salinity. Again, Cl^- was similar between the two pH treatments. Though the small sample size (n = 2) inhibited robust statistical analysis, osmolality appeared higher at low pH (Table 4.3), suggesting an increase of other osmolytes, which could include HCO_3^-. In addition to Cl^-, $GABA_A$ receptors have a lesser affinity for HCO_3^- (Lambert and Grover 1995). Hence, it is possible that the observed pH effect is due to changes in GABAergic signalling during acid-base regulation. However, my behavioral results suggest that the exact mechanism differs from that proposed by Nilsson et al. (2012). Alternatively,

ion regulation may vary significantly in larval crabs, relative to Nilsson et al.'s fish-based hypothesis. For instance, extracellular Cl^- increased after exposure to acidified seawater in a hermit crab (de la Haye et al. 2012). Though, I used gabazine concentrations far below known thresholds for toxicity in another crustacean zooplankter (*Daphnia*; Barry 2002) and I found no difference in heart rate or mortality after gabazine exposure, I cannot entirely eliminate the possibility that gabazine may be acting as an olfactory toxin in these larval crabs. In addition, I recognize the possibility that the effect or even toxicity of gabazine may have varied between seawater types in the pH and dose-response experiment (artificial and filtered seawater, respectively). However, this is unlikely, as I observed similar responses to gabazine (10 μ*M*) at ambient pH in both.

Table 4.3: Osmolality (mOsm kg^{-1}) and Cl^- concentration ($[Cl^-]$, m*M*) in extracellular fluid (ECF) of stage 1 *Hemigrapsus sanguineus* larvae after exposure to various salinities

Seawater			ECF	
pH	Salinity	Osmolality	Osmolality	$[Cl^-]$
8.1	15	307 ± 38	260 ± 60	229 ± 40
8.1	30	680 ± 36	700 ± 200	292 ± 90
8.1	40	907 ± 67	1069 ± 160	304 ± 89
7.6	30	704 ± 69	1059 ± 70	289 ± 81

Values shown are means (± se; n = 2).

To date, most studies assess the effects of CO_2 and/or pH on behavior in the context of future global ocean acidification (Clements and Hunt 2015). However, in estuarine and coastal habitats, present-day pH fluctuations are influenced by biological activity, where pH generally decreases at night and increases during the day (Kemp and Boynton 1980). I found a similar pattern at my *H. sanguineus* collection site (Fig.

4.1), and the observed pH effects to behavior occurred over a timescale similar to these cycles. Since my pH measurements were taken over the course of one day with fair weather, I recognize that pH cycles may also vary over small and large spatial scales and fluctuate due to processes other than biological activity (e.g. river and groundwater input; Bauer et al. 2013). Still, I propose that the observed pH effect on larval crab behavior may be adaptive. Larval crabs maintain depth near an isolume defined by their threshold for light detection (Sulkin 1984), and larvae become more photosensitive after kairomone exposure. Such behaviors contribute to diel vertical migration, a long-proposed strategy for avoidance of visual predators (Cohen and Forward 2009). When pH is highest (daytime), larvae would be most sensitive to kairomones, migrating into deeper, darker water when the threat of visual predators is greatest. Kairomone-induced changes to photobehavior are thought to result in some cost, e.g. separation from food (Ringelberg 2010), therefore losing the kairomone effect during times of least danger (nighttime, when pH is lowest) would provide larvae with an adaptive advantage.

4.4 Conclusion

In this study, I assessed if decreases in pH alter the kairomone effect to zooplankton photobehavior over a diel/tidal timescale and whether altered function of $GABA_A$ receptors during acid-base regulation were the mechanism for this change. I found that exposure to low pH removed the kairomone effect to photobehavior, suggesting that pH inhibits kairomone detection and/or processing over these timescales. Further, GABAergic signalling likely plays a role in detection/processing of kairomones, as addition of gabazine at ambient pH also removed the kairomone effect to photobehavior and this removal was dependent upon gabazine concentration.

Unlike Nilsson et al.'s GABA hypothesis, however, gabazine did not restore this pH effect and extracellular Cl^- concentrations did not vary between the ambient and low pH treatments. Hence, my results suggest that changes in Cl^- transport through the $GABA_A$ receptor may not be the sole mechanism for pH effects to sensation and behavior. Further, acidification and GABAergic signaling independently altered the 'normal' kairomone effect to photobehavior in these zooplankton. Contrary to previous studies, which focused on the deleterious effects of pH in the context of future global ocean acidification, I suggest that the loss of this kairomone effect after exposure to low pH may actually be adaptive in zooplankton that experience present-day diel fluctuations in pH, common in coastal environments.

REFERENCES

Anger, K., Torres, G., Charmantier-Daures, M., and Charmantier, G. (2008). Adaptive diversity in congeneric coastal crabs: Ontogenetic patterns of osmoregulation match life-history strategies in *Armases* spp (Decapoda, Sesarmidae). *J. Exp. Mar. Biol. Ecol*. 367, 28–36.

Barbero, L., Wanninkhof, R., Pierrot, D., Melrose, D. C., and Taylor, C. (2016). Dissolved inorganic carbon, total alkalinity, pH, and other variables collected from surface discrete observations using spectrophotometer and other instruments from R/V Henry B. Bigelow off the northeastern coast of the United States from 2014-09-10 to 2014-11-05 (NCEI Accession 0138983). Version 1.1. NOAA National Centers for Environmental Information. Dataset. [2016-07-19]

Barry, M. J. (2002). Progress toward understanding the neurophysiological basis of predator-induced morphology in *Daphnia pulex*. *Physiol. Biochem. Zool.* 75, 179–86.

Bauer, J. E., Cai, W. J., Raymond, P. A., Bianchi, T. S., Hopkinson, C. S., and Regnier, P. A. G. (2013). The changing carbon cycle of the coastal ocean. *Nature* 504, 61–70.

Baumann, H., Wallace, R. B., Tagliaferri, T., and Gobler, C. J. (2014). Large natural pH, CO_2 and O_2 fluctuations in a temperate tidal salt marsh on diel, seasonal, and interannual time scales. *Estuar. Coast.* 38, 220–231.

Bibby, R., Cleall-Harding, P., Rundle, S., Widdicombe, S., and Spicer, J. (2007). Ocean acidification disrupts induced defences in the intertidal gastropod *Littorina littorea*. *Biol. Lett.* 3, 699–701.

Brauner, C. J. and Barker D. W. (2009). Patterns of acid-base regulation during exposure to hypercarbia in fishes. In *Cardio-respiratory control in vertebrates* (eds. M. L. Glass, S. C. Wood), pp 43–63. Berlin, Germany: Springer-Verlag.

Cai W. J. and Wang Y. (1998). The chemistry, fluxes, and sources of carbon dioxide in the estuarine waters of the Satilla and Altamaha Rivers, Georgia. *Limnol. Oceanogr*. 43, 657–668.

Cai, W. J., Hu, X., Huang, W. J., Jiang, L. Q., Wang, Y., Peng, T. H., and Zhang, X. (2010). Alkalinity distribution in the western North Atlantic Ocean margins. *J. Geophys. Res-Oceans* 115, 1–15.

Charpentier, C. L. and Cohen, J. H. (2015). Chemical cues from fish heighten visual sensitivity in larval crabs through changes in photoreceptor structure and function. *J. Exp. Biol.* 218, 3381–3390.

Chung, W. S., Marshall, N. J., Watson, S. A., Munday, P. L., and Nilsson, G. E. (2014). Ocean acidification slows retinal function in a damselfish through interference with $GABA_A$ receptors. *J. Exp. Biol.* 217, 323–326.

Concas, A., Pierobon, P., Mostallino, M. C., Porcu, P., Marino, G., Minei, R., and Biggio, G. (1998). Modulation of gamma-aminobutyric acid (GABA) receptors and the feeding response by neurosteroids in *Hydra vulgaris*. *Neurosci.* 85, 979–988.

Cohen, J. H. and Forward, R. B. (2009). Zooplankton diel vertical migration – a review of proximate control. *Oceanogr. Mar. Biol.* 47, 77–110.

Clements, J. C. and Hunt, H. L. (2015). Marine animal behavior in a high CO_2 ocean. *Mar. Ecol. Prog. Ser*. 536, 259–279.

Cripps, I. L., Munday, P. L., and McCormick, M. I. (2011). Ocean acidification affects prey detection by a predatory reef fish. *PLoS ONE* 6, e22736

de la Haye, K. L., Spicer, J. I., Widdicombe, S., and Briffa, M. (2011). Reduced sea water pH disrupts resource assessment and decision making in the hermit crab *Pagurus bernhardus*. *Anim. Behav.* 82, 495–501.

de la Haye, K.L., Spicer, J. I., Widdicombe, S., and Briffa, M. (2012). Reduced pH sea water disrupts chemo-responsive behavior in an intertidal crustacean. *J. Exp. Mar. Biol. Ecol.* 412, 134–140.

Devine, B.M., Munday, P.L., and Jones, G.P. (2012a). Homing ability of adult cardinalfish is affected by elevated carbon dioxide. *Oecol*. 168, 269–276.

Devine, B. M., Munday, P.L., and Jones, G.P. (2012). Rising CO_2 concentrations affect settlement behavior of larval damselfishes. *Coral Reefs* 31, 229–238.

Dickson, A. G. (1990). Standard potential of the reaction: $AgCl(s) + 1/2H_2(g) = Ag(s) + HCl(aq)$, and the standard acidity constant of the ion HSO_4 in synthetic sea water from 273.15 to 318.15 K. *J. Chem. Thermodyn.* 22, 113-127.

Dickson, A. G. (1993). The measurement of sea water pH. *Mar. Chem.* 44, 131-142.

Dickson, A. G., Millero, F. J. (1987). A comparison of the equilibrium constants for the dissociation of carbonic acid in seawater media. *Deep-Sea Res.* 34, 1733–1743.

Dixson, D. L., Munday, P. L., and Jones, G. P. (2010). Ocean acidification disrupts the innate ability of fish to detect predator olfactory cues. *Ecol. Lett.* 13, 68–75.

Dodd, L. F., Grabowski, J. H., Piehler, M. F., Westfield, I., and Ries, J. B. (2015). Ocean acidification impairs crab foraging behavior. *Proc. R. Soc. B* 282, 20150333.

Domenici, P., Allan, B., McCormick, M. I., and Munday, P. L. (2012). Elevated carbon dioxide affects behavioral lateralization in a coral reef fish. *Biol. Lett.* 8, 78–81.

Epifanio, C. E., Tilburg, C. E., and Dittel, A. I. (2013). Abundance of invasive and native crab larvae in the mouth of Delaware Bay: *Hemigrapsus sanguineus* and *Uca Pugnax*. *J. Shellfish Res.* 32, 543–550.

Ferrari, M. C. O., McCormick, M. I., Munday, P. L., Meekan, M. G, Dixson, D. L., Lonnstedt, Ö., and Chivers, D. P. (2011). Putting prey and predator into the CO_2 equation--qualitative and quantitative effects of ocean acidification on predator-prey interactions. *Ecol. Lett.* 14, 1143–1148.

Ferrari, M. C. O., Manassa, R. P., Dixson, D. L., Munday, P. L., McCormick, M. I., Meekan, M. G., Sih, A., and Chivers, D. P. (2012). Effects of Ocean Acidification on Learning in Coral Reef Fishes. *PLoS ONE* 7, e31478.

Ferrari, M. C. O., Mccormick, M. I., Munday, P. L., Meekan, M. G., Dixson, D. L., Lonnstedt, Ö., and Chivers, D. P. (2012). Effects of ocean acidification on visual risk assessment in coral reef fishes. *Funct. Ecol.* 26, 553–558.

Forward, R. B. and Rittschof, D. (1999). Brine shrimp larval photoresponses involved in diel vertical migration: activation by fish mucus and modified amino sugars. *Limnol. Oceanogr.* 44, 1904-1916.

Giménez, L. and Anger, K. (2003). Larval performance in an estuarine crab, *Chasmagnathus granulata*, is a consequence of both larval and embryonic experience. *Mar. Ecol. Prog. Ser.* 249, 251–264.

Gran, G. (1952). Determination of the equivalence point in potentiometric titrations Part II. *Analyst* 77, 661–671.

Hamilton, T.J., Holcombe, A., and Tresguerres, M. (2014). CO_2 -induced ocean acidification increases anxiety in Rockfish via alteration of $GABA_A$ receptor functioning CO_2-induced ocean acidification increases anxiety in Rockfish via alteration of $GABA_A$ receptor functioning. *Proc. R. Soc. B* 281, 20132509.

Henry, R. P., Lucu, C., Onken, H., and Weihrauch, D. (2012). Multiple functions of the crustacean gill: osmotic/ionic regulation, acid-base balance, ammonia excretion, and bioaccumulation of toxic metals. *Front. Physiol.* 3, 1-3.

Hosie, A. M. and Sattelle, D. B. (1996). Agonist pharmacology of two Drosophila GABA receptor splice variants. *Br. J. Pharmacol*. 119, 1577–1585.

Huang, W. J., Wang, Y., and Cai, W. J. (2012). Assessment of sample storage techniques for total alkalinity and dissolved inorganic carbon in seawater, *Limnol. Oceanogr.-Meth*. 10, 711–717.

IPCC. (2014). The ocean. *Climate Change 2014: Impacts, Adaptation, and Vulnerability. Part B: Regional Aspects. Contribution of Working Group II to the Fifth Assessment Report of the Intergovernmental Panel on Climate Change* (eds VR Barros et al.), pp 1655-1731. Cambridge, United Kingdom and New York, NY, USA: Cambridge University Press.

Janssen, D., Derst, C., Rigo, J. M., and Van Kerkhove, E. (2010). Cys-Loop Ligand-Gated Chloride Channels in Dorsal Unpaired Median Neurons of *Locusta migratoria*. *J. Neurophysiol.* 103, 2587–2598.

Jiang, L. Q., Cai, W. J., and Wang, Y. (2008). A comparative study of carbon dioxide degassing in river- and marine-dominated estuaries. *Limnol. Oceanogr*. 53, 2603–2615.

Jutfelt, F., Bresolin de Souza, K., Vuylsteke, A., and Sturve, J. (2013). Behavioral disturbances in a temperate fish exposed to sustained high-CO_2 levels. *PLoS ONE* 8, 1–7.

Kemp, W. M. and Boynton, W. R. (1980). Influence of biological and physical processes on dissolved oxygen dynamics in an estuarine system: Implications for measurement of community metabolism. *Estuar. Coast. Mar. Sci.* 11, 407–431.

Lambert, N. and Grover, L. (1995). The mechanism of biphasic GABA responses. *Science* 269, 928–929.

Mehrbach, C., Culberson, C. H., Hawley, J. E., and Pytkowicz, R. M. (1973). Measurement of the apparent dissociation constants of carbonic acid in seawater at atmospheric pressure, *Limnol. Oceanogr*. 18, 897–907.

Munday, P. L., Dixson, D. L., Donelson, J. M., Jones, G. P., Pratchett, M. S., Devitsina, G. V., and Døving, B. (2009). Ocean acidification impairs olfactory discrimination and homing ability of a marine fish. *Proc. Natl. Acad. Sci. U.S.A.* 106, 1848–1852.

Munday, P. L., Dixson, D. L., McCormick, M. I., Meekan, M., Ferrari, M. C. O., and Chivers, D. P. (2010). Replenishment of fish populations is threatened by ocean acidification. *Proc. Natl. Acad. Sci. U.S.A.* 107, 12930–12934.

Nagelkerken, I. and Munday, P. L. (2016). Animal behavior shapes the ecological effects of ocean acidification and warming: Moving from individual to community-level responses. *Global Change Biol.* 22, 974–989.

Nilsson, G. E., Dixson, D. L., Domenici, P., McCormick, M. I., Sørensen, C., Watson, S. A., and Munday, P. L. (2012). Near-future carbon dioxide levels alter fish behavior by interfering with neurotransmitter function. *Nature Clim. Change* 2, 201–204.

Nowicki, J. P., Miller, G. M., and Munday, P. L. (2012). Interactive effects of elevated temperature and CO_2 on foraging behavior of juvenile coral reef fish. *J. Exp. Mar. Biol. Ecol.* 412, 46–51.

Pierobon, P., Tino, A., Minei, R., and Marino, G. (2004). Different roles of GABA and glycine in the modulation of chemosensory responses in *Hydra vulgaris* (Cnidaria, Hydrozoa). *Hydrobiol.* 530/531, 59–66.

Pierrot, D. E., Lewis, and Wallace, D. W. R. (2006). MS Excel Program Developed for CO_2 System Calculations. ORNL/CDIAC-105a. *Carbon Dioxide Information Analysis Center*, Oak Ridge National Laboratory, U.S. Department of Energy, Oak Ridge, Tennessee.

Riebesell, U., Fabry, V. J., Hansson, L., and Gattuso, J. P. (2010). Guide to Best Practices for Ocean Acidification Research and Data Reporting. Luxembourg: Publications Office of the European Union.

Ringelberg, J. (2010). *Diel vertical migration of zooplankton in lakes and oceans*. Dordrecht, Holland: Springer.

Rodgers, R. J. and Dalvi, A. (1997). Anxiety, defence and the elevated plus-maze. *Neurosci. Biobehav. Rev.* 21, 801–810.

Simpson, S. D., Munday, P. L., Wittenrich, M. L., Manassa, R., Dixson, D. L., Gagliano, M., and Yan, H. Y. (2011). Ocean acidification erodes crucial auditory behavior in a marine fish. *Biol. Lett.* 7, 917–920.

Sulkin, S. (1984). Behavioral basis of depth regulation in the larvae of brachyuran crabs. *Mar. Ecol. Prog. Ser.* 15, 181–205.

Uppstrom, L. R. (1974). The boron/chlorinity ratio of the deep-sea water from the Pacific Ocean. *Deep-Sea Res. Pt. I* 21, 161–162.

Wachowiak, M., Cohen, L. B., and Ache, B. W. (2002). Presynaptic inhibition of olfactory receptor neurons in crustaceans. *Microsc. Res. Tech.* 58, 365–75.

Watson, S. A., Lefevre, S., McCormick, M. I., Domenici, P., Nilsson, G.E., and Munday, P. L. (2014). Marine mollusc predator-escape behavior altered by near-future carbon dioxide levels. *Proc. R. Soc. B* 281, 1–8.

Chapter 5

FISH KAIROMONES INDUCE SPINE ELONGATION AND REDUCE PREDATION IN MARINE CRAB LARVAE

Specialized defense strategies are induced in zooplankton upon detection of predator chemical cues or kairomones. These defenses are well-described for freshwater zooplankters, with morphological defenses being particularly striking, but few studies have reported kairomone-induced morphological defenses in marine zooplankton. Here, I compare morphological responses to kairomones in the larvae of two marine crab species, estuarine mud crabs (*Rhithropanopeus harrisii*) and Asian shore crabs (*Hemigrapsus sanguineus*). When reared in the presence of fish kairomones, spine length increased by 2–3% in larval *R. harrisii*, while no morphological changes were identified in *H. sanguineus*. In subsequent feeding assays with a co-occurring fish predator (Atlantic silversides, *Menidia menidia*), consumption of *R. harrisii* was lower on larvae that had been reared with kairomones. In addition, I found that broods with smaller larvae are more likely to exhibit increases in spine length after kairomone exposure. Hence, the observed morphological response is likely influenced by larval size.

5.1 Introduction

Marine and freshwater zooplankton exhibit a variety of specialized defense strategies, including changes to morphology, behavior, and life history. Such defenses are often induced by detection of predator chemical cues (Lass and Spaak, 2003,

Ferrari et al. 2010). These chemical cues are commonly defined as *kairomones*, i.e. interspecific chemical signals that benefit the receiver (Brönmark and Hansson 2012). Predator-induced morphological defenses have been most thoroughly described in freshwater systems. The cladoceran *Daphnia* has become a textbook example of phenotypic plasticity in morphological defenses. When exposed to predator kairomones, *Daphnia* produce various defensive structures (e.g. helmets, tail spines) via cyclomorphosis (Tollrian and Dodson 1999). Kairomones also induce spine elongation in rotifers (Gilbert 2013) as well as dorsal crests and increased cell width in *Euplotes* ciliates (Kuhlmann et al. 1999), both strategies effective against gape-limited predators.

In marine zooplankton, kairomones increased growth rate in copepods (Bjærke et al. 2014) and altered photobehavior in several species (Cohen and Forward 2009). Kairomone exposure also induced larger shells with smaller apertures in larvae of a marine snail, which effectively deterred predators (Vaughn 2007). However, studies investigating similar morphological responses in other marine species are lacking.

The specific kairomone molecules known to evoke changes to phototactic swimming behaviors in marine zooplankton are sulfated or acetylated amino sugars, derived from fish mucus (Rittschof and Cohen 2004). Behavioral responses to these molecules have been described in several marine crustacean zooplankton (Cohen and Forward 2009), including the larvae of two crab species, estuarine mud crabs, *Rhithropanopeus harrisii* and Asian shore crabs, *Hemigrapsus sanguineus*. Larval *R. harrisii* are more responsive to shadows, descending upon detection to evade predators lurking overhead (Cohen and Forward 2003). In addition, larvae of *R. harrisii* and *H. sanguineus* exhibit descent responses following dimmer increases in downwelling

light, which would exaggerate diel vertical migration (DVM), the habitual daytime descent to darker waters in avoidance of visual predators (Charpentier and Cohen 2015). DVM is thought to be a nearly universal defense amongst zooplankton, making plasticity in this behavior of considerable ecological significance.

In addition to phenotypically plastic behavioral defenses, many estuarine crab larvae are advected offshore during their early planktonic stages, a strategy which decreases vulnerability to predation by avoidance of predator-dense estuaries (Christy 2011). Previous work suggests that *H. sanguineus* follow this 'export-and-return' pattern of larval development and recruitment (Cohen et al. 2015, Epifanio 2013). Larval *R. harrisii*, however, are retained within the estuary throughout development (Cronin 1982). Elongated *R. harrisii* spines (Fig. 5.1a,b) provide some protection in estuarine waters (Morgan 1989).

With well-established inducible behavioral defenses and interspecific morphological variation in defensive structures, larval crabs provide a fitting model for testing whether common morphological defenses in freshwater zooplankton also occur in marine taxa. The aim of this study was to assess whether predator kairomones known to induce behavioral defenses in brachyuran crab larvae also induce morphological defenses (e.g. spine elongation) in two crab species with varying larval morphology and ecology (*R. harrisii* and *H. sanguineus*). Further, I test whether potential differences in morphology affect predation by a visual planktivore and if differences between individual broods impact induction of morphological defenses.

5.2 Methods

5.2.1 Morphology experiment

I assessed whether kairomones induce changes to larval morphology of two crab species, *R. harrisii* and *H. sanguineus* (see Appendix B.1 for collection/rearing details). On the day of hatching, larvae from single-female broods were divided and exposed to either (1) control seawater or (2) kairomones from fish mucus. Control seawater was collected from Indian River Inlet, DE, USA, and biologically active molecules were removed by ultrafiltration (100 kDa; GE Life Sciences UFP-100-C-5A, Pittsburgh, PA, USA) and aging in darkness for at least 1 week (Forward and Rittschof 1999). I produced kairomone solutions by isolating mucus from *Fundulus heteroclitus* with a previously described body wipe method (Forward and Rittschof 1999), followed by dilution with control seawater to 0.1 g wet weight mucus L^{-1} seawater. Mucus from *F. heteroclitus* at this concentration elicits strong phenotypic plasticity in photobehavior of larval *R. harrisii* and *H. sanguineus* (Charpentier and Cohen 2015). Larvae were continuously exposed to their respective treatments until the conclusion of larval development (see Appendix B.1 for details).

At each zoeal stage, 10 larvae from each treatment within a brood were randomly selected, anesthetized with 0.1 *M* urethane, and digitally photographed at 40x on a compound microscope (Canon EOS Rebel T3i, Tokyo, Japan; Olympus CX31, Waltham, MA, USA). One single female brood represented a replicate with two treatments (control, kairomones), of which there were five total replicates. Sample size was reduced to four broods in Z2 *R. harrisii*. Broods were paired between control and kairomone treatments at each stage. However, the same five broods were not necessarily measured throughout development. For example, if there were too few

individuals remaining within a brood of *R. harrisii* to continue measurements after Z2, I would use a different brood for Z3 and Z4 that had not been included in previous measurements (Z1, Z2). Morphometric analysis of digital images was conducted using ImageJ software (Schneider et al. 2012) calibrated to a stage micrometer image. In each larva, I measured (1) *body length* – posterior margin of the carapace to the base of the rostral spine and (2) *spine length* – tip of the dorsal spine to the tip of the rostral spine.

I compared the spine length of zoeae reared in control seawater or kairomones throughout larval development using linear mixed models with likelihood ratio tests (Bolker et al. 2008) and false discovery rate *post hoc* analyses (Benjamini and Hochberg 1995). In these models, direct effects were treatment (control, kairomones) and zoeal stage (Z1–Z4 in *R. harrisii*; Z1–Z5 in *H. sanguineus*). Body length was included as a covariate, and brood was added as a random effect to account for potential maternal effects, e.g. Giménez and Anger (2003). These statistical analyses were conducted in R (R Core Team 2016), using the lme4 (Bates et al. 2015) and lsmeans (Lenth 2016).

5.2.2 Predation experiment

I assessed whether morphological responses to kairomones influenced predation of zoeae by fish. In feeding assays, Z3 *R. harrisii* were preyed upon by juvenile *Menidia menidia*. Previous studies confirm that juvenile *M. menidia* consume crab larvae in the field (Cadigan and Fell 1985). Prior to experiments, zoeae were exposed to either control seawater or kairomones over two timescales: (1) developmental [since time of hatching], or (2) acute [1–3 h prior to experiments]. Here, the acute treatment was added to account for behavioral and physiological

responses to kairomones that have been observed in zoeae over this timescale (e.g. Charpentier and Cohen 2015). Fish were collected from Roosevelt Inlet, DE, USA and maintained in the laboratory, unfed, for 24 h before the start of feeding assays (see Appendix B.1 for details). Standard length and vertical mouth gape did not vary between fish that fed on zoeae exposed to control or kairomone treatments (Appendix B.2, Table B.1).

I conducted feeding assays in an apparatus that mimics the underwater angular light distribution, under white light with an irradiance of 1.92×10^{16} photons $m^{-2}s^{-1}$ (see Appendix B.2.2 for details). The spectral irradiance in the experimental apparatus was similar to that observed during civil twilight at my field site (see Appendix B.2.2: Fig. B.1). During experiments, animals were held in a 3.2 L feeding chamber at the center of the apparatus. Prior to each experiment, a removable insert was positioned at the center of chamber. Zoeae (n = 20) were placed outside of the insert and a fish was placed inside of the insert, and allowed to acclimate separately to the experimental apparatus for 15 minutes. This density of zooplankton is similar to that found locally (Maurer et al. 1978). After acclimation, the insert was removed and the fish was allowed to feed for 30 minutes, with the possibility of 20 successes (i.e. zoea consumption). At the conclusion of each experiment, fish were removed from the feeding chamber with a net (1.5 mm mesh). In addition, I quantified the number of zoeae consumed by removing the remaining zoeae with a sieve (190 μm mesh) and inspecting the net used for fish retrieval for zoea bycatch. In a preliminary experiment, this method was used to quantify zoeae in the absence of fish, and mean ± standard error [SE] retrieval efficiency was 98 ± 0.9% (n = 5). I repeated feeding experiments

10 times, where each replicate included three treatments (control, acute, developmental) and represented a brood from a single female.

I assessed whether kairomone exposure impacted predation of zoeae by *M. menidia* using a general linear mixed effects model with binary error and a logit link. In this analysis, the effect of kairomone treatment (direct effect) was assessed with a likelihood ratio test (Bolker et al. 2008) and false discovery rate *post hoc* analysis (Benjamini and Hochberg 1995). Brood was included as a random effect, since one brood of crab larvae comprised all the larvae used in one replicate of the predation experiment. In addition, larval morphology and swimming speed were measured during the predation experiment and later analyzed for differences between kairomone treatments (see Appendix B.2.3 for details). I conducted all statistical analyses for the predation experiment in R (R Core Team 2016), using the lme4 and lsmeans packages (Bates et al. 2015, Lenth 2016, respectively).

5.2.3 Brood effects (combined comparison)

Here, I combined data from the morphology (n = 5) and predation experiment (n = 10) to assess brood differences in spine length and the kairomone effect to spine length. Hence, this grouping narrowed my analysis to Z3 *R. harrisii* but expanded the sample size (n = 15). With these combined data, I first assessed whether developmental kairomone exposure impacted spine length in Z3 larvae using a mixed model with likelihood ratio tests (Bolker et al. 2008). In this model, I included body length as a covariate as well as brood and experiment (morphology, predation) as random effects. Using a similar procedure, I then conducted a second mixed model to determine the direct effect of brood on spine length, with body length as a covariate and experiment as a random effect.

Lastly, between broods, I assessed differences in the morphological response to kairomones with linear regressions. Further, the relative kairomone effect was compared to the initial trait (body and spine length). The relative kairomone effect was defined as the mean trait value with kairomone exposure divided by that without. Hence, a value of 1 would indicate no effect. The mean length without kairomone exposure represented the "initial" condition. All brood comparison analyses were conducted in R (R Core Team 2016), using lme4 and lsmeans packages (Bates et al. 2015, Lenth 2016, respectively).

5.3 Results

5.3.1 Morphology experiment

I assessed whether kairomones affect spine length throughout larval development. In *R. harrisii*, spine length varied between control and kairomone treatments ($\chi^2(4) = 11.2$, $P = 0.02$, linear mixed model). After the time of exposure at Z1, mean spine length increased by 2–3% (Fig. 5.1e; Z2–Z4). This difference was significant in Z2 ($P = 0.01$; false discovery rate *post hoc* tests). In *H. sanguineus*, mean spine length was approximately 3.8% greater in kairomone-exposed Z3 and Z4 larvae (Fig. 5.1f). Despite this apparent difference, spine length did not differ between control and kairomone-treated zoeae throughout development ($\chi^2(5) = 7.1$, $P = 0.2$).

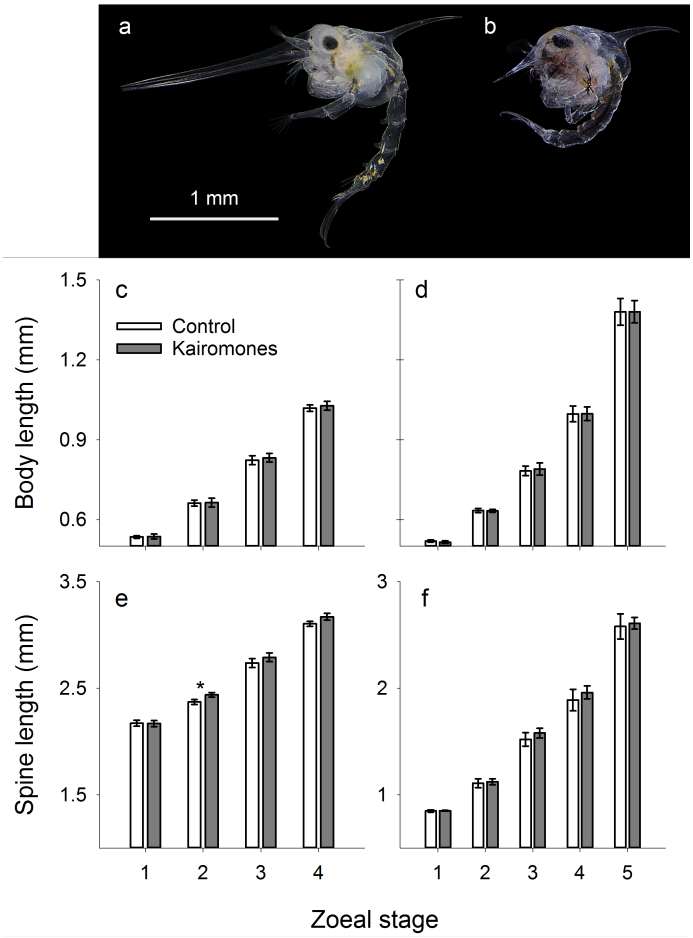

Figure 5.1: Interspecific variation in morphology and response to kairomones in (a) Z3 *Rhithropanopeus harrisii* and (b) Z3 *Hemigrapsus sanguineus*. Mean ± SE body and spine length of *R. harrisii* (c, e respectively) and *H. sanguineus* (d, f respectively) across all zoeal stages, reared in control seawater or kairomones (n = 5 broods except for in Z2 *R. harrisii* where n = 4 broods). Asterisks indicate significant differences in morphology between control and kairomone-treated animals ($P \leq 0.05$; linear mixed models, false discovery rate *post-hoc* tests).

5.3.2 Predation experiment

Predation of Z3 *R. harrisii* by juvenile *M. menidia* was evaluated to determine whether the observed spine elongation (Fig. 5.1e) impacts predation. Larvae were

exposed to either control seawater or kairomones over developmental and acute timescales. Predation differed significantly between the three treatments ($\chi^2(2) = 66$, $P < 0.001$; general linear mixed effects model). Specifically, the number of larvae consumed was approximately three times lower in zoeae exposed to kairomones throughout development, compared to those given control seawater or an acute exposure to kairomones ($P < 0.01$; false discovery rate *post hoc* test; Fig. 5.2).

In addition to the number of larvae consumed, I also assessed whether spine length or swimming speed differed after kairomone exposure in the predation experiment. Here, I found no significant differences between treatments in either spine length ($\chi^2(1) = 2.3$, $P = 0.13$) or swimming speed ($\chi^2(2) = 0.08$, $P = 0.96$, mixed model; see Appendix B.2.3: Table B.2). Though, mean spine length was approximately 2% greater in Z3 *R. harrisii* exposed to kairomones throughout development, similar to my previous finding in the morphology experiment (Fig. 5.1e).

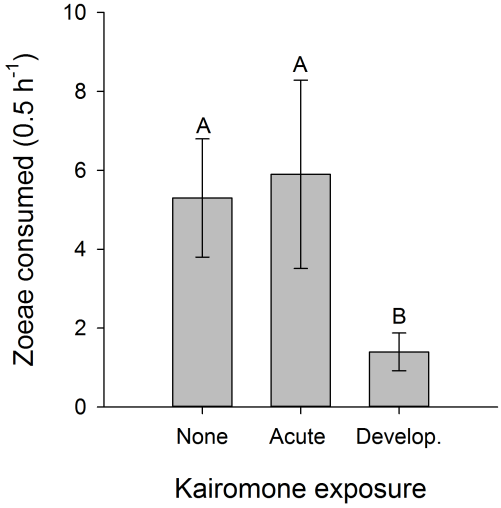

Figure 5.2: Kairomones effect predation of zoeae by fish planktivore. Mean ± SE Z3 *Rhithropanopeus harrisii* consumed (0.5 h^{-1}) by juvenile *Menidia menidia* was compared between zoeae given prior exposure to control seawater ("none") or kairomones over acute and developmental ("develop.") timescales (n = 10). Different letters indicate significant differences in the number of zoeae consumed between kairomone exposures ($P \leq 0.05$; general linear mixed effects model, false discovery rate *post hoc* tests).

5.3.3 Brood effects (combined comparison)

Using data from both the morphology and predation experiment, I evaluated whether Z3 *R. harrisii* from different broods varied in spine length and/or in their response to kairomones. With this combined dataset, I first confirmed that developmental exposure to kairomones resulted in greater spine length in Z3 larvae ($\chi^2(1) = 6.9$, $P = 0.009$; mixed model), with a mean increase of 2.3%. I then found that brood influenced both spine length and the kairomone effect to spine length (Fig. 5.3) ($\chi^2(28) = 128$, $P < 0.001$; mixed model). One brood exhibited significant kairomone-induced increases in spine length after kairomone exposure ($t(244) = -5.4$, $P < 0.001$, false discovery rate *post hoc* test; red in Fig. 5.3b).

Since spine length varies between broods, regression analyses were conducted to determine whether initial body length and/or spine length influenced the observed kairomone response. The relative kairomone effect was negatively related to initial body and spine length (Fig. 5.4) ($F(1,13) = 5.0$, $P = 0.04$ and $F(1,13) = 8.1$, $P = 0.01$, respectively.

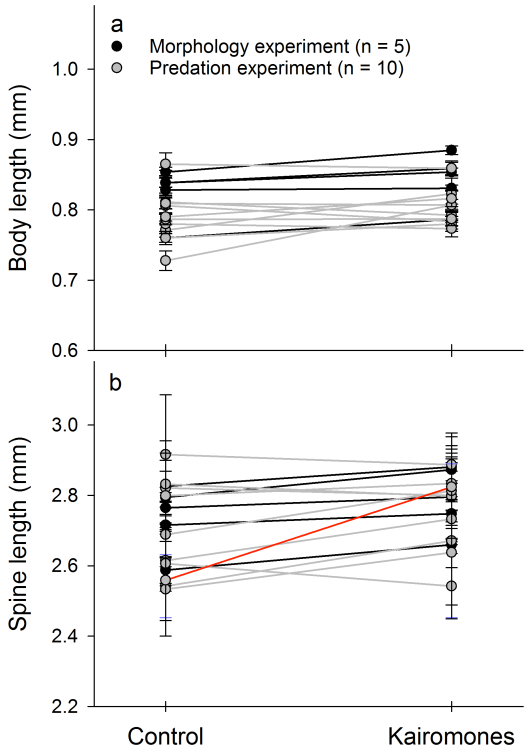

Figure 5.3: Variation amongst broods. Mean ± SE of (a) body length and (b) spine length of Z3 *Rhithropanopeus harrisii* from individual broods during the morphology experiment (n = 5) and the predation experiment (n = 10). Connection between two symbols represents zoeae within the same brood. One brood exhibited kairomone-induced changes to spine length ($P < 0.05$; mixed model, false discovery rate *post hoc* test), which is shown in red.

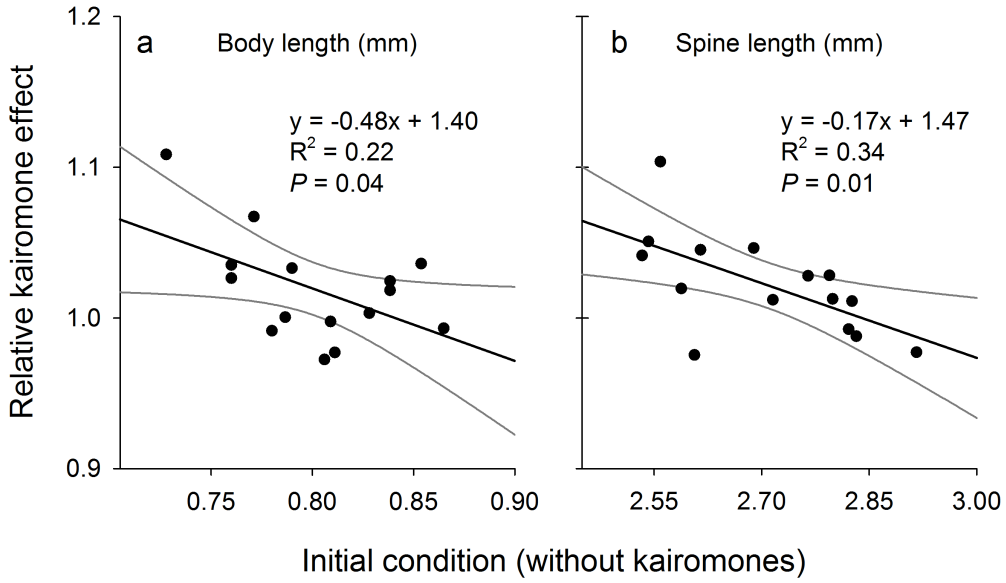

Figure 5.4: Kairomone effect varies with body and spine length. Relationship between the relative kairomone effect (with/without kairomones) and initial condition (without kairomones) for (a) body length and (b) spine length of Z3 *Rhithropanopeus harrisii* (n = 15). Regressions are shown with 95% CI as well as corresponding equations, R^2, and *P* values (top right).

5.4 Discussion

By increasing spine length, crab larvae can effectively deter gape-limited predators (Morgan 1989, Gilbert 2013, Engel et al. 2014). Since prey size is limited by mouth/throat gape in fish (Scharf et al. 2000), effectiveness of defensive spines increases with length. For example, Hovel and Morgan (1997) found that *M. menidia* preferentially ate crab larvae from species with shorter spines. Here, spines of larval *R. harrisii* were longer after exposure to kairomones at the Z1 stage (Fig. 5.1e). Kairomone exposure did not significantly impact spine length in larval *H. sanguineus*, despite apparent increases in Z3 and Z4 larvae (Fig. 5.1f). It is possible that kairomones do induce spine elongation in *H. sanguineus*, but I was unable to detect

this effect (power analysis; see Appendix B.3). Alternatively, this interspecific difference may be due to varying levels of predation pressure experienced by *R. harrisii* and *H. sanguineus* during larval development. Unlike *R. harrisii*, *H. sanguineus* are exported offshore to the continental shelf during planktonic larval stages (Cohen et al. 2015, Epifanio 2013), and therefore avoid the high abundance of planktivorous fish in estuaries (Christy 2011). Both larval *R. harrisii* and *H. sanguineus* exhibit DVM behavior, descending to deeper, darker waters during daytime, likely in avoidance of visual predators (Cronin 1982, Cohen et al. 2015). Superimposed on these migrations, larval *R. harrisii* ascend during flood tides to maintain estuarine retention, regardless of the time of day (Cronin 1982). Estuarine retention and flood tide ascents, which necessarily make larval *R. harrisii* more vulnerable to predators, have not been observed in larval *H. sanguineus*. Hence, selection for phenotypic plasticity in morphological defenses may be particularly beneficial to larvae of *R. harrisii*, developing in predator-dense estuaries.

The observed changes in spine length were slight (<3%), and this kairomone response varied between broods in *R. harrisii* (Fig. 5.3). Further, the relative kairomone effect decreased with initial body and spine length of individual broods (Fig. 5.4), suggesting that broods of smaller larvae are more likely to exhibit spine elongation after kairomone exposure. Relative to the freshwater zooplankton *Daphnia*, spine elongation after kairomone exposure is considerably less distinct in these larval crabs. Some *Daphnia* species exhibit nearly 40% increases in spine:body length following kairomone exposure throughout development (Tollrian and Dodson 1999). Similar to my observations, however, formation of defensive neck spines was related to body size in *Daphnia* (Riessen and Trevitt-Smith 2009). Here, spine elongation may

be reduced or absent in larger larvae, because further increases in spine length would be ineffectual in predator deterrence or associated with some cost. For example, increased drag from elongated structures can slow speed and increase the energy required for swimming. Comparing two cladocerans from the subgenus *Eubosmina*, one typical and one extreme (high carapax and long antennule body form), Lagergren et al. (1997) found that the extreme *Eubosimina* swam 40% slower and had to work 12% harder to swim at the same speed as the typical form. Induction of morphological defenses has also been shown to decrease reproduction (Gilbert 2013), reduce population growth (Kuhlmann et al. 1999), and lower relative fitness (Riessen 2012). Similar costs may surpass the benefit of predator deterrence through spine elongation after spines exceed a certain size in larval *R. harrisii*, which may explain the subtlety of the changes observed here.

Spine elongation in *Daphnia* improved survival during feeding assays (Engel et al. 2014). Here, in a similar feeding assay, the consumption of Z3 *R. harrisii* by *M. menidia* was three times lower in zoeae that had been exposed to kairomones throughout development, compared to those given either no kairomone exposure, or an acute exposure (Fig. 5.2). Hence, developmental exposure to kairomones induced spine elongation and reduced predation in *R. harrisii*. However, I lack definitive evidence that the observed increases in spine length (2–3%) directly and independently reduced predation. Further, it is possible that a factor other than spine elongation contributed to lower predation of zoeae, e.g. behavior. However, swimming speed did not vary between kairomone exposures, and the similarity between the control and acute kairomone exposure suggests that predation was not impacted by previously observed changes to photobehavior (Cohen and Forward 2003, Charpentier

and Cohen 2015). Zoeae may have evaded predators by retreating during an encounter or pursuit, but evaluation of fish-zoea interactions was limited by my inability to observe capture success or handling time at all locations of the behavioral chamber, and hence cannot be reliably reported here. In addition to behavior, kairomones may induce chemical defenses, a strategy common in other arthropods (e.g. insects, Pasteels et al. 1983).

Inducible defenses are defined by four basic criteria (Tollrian and Harvell 1999). First, the selective pressure of the inducing agent must vary in concentration over time, as constantly high concentrations would likely result in a permanent defense. Abundance of fish planktivores varies seasonally at my collection site (Broadkill River; [Chapter 6]). Second, the cue must reliably convey the magnitude of the threat (e.g. predator concentration). Kairomones from fish mucus accurately indicate predator abundance, as mucus is constantly sloughed from fish and active cues degrade quickly (McKelvey 1997, Parrish and Kroen 1988). Third, the induced defense must be effective. Predation decreased in larvae that were reared with kairomones, some of which exhibited significant increases in spine length. Fourth, the defense must have an associated cost trade-off. Here, my analyses indirectly indicate a cost tradeoff, or at least size selectivity, through the negative relationship between the relative kairomone effect and initial body/spine length. Arguably, spine elongation may be considered an inducible defense in larval *R. harrisii*. However, morphological responses in these animals seem to depend strongly on brood and size.

REFERENCES

Bates, D., M. Maechler, B. Bolker, and S. Walker. 2015. Fitting linear mixed-effects models using lme4. Journal of Statistical Software 67:1–48.

Benjamini, Y. and Y. Hochberg. 1995. Controlling the false discovery rate: A practical and powerful approach to multiple testing. Journal of the Royal Statistical Society B 57:289–300.

Bjærke, O., T. Andersen, and J. Titelman. 2014. Predator chemical cues increase growth and alter development in nauplii of a marine copepod. Marine Ecology Progress Series 510:15–24.

Bolker, B.M., M.E. Brooks, C.J. Clark, S.W. Geange, J.R. Poulsen, M.H.H. Stevens, and J-S.S. White. 2009. Generalized linear mixed models: a practical guide for ecology and evolution. Trends in Ecology and Evolution 24:127–135.

Brönmark, C. and L.A. Hansson. 2012. Chemical ecology in aquatic systems-an introduction. Pages 1–19 *in* C. Brönmark and L.A. Hansson, editors. Chemical Ecology in Aquatic Systems. Oxford University Press, New York, New York, USA.

Cadigan, K.M. and P.E. Fell. 1985. Reproduction, growth and feeding habits of *Menidia menidia* (Atherinidae) in a tidal marsh-estuarine system in southern New England. Copeia 1:21–26.

Charpentier, C.L. and J.H. Cohen. 2015. Chemical cues from fish heighten visual sensitivity in larval crabs through changes in photoreceptor structure and function. Journal of Experimental Biology 218:3381–3390.

Christy, J.H. 2011. Timing of hatching and release of larvae by brachyuran crabs: patterns, adaptive significance and control. Integrative and Comparative Biology 51:62–72.

Cohen, J.H. and R.B. Forward. 2003. Ctenophore kairomones and modified aminosugar disaccharides alter the shadow response in a larval crab. Journal of Plankton Research 25:203–214.

Cohen J.H. and R.B. Forward. 2009. Zooplankton diel vertical migration: a review of proximate control. Oceanography and Marine Biology: An Annual Review 47:77–110.

Cohen, J.H., C.K. Hanson, A.I. Dittel, D.C. Miller, and C.E. Tilburg. 2015. The ontogeny of larval swimming behavior in the crab *Hemigrapsus sanguineus*: Implications for larval transport. Journal of Experimental Marine Biology and Ecology 462:20–28.

Cronin, T.W. 1982. Estuarine retention of larvae of the crab *Rhithropanopeus harrisii*. Estuarine, Coastal and Shelf Science 15:207–220.

Engel, K., T. Schreder, and R. Tollrian. 2014. Morphological defences of invasive *Daphnia lumholtzi* protect against vertebrate and invertebrate predators. Journal of Plankton Research 36:1140–1145.

Epifanio, C.E. 2013. Invasion biology of the Asian shore crab *Hemigrapsus sanguineus*: A review. Journal of Experimental Marine Biology and Ecology 44:33–49.

Ferrari, M.C.O., B.D. Wisenden, and D.P. Chivers. 2010. Chemical ecology of predator–prey interactions in aquatic ecosystems: a review and prospectus. Canadian Journal of Zoology 88:698–724.

Forward, R.B. and D. Rittschof. 1999. Brine shrimp larval photoresponses involved in diel vertical migration: Activation by fish mucus and modified amino sugars. Limnology and Oceanography 44:1904–1916.

Gilbert, J.J. 2013. The cost of predator-induced morphological defense in rotifers: experimental studies and synthesis. Journal of Plankton Research 35:461–472.

Giménez, L. and K. Anger. 2003. Larval performance in an estuarine crab, *Chasmagnathus granulata*, is a consequence of both larval and embryonic experience. Marine Ecology Progress Series 249:251–264.

Hovel, K. and Morgan, S. (1997). Planktivory as a selective force for reproductive synchrony and larval migration. *Mar. Ecol. Prog. Ser.* 157, 79–95.

Kuhlmann, H.W., J. Kusch, and K. Heckmann. 1999. Predator-induced defenses in ciliated protozoa. Pages 142–159 *in* R. Tollrian and C.D. Harvell. The Ecology an Evolution of Inducible Defenses, Princeton University Press, Princeton, New Jersey, USA

Lagergren, R., M. Hellsten, and J.A.E. Stenson. 1997. Increased drag, and thus lower speed: a cost for morphological defence in *Bosmina* (*Eubosmina*) (Crustacea: Cladocera). Functional Ecology 11:484–488.

Lass, S. and P. Spaak. 2003. Chemically induced anti-predator defences in plankton: a review. Hydrobiology 491:221–239.

Lenth, R.V. 2016. Least-squares means: The R package lsmeans. Journal of Statistical Software 69:1–33.

Maurer, D., L. Watling, R. Lambert, and A. Pembroke. 1978. Seasonal fluctuation of zooplankton populations in lower Delaware Bay. Hydrobiology 61:149–160.

McKelvey, L.M. 1997. Predator chemical cues mediate zooplankton diel vertical migration. Ph.D. Dissertation, Duke University, Beaufort, NC, USA.

Morgan, S.G. 1989. Adaptive significance of spination in estuarine crab zoeae. Ecology 70:464–482.

Parrish, J.K. and W.K. Kroen. 1988. Sloughed mucus and drag-reduction in a school of Atlantic silversides *Menidia menidia*. Marine Biology 97:165–169.

Pasteels, J. M., J.-C. Gregoire, and M. Rowell-Rahier. 1983. The chemical ecology of defense in arthropods. Annual Review of Entomology 28: 263–289.

R Core Team. 2016. R: A language and environment for statistical computing. R Foundation for Statistical Computing, Vienna, Austria. URL http://www.R-project.org/.

Riessen, H.P. 2012. Costs of predator-induced morphological defences in *Daphnia*. Freshwater Biology 57:1422–1433.

Riessen, H.P. and J.B. Trevett-Smith. 2009. Turning inducible defenses on and off: adaptive responses of *Daphnia* to a gape-limited predator. Ecology 90:3455–3469.

Rittschof, D. and J.H. Cohen. 2004. Crustacean peptide and peptide-like pheromones and kairomones. Peptides 25:1503–1516.

Scharf, F.S., F. Juanes, and R.A. Rountree. 2000. Predator size – prey size relationships of marine fish predators: interspecific variation and effects of ontogeny and body size on trophic-niche breadth. Marine Ecology Progress Series 208:229–248.

Schneider, C.A., W.S. Rasband, and K.W. Eliceiri. 2012. NIH Image to ImageJ: 25 years of image analysis. Nature Methods 9:671–675.

Tollrian, R. and S.I. Dodson. 1999. Inducible defenses in Cladocera: constraints, costs, and multipredator environments. Pages 177– 202 *in* R. Tollrian and C.D. Harvell, editors. The Ecology and Evolution of Inducible Defenses, Princeton University Press, Princeton, New Jersey, USA.

Tollrian, R. and C.D. Harvell. 1999. Why inducible defenses? Pages 3– 9 *in* R. Tollrian and C.D. Harvell, editors. The Ecology and Evolution of Inducible Defenses, Princeton University Press, Princeton, New Jersey, USA.

Vaughn, D. 2007. Predator-induced morphological defenses in marine zooplankton: a larval case study. Ecology 88:1030–1039.

Chapter 6

QUANTIFYING FISH KAIROMONES IN ESTUARINE WATER: IS THE KAIROMONE EFFECT TO ZOOPLANKTON PHOTOBEHAVIOR A LABORATORY ARTIFACT?

Chemical cues, *kairomones*, from fish induce defensive strategies in zooplankton. For example, these cues affect predator avoidance behaviors, like vertical migration, by making zooplankton more responsive to light. Previous laboratory studies found that some fish kairomones in marine systems are derived from body mucus and include sulfated glycosaminoglycans (sGAGs). However, no reports quantify these cues in estuarine/marine environments or to assess whether laboratory studies with zooplankton reflect natural scenarios. I collected fish and water samples weekly in the Broadkill River, Delaware, USA. Using this field-collected water, I measured sGAG concentration with a colorimetric assay and determined behavioral sensitivity to light in a zooplankton model (*Artemia* spp. nauplii), following exposure of nauplii to these water samples. *Artemia* nauplii only undertake a descent response to increases in downwelling light after kairomone exposure, providing a standardized laboratory bioassay to test kairmone level in field-collected water. I determined the "behavioral threshold," the lowest light increase that induced a descent response, which decreases with increasing photosensitivity. Fish quantity (m^{-2}) was positively related to sGAG concentration and negatively related to behavioral thresholds. Hence, I was able to assess relative concentrations of fish kairomones in the field, and my results support that kairomone-induced changes to zooplankton photobehavior in laboratory assays are consistent with kairomone levels found in the

field. Future work should investigate how temporal changes in kairomone levels impact zooplankton behavior and vertical distribution in the field.

6.1 Introduction

In marine and freshwater zooplankton, chemical cues from fish induce strategies for predator avoidance. These cues, also known as *kairomones*, impact the behavior, morphology, and life history of zooplankton. A nearly universal behavior amongst zooplankton, diel vertical migration (DVM) generally describes the nighttime ascent to feed and daytime descent to avoid visual predators (Hays 2003), and DVM is primarily mediated by light (reviewed by Cohen and Forward 2009; Ringelberg 2010). Many zooplankton become more sensitive to light after kairomone exposure, responding to smaller changes in downwelling light than in the absence of kairomones. This increased photosensitivity likely deepens DVM (Cohen and Forward 2009; Charpentier and Cohen, 2015 [Chapter 2]), and results in a more dramatic avoidance of overhead shadows (Cohen and Forward 2003). Kairomone-induced morphological defenses are well documented in freshwater zooplankton (Kuhlmann et al. 1999; Tollrian and Dodson 1999; Gilbert 2013), with only a few examples for zooplankton in marine environments (Vaughn 2007; Charpentier et al. *submitted* [Chapter 5]). Kairomones also impact the growth, development, and reproduction of marine and freshwater zooplankton (Riessen 1999; Bjærke et al. 2014).

Although responses to predator kairomones are comparable between marine and freshwater zooplankton, the similarity of the chemical composition of these cues is still up for debate. In marine systems, kairomones from fish predators are degradation products from external body mucus. Biologically active cues are sulfated, acetylated, and/or aminated amino sugars (< 10 kDa), released by lyases including

heparinases and chondroitinases from glycosaminoglycans and glycoproteins (Rittschof and Cohen 2004). Molecules from different species of marine fish are equally effective in inducing defensive responses (McKelvey and Forward 1995). In freshwater environments, fish kairomones are low-molecular weight (< 500 Da), soluble compounds of intermediate lipophilicity, and glucuronic acids, phosphate, sulfate, and carboxyl groups are not required for biological activity (Von Elert and Pohnert 2000). In freshwater environments, fish-associated bacteria are necessary for production of the cue (Ringelberg and Van Gool, 1998). Although kairomones are chemically similar between different fish species (Loose et al. 1993; Von Elert and Pohnert 2000), freshwater zooplankton can likely distinguish between fish and invertebrate kairomones, as they induce different defensive responses (Lass and Spaak 2003). Several of the functional groups that are not required for biological activity in freshwater kairomones are found in some marine kairomones (e.g. glucuronic acids, sulfate, and carboxyl groups). However, marine zooplankters also respond to biologically active monosaccharide amino sugars that similarly do not include these groups (e.g. N-acetyl-D-glucoseamine; Forward and Rittschof 1999, 2000).

To identify inducible defenses and the chemical composition of active cues, previous work used bioassays as well as high-performance liquid chromatography (HPLC) in the laboratory (e.g. Forward and Rittschof 1999; Von Elert and Pohnert 2000). However, we generally lack an understanding of kairomone concentrations in the field, especially in marine environments. In a freshwater lake, Van Gool and Ringelberg (2002) found that collected lake water, which had previously contained greater fish biomass, resulted in an increase in DVM-related photobehavior of a resident zooplankter. These observations suggest that field concentrations of

kairomones are positively related to a common defensive strategy, DVM. To my knowledge, a similar study has not been conducted in a marine ecosystem. Hence, further work is needed to support previous laboratory studies.

Here, I quantified fish kairomones in water collected from an estuarine environment and assessed if kariomone levels are consistent with responses observed in laboratory tests. First, paired fish and water samples were collected during two consecutive field seasons. I then compared quantities of fish (abundance, mass, and surface area) to chemical and behavioral indicators of kairomone concentrations in the field water samples. Specifically, I determined the concentration of sulfated glycosaminoglycans (sGAGs) in a chemical assay, and the photosensitivity of zooplankton in a behavioral assay. In addition, I compared sGAG concentrations between field water samples and mucus extracts used in previous laboratory experiments. I expected that sGAG concentration and zooplankton photosensitivity would increase with fish quantity.

6.2 Methods

6.2.1 Field collection

I collected and quantified fish from Broadkill River, DE, USA for 20 consecutive weeks in 2014 (June 17th – October 29th) and 23 consecutive weeks in 2015 (May 27th – October 29th), with all samples collected ± 3 h around low tide. For each sample, a seine net was towed perpendicularly to shore at three adjacent sites (Fig. 6.1), which were 28, 77, and 39 m in length. I used a 3.0 x 0.9 m bagless seine net with 8 mm mesh in 2014 and a 3 x 1.2 m net with 6.4 mm mesh and a bag in 2015 (Memphis Net and Twine, Memphis, TN, USA). Given the use of different nets,

collections from each year were kept separate in all analyses. For each tow, I recorded the abundance of all captured species as well as length (mm) and mass (g) of each individual fish with a digital caliper (Traceable Products, Friendswood, TX, USA) and a top-loading balance (V-333, Acculab, Bradford, MA, USA), respectively. Sloughing of fish mucus occurs across the entire surface area of the body (Shephard 1994). Hence, I also calculated surface area using a previously described relationship between mass (*M*) and total surface area (*S*) in seatrout, *Salmo trutta* (Equation 6.1; O'Shea et al. 2006).

$$S = 12.62M^{0.63} \qquad \text{Equation 6.1}$$

In addition to fish collection, water samples were taken at site 2 each week (Fig. 6.1), and frozen at -80 °C until use in chemical (~ 15 mL) and behavioral assays (~ 2 L). At site 2, I also recorded temperature (°C), salinity, and dissolved oxygen (mg L^{-1}) with a YSI Pro2030 meter (YSI Incorporated, Yellow Spring, OH, USA) as well as current (m/s) with a mechanical flow meter (General Oceanics, Miami, FL, USA). Means and ranges of each measured environmental parameter are shown in Table 6.1.

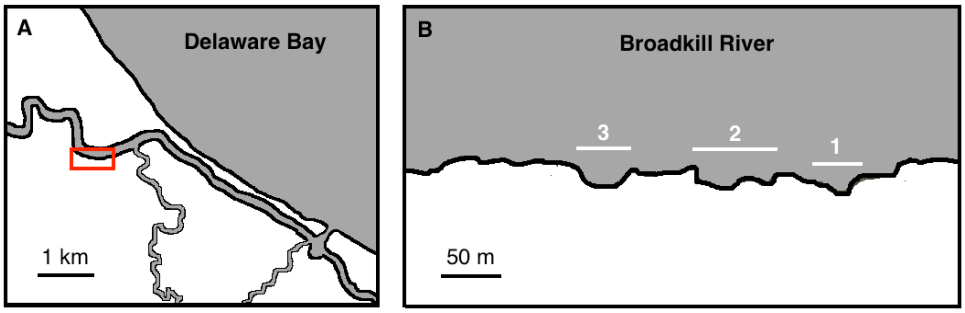

Figure 6.1: Map of field collection sites. Samples were taken from three sites in Broadkill River, Delaware, USA (within red box of panel A). Site numbers are shown in white (B) and indicate the order in which samples were collected each week, including site 1 (38.802166°, -75.201915°), 2 (38.802166°, -75.201915°), and 3 (38.802141°, -75.201633°). Scale bar is shown on the bottom left of each panel.

Table 6.1: Environmental parameters of field water at the time of collection

		Temp (°C)	Salinity	DO (mg/L)	Current (m/s)
2014	Mean ± se	23 ± 0.7	16 ± 1.0	5.1 ± 0.4	0.11 ± 0.03
	Range	15 – 27	10 – 25	3.6 – 9.2	0 – 0.37
2015	Mean ± se	24 ± 0.8	16 ± 1.0	4.1 ± 0.3	0.07 ± 0.02
	Range	15 – 28	8 – 27	2.3 – 6.8	0 – 0.33

Values are means ± standard error (se) and ranges (n = 20 in 2014 and n = 23 in 2015). Temperature and dissolved oxygen are abbreviated to "Temp" and "DO", respectively.

6.2.2 Chemical assay

I used a colorimetric assay (Proteoglycan Detection Kit, Astarte Biologics, Bothell, WA, USA) to determine the sGAG concentration in field water samples. A dye, 1,9-dimethylmethylene blue, was added to all samples, and absorbance at 525 nm was compared to a standard curve of chondroitin sulfate with a spectrophotometer (Evolution 201, Thermo Fisher Scientific, Waltham, MA, USA). During calibration, reagent blanks were seawater from my collection site that had been aged in darkness at

approximately 21 °C for at least two months prior to assays. Prior to calculation of sGAG concentration, the I subtracted the absorbance of the blank from the absorbance of each sample, such that the absorbance of the blank was now zero. Detectable compounds in mucus degrade well before this timeframe (McKelvey 1997). In addition, I assayed for sGAG concentration in crude mucus solutions. I extracted fish body mucus from *Fundulus heteroclitus*, using a previously described body wipe method (Forward and Rittschof 1999). Just prior to assays, concentrated mucus was diluted to 0.001, 0.01, 0.1, 1, and 10 g mucus L^{-1} seawater. These wet weight concentrations reflect those used in previous behavioral studies (e.g. Forward and Rittschof 1999, 2000; Cohen and Forward 2005; Charpentier and Cohen 2015). Standards and mucus solutions were diluted with aged field water. In both years, duplicate samples were measured for each field sample and each concentration of crude mucus. Dimethylmethylene blue assays for polysaccharide chains of sGAGs (Farndale et al. 1986). The active compounds detected by zooplankton are smaller (< 10 kDa), generally disaccharide degradation of products of these polysaccharides (Rittschof and Cohen 2004). Hence, I recognize that the results of this assay provide a relative rather than an absolute measure of the sGAG kairomones detected by zooplankton.

In addition to measurement of sGAG concentration, I conducted assays to determine total protein (Coomassie Bradford Protein Assay, Thermo Scientific, Rockford, IL, USA) and total sugar (Dubois et al. 1956) in my samples. In 2014, I found that the concentration of protein and sugar in several samples was near or below the detection limit of these assays. To improve detection in 2015, I concentrated my samples using centrifugal filters (3 kDa; EMD Millipore, Darmstadt, Germany). After

which, samples were 1.4 times more concentrated at the time of measurement. Given that a few samples still had concentrations of protein and sugar below detection limits, I do not report the results for these assays in either 2014 or 2015. However, reported sGAG values have been corrected for the described concentration procedure in 2015.

6.2.3 Behavioral assay

Behavioral experiments were conducted to determine zooplankton photosensitivity after exposure to collected field water samples. Specifically, I assessed descent responses to downwelling light, an important cue for depth regulation and DVM (Cohen and Forward 2009). Naupliar *Artemia* spp. were used in these assays, because nauplii are known to become more sensitive to downwelling light stimuli after exposure to fish kairomones and sensitivity increases with kairomone concentration (Forward and Rittschof 1999). *Artemia* can be hatched in the laboratory year-round from a single batch of cysts.

Two days prior to an experiment, preserved cysts of *Artemia* spp. (Grade A; Brine Shrimp Direct, Ogden, Utah, USA) were hatched under incandescent light in a separator funnel. Nauplii hatching within 24 h were moved into a 500 mL beaker and fed *Nannochloropsis* algal paste (Brine Shrimp Direct) at a concentration of 10^{10} cells L^{-1} for 5 h. After feeding, nauplii were filtered from the food mixture with a 200 μm sieve and then starved for 18 to 20 h before experiments. Feeding then starving was used to heighten swimming responses in brine shrimp nauplii (Forward and Hettler 1992; Forward and Rittschof 1999). Seawater used for rearing was collected from Indian River Inlet, Delaware, USA, and biologically active molecules were removed by ultrafiltration (100 kDa;GELife Sciences UFP- 100-C-5A, Pittsburgh, PA, USA) and aging in darkness for at least one week (Forward and Rittschof 1999), henceforth

referred to as *control seawater*. Nauplii were hatched, fed, and starved in control seawater with a salinity of 30.

Behavioral experiments were conducted in an apparatus that mimics the underwater angular light distribution, similar to that described by Forward et al. (1984). Inside of a light-tight enclosure, I placed groups of animals ($n \approx 50$) in a transparent acrylic chamber (5 × 5 × 5 cm), which was positioned at the center of a larger acrylic water bath painted flat black (40 × 40 × 15 cm; ~ 23°C). Downwelling light within the chamber was produced by a 300 W ozone-free Xe Arc Lamp (6258; Oriel Instruments, Stratford, CT, USA), and wavelength was set by a blue/green broadband pass filter (BG-18, Schott, Elmsford, NY, USA), which encompasses the peak spectral sensitivity of *Artemia* (Bradley and Forward 1984). Intensity of light stimuli was controlled with fixed neutral density filters (Melles Griot, Irvine, CA, USA). Light passed horizontally through a collimating lens, wavelength and intensity filters, and then reflected off a mirror positioned inside of the light-tight enclosure to pass vertically through a white acrylic diffuser that covered the water bath. Downwelling irradiance within the larval chamber was measured with an optometer and calibrated radiometric probe (models S471 and 247; Gamma Scientific, Baltimore, MD, USA) to select an appropriate range and resolution of light stimuli.

Prior to experiments, animals were exposed to either control seawater or field water for 1 – 3 h. Control seawater was diluted with de-ionized water to match the salinity of the respective field water sample as it varied with sample. In addition, nauplii were acclimated to 1.1×10^{15} photons m^{-2} s^{-1} (2014) or 2.4×10^{15} photons m^{-2} s^{-1} (2015) for at least 15 minutes in the experimental chamber. After the acclimation period, experimental animals were given a series of seven 3 s increases in light

intensity, which ranged from a 26 to 600 % increase from the acclimation level. During these experiments, two minutes of acclimation to dim light (1.1 or 2.4×10^{15} photons m^{-2} s^{-1}) separated each stimulus. Swimming behavior was recorded 3 s prior to and after each light increase through two narrow transparent sections in the black water bath with a digital camera (scA750-60gm; Basler AG Electronics, Ahrensburg, Germany) and a 16 mm varifocal lens (HF16HA-1B; Fujinon Corp, Edison, NJ, USA), backlit by an infrared LED array (880 nm; Advanced Illumination, Edmund Optics, Barrington, NJ, USA). I used a custom program in LabVIEW (National Instruments, Austin, TX, USA) to control the timing of video recordings. For each sampling week, behavioral assays were conducted with both control seawater (n = 5) and field-collected water (n = 5).

I determined the direction of travel for each swimming individual in the last 2 s of video recordings. Further, an individual was considered to be descending if the line between its start and end XY-coordinates was within the nadir ± 30°. I assessed whether the percentage of animals descending differed after increased light intensity, relative to prior swimming behavior in dim light, with one-way repeated measures (RM) ANOVAs. Within treatments of all samples, the percentage descending in dim light did not vary with replicate or intensity of the subsequent light increase ($P > 0.05$, two-way ANOVAs). Hence, within each treatment, I used the mean percentage of animals descending to represent swimming behavior before a light increase. Given a significant RM ANOVA ($P < 0.05$), I determined the smallest percent increase in light that evoked a descent response with Holm–Šidák *post-hoc* tests. This increase was deemed the 'behavioral threshold'. A lower behavioral threshold indicates greater photosensitivity (Appendix C, Fig. C.1).

Behavioral experiments were conducted for the latter 10 samples in 2014 (8/28/14 – 10/29/14) and for the entire sampling season in 2015 (n = 23). I verified experimental consistency by pairing observations in field water with a control group. Further, previous work indicates that naupliar *Artemia* do not descend in response to light increases in control seawater (Forward and Rittschof 1999). In 2015, however, behavioral thresholds were significant in the control group of two sampling weeks (6/3/15, 6/23/15). Hence, these samples were removed from analysis, reducing sample size to n = 21 in 2015. If descent responses were not significant in field water, samples were given a behavioral threshold of 175% for analysis. This percent increase in light surpassed the behavioral threshold of responding individuals (Appendix C, Table C.1).

6.2.4 Statistical analyses

First, I determined whether fish parameters differed significantly across each of the sampling seasons with one-way ANOVAs, comparing raw data of fish abundance, mass, and surface area between sample weeks, where replicates represent individual sampling locations (n = 3). Second, regression analysis was used to determine (1) whether any of the measured environmental parameters influenced fish quantity (abundance, mass, surface area), sGAG concentration, and/or behavioral threshold, and (2) whether sGAG concentrations and behavioral thresholds were related to the quantity of fish. If a response variable was related to more than one parameter (e.g. $P \leq 0.05$ in two regressions), I also performed multiple linear regressions to build a model that best fit my data. However, multiple regressions were only conducted with independent parameters, i.e. not with multiple measures of fish quantity. In all regression analyses, I used the mean values of fish quantity and sGAG concentration per sampling day. Third, I assessed whether sGAG concentration

differed between crude mucus solutions (0.001 – 10 g L^{-1}) and field samples using a mixed model with a likelihood ratio test (Bolker et al. 2008). In this analysis, I used the minimum and maximum sGAG concentrations measured in 2014 and 2015, and included year as a random effect. For all analyses, I applied a log transformation for fish abundance, mass, surface area, and behavioral thresholds, and relationships were considered significant when $P \leq 0.05$. All statistical analyses were performed in R (R Core Team, 2016), using lmtest (Zeileis and Hothorn 2002), MASS (Venables and Ripley 2002), and lme4 packages (Bates et al. 2015).

During my original analysis, I found that sGAG concentration was positively related to salinity (linear regression). I was concerned that salt concentrations may be interfering with the assay results. Further, Templeton (1988) showed that, in the absence of sGAGs, absorbance was 5% greater in samples containing 0.3 *M* NaCl than in the blank. Though present, this effect decreased in samples containing 5 μg of heparin. To conservatively compensate for this salt effect, I subtracted 5% of the original absorbance value before calculating sGAG concentration for all samples with a salinity > 20 (i.e. ~ 0.3 *M* NaCl). I made this salinity correction to samples in both 2014 (salinity of 21 – 28; n = 4) and 2015 (salinity of 21 – 27; n = 3).

6.3 Results

6.3.1 Fish quantity

I collected a total of 2163 fish in 2014 and 3579 fish in 2015. Fish abundance, mass, and surface area ranged from 0.07 – 3.6 fish m^{-2}, 0.13 – 7.5 g m^{-2}, and 1.80 – 99.07 $cm^{-2}m^{-2}$ in 2014 and 0.15 – 8.97 fish m^{-2}, 0.065 – 15.03 g m^{-2}, and 1.08 – 145.97 cm^{-2} m^{-2} in 2015, respectively. With the exception of fish mass in 2014, all fish

parameters varied significantly throughout the sampling season in both years (Fig. 6.2) ($F(19, 40) = 3$, $P < 0.003$ in 2014 and $F(22, 45) \geq 2.1$, $P \leq 0.02$ in 2015; one-way ANOVAs).

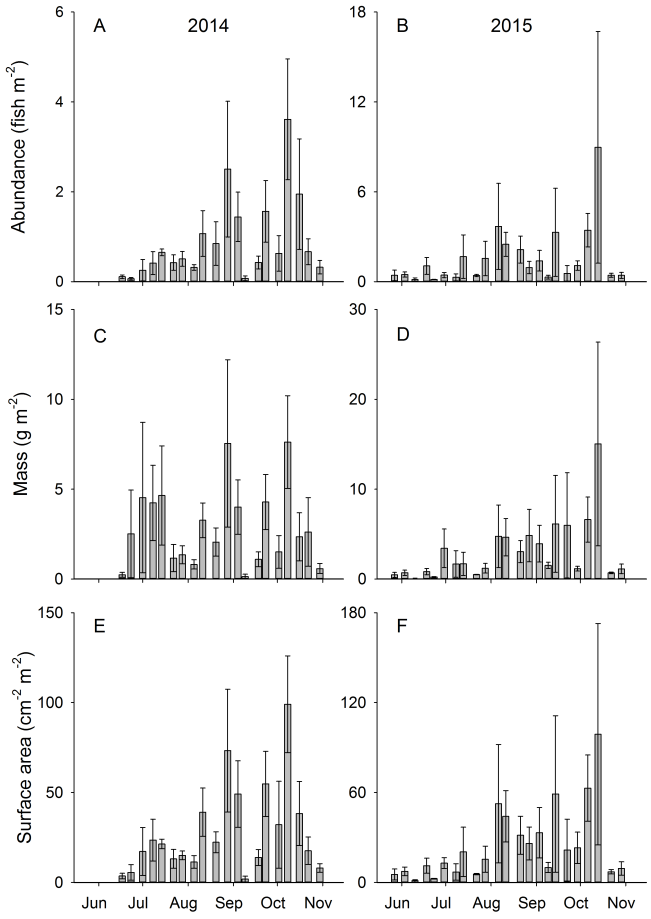

Figure 6.2: Variability in fish quantity. Mean ± se fish abundance (fish m^{-2}), mass (g m^{-2}) and surface area (cm^{-2} m^{-2}) across the sampling season in 2014 (A, C, E) and 2015 (B, D, F), respectively. Fish were collected with a 3.0 x 0.9 m bagless seine net (8 mm mesh) in 2014 and a 3 x 1.2 m seine net with a bag (6.4 mm mesh) in 2015. The scale of fish quantity is also different between 2014 and 2015.

I identified a total of 21 species in 2014 and 19 species in 2015, where 3 species comprised > 90% of the total catch in both years. *Menidia menidia*, *Bairdiella chrysoura*, and *Fundulus heteroclitus* represented 81, 5.6, and 4.3% of the catch in 2014 and 86, 7.2, and 1.5% of the catch in 2015, respectively. In both 2014 and 2015, fish abundance, mass, and surface area did not vary with any of the measured environmental parameters ($F(1, 18) < 0.2$, $P > 0.7$ and $F(1, 21) < 3.8$, $P \geq 0.1$, respectively; linear regressions).

6.3.2 Chemical assay

Concentration of sGAGs varied significantly with fish quantity (Fig. 6.3) (linear regressions). In 2014, sGAG concentration increased with fish abundance ($F(1, 18) = 5.7$, $P = 0.03$), mass ($F(1, 18) = 7.1$, $P = 0.02$), and surface area ($F(1, 18) = 7.1$, $P = 0.02$). In 2015, concentration of sGAGs was also positively related to fish mass and surface area ($F(1, 21) = 9.5$, $P = 0.006$ and $F(1, 21) = 10.2$, $P = 0.004$, respectively). Though not statistically significant, sGAG concentration appears to increase similarly with fish abundance in 2015 ($F(1, 21) = 4.1$, $P = 0.06$).

In 2014, sGAG concentration also increased with temperature ($F(1, 18) = 4.7$, $P = 0.04$; linear regressions). Using an additive model, multiple regression analysis with temperature and individual fish parameters (abundance, mass, surface area) further demonstrated that sGAG concentration was positively related to both temperature and all measures of fish quantity (Fig. 6.4) ($F(2, 17) > 7.5$, $P < 0.005$). I found no other significant relationships between sGAG concentration and environmental parameters in 2014 ($F(1, 18) < 3.8$, $P \geq 0.07$) or 2015 ($F(1, 21) < 2.3$, $P \geq 0.2$).

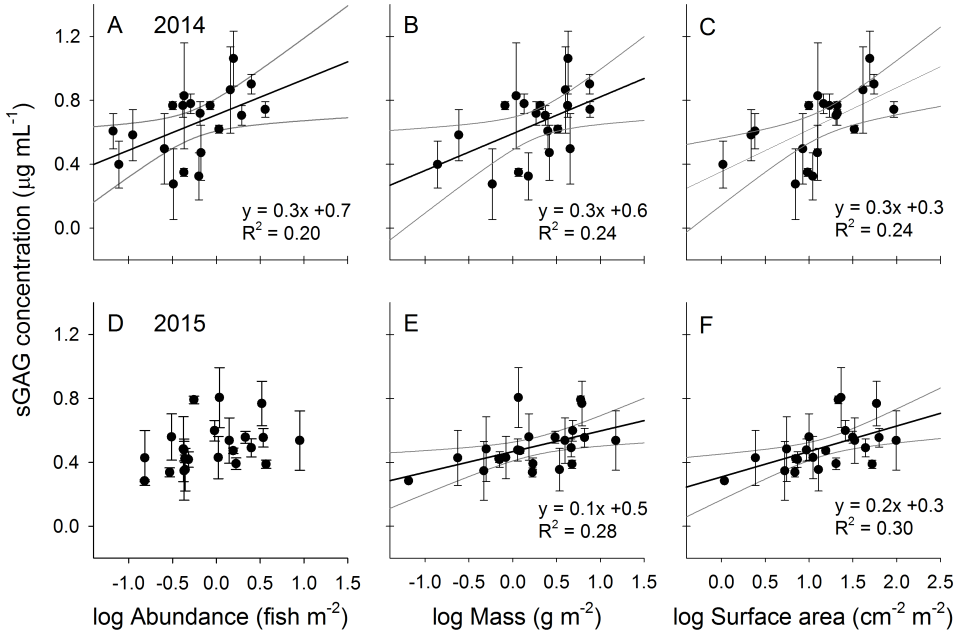

Figure 6.3: Relative kairomone concentration increases with fish quantity. Mean ± se sGAG concentration (µg mL^{-1}) across log abundance (fish m^{-2}), log mass (g m^{-2}), and log surface area (cm^{-2} m^{-2}) in 2014 (A, B, C; n = 20) and 2015 (D, E, F; n = 23). For all significant relationships ($P \leq 0.05$), regression lines are shown with 95% confidence intervals, equations, and adjusted R^2 values in the bottom right of the panel.

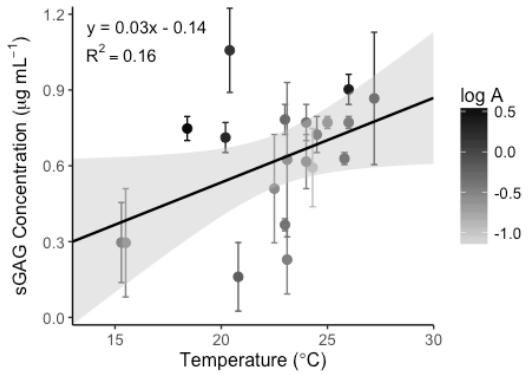

Figure 6.4: Temperature affects sGAG concentration in 2014. Mean ± se sGAG concentration (µg mL^{-1}) across temperature (°C) in 2014 field samples (n = 20). Regression line is shown with 95% confidence intervals, equation, and adjusted R^2 value (top left). Symbol gradient represents log fish abundance ("log A"; fish m^{-2}).

In crude mucus solutions, mean sGAG concentration increased with wet weight concentrations, from 0.001 to 10 g mucus L^{-1} (Fig. 6.5). When comparing sGAG concentration between the range found in crude mucus solutions and in field samples (dashed red lines in Fig. 6.5), I found no significant difference ($\chi^2(5) = 10.0$, $P = 0.08$; mixed model).

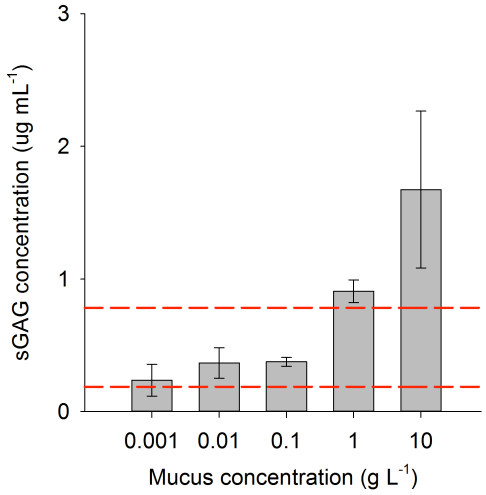

Figure 6.5: Mucus solutions resemble field sGAG concentrations. Mean ± se sGAG concentration (µg mL^{-1}) of crude mucus solutions, across a range of concentrations used in previous laboratory experiments (0.001 – 10 g mucus L^{-1} seawater). Concentrations shown are the combined results from assays conducted in 2014 (n = 2) and 2015 (n = 2). The red dashed lines represent the mean minimum and maximum sGAG concentrations of field seawater in 2014 (n = 2) and 2015 (n = 2).

6.3.3 Behavioral assay

Lower behavioral thresholds indicate greater photosensitivity, and behavioral thresholds decreased with some measure of fish quantity in both years (Fig. 6.6; linear regressions). In 2014, behavioral thresholds ranged from 26 – 175% increases in light,

and were negatively related to fish mass (F(1,8) = 5.5, $P = 0.05$). Thresholds appear to also decrease with increasing fish abundance and surface area. However, I did not find a significant relationship between these variables (F(1,8) = 3, $P = 0.14$). The range of behavioral thresholds in 2015 was 26 – 162% increases in light. Thresholds decreased with increasing fish abundance (F(1,19) = 7.2, $P = 0.02$) and surface area (F(1,19) = 4.6, $P = 0.05$). Though the trend appears similar, the relationship between threshold and fish mass was not significant in 2015 (F(1,19) = 2.8, $P = 0.11$). In both 2014 and 2015, behavioral thresholds did not vary with any of the measured environmental parameters (F(1,8) < 1.8, $P > 0.22$; F(1,19) < 2.10, $P > 0.16$, respectively).

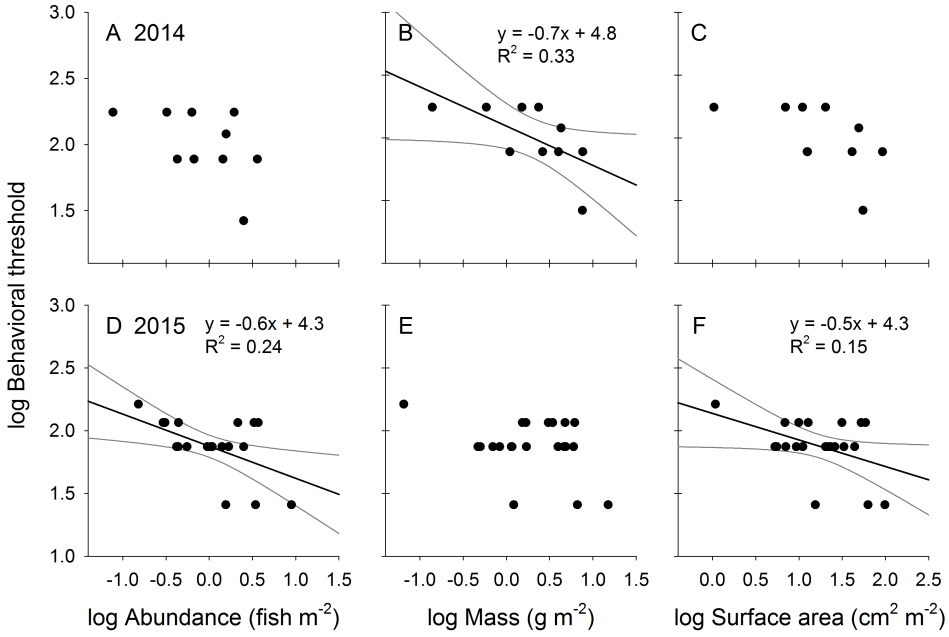

Figure 6.6: Photosensitivity increases with fish quantity. Behavioral threshold across log abundance (fish m^{-2}), log mass (g m^{-2}), and log surface area (cm^{-2} m^{-2}) in 2014 (A, B, C; n = 10) and 2015 (D, E, F; n = 21). For all significant relationships ($P \leq 0.05$), regression lines are shown with 95% confidence intervals, equations, and adjusted R^2 value in the top right of the panel.

6.4 Discussion

Many predator avoidance strategies in zooplankton are phenotypically plastic, where defensive traits are induced after exposure to kairomones. To be an effective signal, kairomone molecules must reliably convey the proximity of the threat (Tollrian and Harvell 1999). Kairomones from fish mucus represent a reliable cue, as mucus is constantly sloughed from fish and the active cues degrade quickly (Parrish and Kroen 1988; Forward and Rittscof 1993; McKelvey 1997). At my field site, fish abundance, mass, and surface area varied across the sampling season, with peak quantities in the fall (Fig. 6.2). Further, I found that two indicators of kairomone concentration, sGAG concentration and zooplankton photosensitivity, increased with some measure of fish quantity in two consecutive field seasons (Fig 6.3,6.6). Hence, I was able to quantify relative concentrations of fish kairomones in a marine ecosystem. Similar results have only been reported in a freshwater lake (Van Gool and Ringelberg 2002).

Although the described relationships between kairomone indicators and fish were directionally consistent between the two sampling years, I did not find that one measure of fish quantity best described kairomone concentration, and there were some absolute differences between the 2014 and 2015 samples. With the exception of fish abundance in 2015, sGAG concentration increased with fish quantity in both years (Fig. 6.3). However, relationships between behavioral thresholds and fish were only significant when using fish mass in 2014 and fish abundance as well as surface area in 2015 (Fig. 6.6). Hence, no one descriptor of fish quantity (i.e. abundance, mass, surface area) was the best predictor of kairomone concentration. In addition, the slope of fish-kairomone relationships and range of kairomone indicators were greater in 2014 (Fig. 6.3,6.6). This difference may be due to a slight variation in fish sampling between the two years, i.e. using a seine net without (2014) and with a bag (2015),

where larger catch in 2015 may be due to better sampling efficiency rather than a greater abundance of fish (Hahn et al. 2007).

In addition to fish-kairomone comparisons, I also assessed the impact of environment at the time of fish and water collection. Generally, indicators of fish quantity and kairomone concentration were not influenced by the measured environmental parameters (Table 6.1), with one exception. Concentration of sGAGs was positively related to temperature at the time of collection in 2014 (Fig. 6.4). It is possible that fish activity decreased at cooler temperatures (Beyan et al. 2015), resulting in less mucus being sloughed from fish. Parrish and Kroen (1988) found that mucus concentration in seawater decreased as fish swam at slower speeds. However, there was no significant temperature effect to sGAG concentration in 2015 or to behavioral thresholds in either year. Further, the 2014 sGAG-temperature relationship was primarily driven by two samples at relatively low temperatures (Fig. 6.4). Both of these were collected at the end of the sampling season, when temperature and fish quantity decreased simultaneously (Fig. 6.2). Hence, it is also possible that the temperature effect to sGAG concentration was not independent of fish quantity in the 2014 sampling season. Though not reported here, future work should also assess the influence of pH/pCO_2 on kairomone molecules. Seawater acidification impacts the behavior and sensation of marine animals (Clements and Hunt 2015), even over diel cycles commonly found in estuaries (Baumann et al. 2014; Charpentier and Cohen 2016 [Chapter 4]), as well as the function of peptide signaling molecules (Roggatz et al. 2016). In this study, for example, I sampled at low tide ± 3 h at a field site with a semidiurnal tidal cycle (Broadkill River, Delaware, USA). Further, at certain times of year, the pH of my field site at low tide is well below levels that induce behavioral

changes in a crustacean zooplankton (Appendix C, Fig. C.2; Charpentier and Cohen 2016 [Chapter 4]).

In aquatic environments, chemical information exists in a mixture, with different cues varying in composition and concentration (Atema 1995). However, most laboratory studies with zooplankton have assessed behavioral responses to chemical cues from just one predator at a time, although kairomones from different fish species similarly increase photosensitivity (McKelvey and Forward 1995). To collect kairomones from marine fish, Forward and Rittschof (1999) described a body wipe method to standardize extraction and dilution of fish mucus. Using this methodology, mucus concentrations known to induce changes in behavior and physiology range from 10^{-4} to 10 g mucus L^{-1} seawater (Forward and Rittschof 1999, 2000; Cohen and Forward 2005; Charpentier and Cohen 2015). To date, little work has been conducted to determine whether these laboratory exposures represent relevant compositions or concentrations of fish kairomones in marine ecosystems. Here, I found that photosensitivity of *Artemia* increases with fish concentration in estuarine water (Fig. 6.6), as it does with concentration of mucus extracts (Forward and Rittschof 1999). In addition, sGAG concentrations in field water were comparable to those found in crude mucus solutions at 0.001 – 10 g mucus L^{-1} seawater (Fig. 6.5). Hence, both behavioral responses and sGAG concentrations were comparable between my study with field water and laboratory studies with mucus solutions, supporting that previous findings were not a laboratory artifact. However, I recognize that my chemical assay specifically assessed large sGAG chains (Farndale et al. 1986), while the active cues that alter zooplankton behavior are likely mono- and disaccharide degradation products of these molecules, containing N-acetyl and/or sulfate groups

(Forward and Rittschof 1999, 2000). Hence, I cannot directly compare my findings to the concentration of these cues that are known to induce behavioral changes (10^{-6} – 10^{-9} *M*; Forward and Rittschof 1999). Alternatively, exudes from other organisms may have contributed to my sGAG estimation. For example, a marine phytoplankton, *Bacteriastrum jadranum* uses glycosaminoglycans in colony formation (Bosak et al. 2012), suggesting that these compounds may also contribute to bottom-up control of zooplankton behavior.

In the laboratory, previous work described kairomone-induced defenses in marine zooplankton as well as the chemical characteristics of these important signaling molecules. Using relatively simple chemical and behavioral assays, I quantified kairomone concentrations in a marine ecosystem, and my results support that previous findings, e.g. kairomone-induced photosensitivity, are not an artifact of laboratory experiments. However, further study in the field is necessary to confirm that kairomones impact ecologically relevant behaviors in marine ecosystems. For example, the amplitude of vertical migrations or daytime depth of zooplankton could be compared to fish quantity and/or the described indicators of kairomone concentration, i.e. sGAG concentration and behavioral threshold. Vertical distribution may be determined by collection of zooplankton at different depths, either by pumping samples in shallow, coastal environments (Cohen and Forward 2005) or by deploying multiple opening and closing plankton nets in deeper water (Criales-Hernández et al. 2008; Daase et al. 2008). Alternatively, less invasive acoustic methods accurately track depth and migration patterns at high spatial and temporal resolution, and may prove most informative, as both fish and zooplankton distributions can be deduced from acoustic backscatter data (Benoit-Bird and Lawson 2016). Given the

quantification of fish kairomones, future observation of migration patterns in the field is an important next step in determining how kairomones impact fish-zooplankton dynamics in marine environments.

REFERENCES

Atema, J. (1995). Chemical signals in the marine environment: dispersal, detection, and temporal signal analysis. *Proc. Natl. Acad. Sci.* 92, 62–66.

Bates, D., Maechler, M., Bolker, B., and Walker, S. (2015). Fitting linear mixed-effects models using lme4. *J. Stat. Softw.* 67, 1–48.

Baumann, H., Wallace, R. B., Tagliaferri, T., and Gobler, C. J. (2014). Large natural pH, CO_2 and O_2 fluctuations in a temperate tidal salt marsh on diel, seasonal, and interannual time scales. *Estuar. Coast.* 38, 220–231.

Benoit-Bird, K. J. and Lawson, G. L. (2016). Ecological insights from pelagic habitats acquired using active acoustic techniques. *Annu. Rev. Mar. Sci.* 8, 463–490.

Beyan, C., Boom, B. J., Liefhebber, J. M., Shao, K.-T., and Fisher, R. B. (2015). Natural swimming speed of *Dascyllus reticulatus* increases with water temperature. *ICES J. Mar. Sci.* 72, 2506–2511.

Bjærke, O., Andersen, T., and Titelman, J. (2014). Predator chemical cues increase growth and alter development in nauplii of a marine copepod. *Mar. Ecol. Prog. Ser.* 510, 15–24.

Bolker, B.M., Brooks, M.E., Clark, C.J., Geange, S. W., Poulsen, J. R., Stevens, M. H. H., and White, J-S. S. (2009). Generalized linear mixed models: a practical guide for ecology and evolution. *Trend. Ecol. Evol.* 24:127–135.

Bosak, S., Pletikapić, G., Hozić, A., Svetličić, V., Sarno, D., and Viličić, D. (2012). A novel type of colony formation in marine planktonic diatoms revealed by atomic force microscopy. *PLoS ONE* 7, e44851.

Bradley, D. J. and Forward, R. B. (1984). Phototaxis of adult brine shrimp, *Artemia salina*. *C. J. Zool.* 62, 2357–2359.

Charpentier, C. L. and Cohen, J. H. (2015). Chemical cues from fish heighten visual sensitivity in larval crabs through changes in photoreceptor structure and function. *J. Exp. Biol.* 218, 3381–3390.

Charpentier, C. L. and Cohen, J. H. (2016). Acidification and γ -aminobutyric acid independently alter behaviour. *R. Soc. Open Sci.* 3, 160311.

Charpentier, C. L., Wright, A. J., and Cohen, J. H. *submitted*. Fish kairomones induce spine elongation and reduce predation in marine crab larvae. *Ecology*.

Clements, J. C. and Hunt, H. L. (2015). Marine animal behaviour in a high CO_2 ocean. *Mar. Ecol. Prog. Ser.* 536, 259–279.

Cohen, J. H. and Forward, R. B. (2003). Ctenophore kairomones and modified aminosugar disaccharides alter the shadow response in a larval crab. *J. Plankton Res.* 25, 203–214.

Cohen, J. H. and Forward, R. B. (2005). Photobehavior as an inducible defense in the marine copepod *Calanopia americana*. *Limnol. Oceanogr.* 50, 1269–1277.

Cohen, J. H. and Forward, R. B. (2009). Zooplankton diel vertical migration - A review of proximate control. *Oceanogr. Mar. Biol.* 47, 77–110.

Criales-Hernández, M. I., Schwamborn, R., Graco, M., Ayón, P., Hirche, H. J., and Wolff, M. (2008). Zooplankton vertical distribution and migration off Central Peru in relation to the oxygen minimum layer. *Helgol. Mar. Res.* 62, 85–100.

Daase, M., Eiane, K., Aksnes, D. L., and Vogedes, D. (2008). Vertical distribution of *Calanus* spp. and *Metridia longa* at four Arctic locations. *Mar. Biol. Res.* 4, 193–207.

DuBois, M., Gilles, K. A., Hamilton, J. K., Rebers, P. A., and Smith, F. (1956). Colorimetric method for determination of sugars and related substances. *Anal. Chem.* 28, 350–356.

Farndale, R. W., Buttle, D. J., and Barrett, A. J. (1986). Improved quantitation and discrimination of sulphated glycosaminoglycans by use of dimethylmethylene blue. *Biochim. Biophys. Acta* 883, 173–1777.

Forward, R. B., Cronin, T. W., and Stearns, D. E. (1984). Control of diel vertical migration: Photoresponses of a larval crustacean. *Limnol. Oceanogr.* 29, 146–154.

Forward, R. B. and Hettler, W. F. (1992). Effects of feeding and predator exposure on photoresponses during diel vertical migration of brine shrimp larvae. *Limnol. Oceanogr.* 37, 1261–1270.

Forward, R. B., & Rittschof, D. (1993). Activation of photoresponses of brine shrimp nauplii involved in diel vertical migration by chemical cues from fish. *J. Plankton Res*. 15, 693–701.

Forward, R. B. and Rittschof, D. (1999). Brine shrimp larval photoresponses involved in diel vertical migration: Activation by fish mucus and modified amino sugars. *Limnol. Oceanogr*. 44, 1904–1916.

Forward, R.B. and Rittschof, D. (2000). Alteration of photoresponses involved in diel vertical migration of a crab larva by fish mucus and degradation products of mucopolysaccharides. *J. Exp. Mar. Biol. Ecol*. 245, 277–292.

Gilbert, J. J. (2013). The cost of predator-induced morphological defense in rotifers: experimental studies and synthesis. *J. Plankton Res*. 35, 461–472.

Hahn, K. J., Bailey, R. E., and Ritchie, A. (2007). Beach seining. In *Salmonid Field Protocols Handbook: Techniques for Assessing Status and Trends in Salmon and Trout Populations* (eds. D. H. Johnson, B. M. Shrier, J. S. O'Neal, J. A. Knutzen, X. Augerot, T. A. O'Neil, and T. N. Pearsons), pp. 267–324. American Fisheries Society.

Hays, G. C. (2003). A review of the adaptive significance and ecosystem consequences of zooplankton diel vertical migrations. *Hydrobiologia* 503: 163–170.

Kuhlmann, H.W., Kusch, J., and Heckmann, K. (1999). Predator-induced defenses in ciliated protozoa. In *The Ecology and Evolution of Inducible Defenses* (eds. R. Tollrian and C.D. Harvell), pp. 142-159. Princeton: Princeton University Press.

Lass, S. and Spaak, P. (2003). Chemically induced anti-predator defences in plankton: a review. *Hydrobiologia* 491, 221–239

Loose, C., Von Elert, E., and Dawidowicz, P. (1993). Chemically-induced diel vertical migration in *Daphnia*: a new bioassay for kairomones exuded by fish. *Archiv Fur Hydrobiologie* 126, 329–337.

McKelvey, L.M. (1997). Predator chemical cues mediate zooplankton diel vertical migration. Ph.D. Dissertation, Duke University, Beaufort, NC, USA.

Mckelvey, L. M. and Forward, R. B. (1995). Activation of brine shrimp nauplii photoresponses involved in diel vertical migration by chemical cues from visual and non-visual planktivores. *J. Plankton Res*. 17, 2191–2206.

O'Shea, B., Mordue-Luntz, A. J., Fryer, R. J., Pert, C. C., and Bricknell, I. R. (2006). Determination of the surface area of a fish. *J. Fish Dis*. 29, 437–440.

Parrish, J. K. and Kroen, W. K. (1988). Sloughed mucus and drag-reduction in a school of Atlantic silversides *Menidia menidia*. *Mar. Biol*. 97, 165–169.

R Core Team. (2016). R: A language and environment for statistical computing. R Foundation for Statistical Computing, Vienna, Austria. URL http://www.R-project.org/.

Riessen, H. P. (1999). Predator-induced life history shifts in *Daphnia*: a synthesis of studies using meta-analysis. *Can. J. Fish. Aquat. Sci*. 56, 2487–2494.

Ringelberg, J. 2010. Diel Vertical Migration of Zooplankton in Lakes and Oceans. Dordrecht: Springer.

Ringelberg, J. and Van Gool, E. (1998). Do bacteria, not fish, produce "fish kairomone"? *J. Plankton Res*. 20, 1847–1852.

Rittschof, D. and Cohen, J. H. (2004). Crustacean peptide and peptide-like pheromones and kairomones. *Peptides* 25, 1503–1516.

Roggatz, C. C., Lorch, M., Hardege, J. D., and Benoit, D. M. (2016). Ocean acidification affects marine chemical communication by changing structure and function of peptide signalling molecules. *Glob. Change Biol*. 22, 3914–3926.

Shephard, K. L. (1994). Functions for fish mucus. *Rev. Fish Biol. Fisher*. 4, 401–429.

Templeton, D. M. (1988). The basis and applicability of the dimethylmethylene blue binding assay for sulfated glycosaminglycans. *Connect. Tissue Res*. 17, 23–32.

Tollrian, R. and Dodson, S. I. (1999). Inducible defenses in *Cladocera*: constraints, costs, and multipredator environments. In *The Ecology an Evolution of Inducible Defenses* (eds. R. Tollrian and C.D. Harvell), pp. 177–202. Princeton: Princeton University Press.

Vaughn, D. (2007). Predator-induced morphological defenses in marine zooplankton: a larval case study. *Ecology* 88, 1030–1039.

Von Elert, E. and Pohnert, G. (2000). Predator specificity of kairomones in diel vertical migration of Daphnia: a chemical approach. *Oikos* 88, 119–128.

Van Gool, E. and Ringelberg, J. (2002). Relationship between fish kairomone concentration in a lake and phototactic swimming by *Daphnia*. *J. Plankton Res*. 24, 713–721.

Venables, W. N. and Ripley, B. D. (2002). Modern Applied Statistics with S. Fourth Edition. Springer, New York.

Zeileis, A. and Hothorn, T. (2002). Diagnostic Checking in Regression Relationships. *R News* 2(3), 7-10. URL http://CRAN.R-project.org/doc/Rnews/

Chapter 7

CONCLUDING REMARKS

In the preceding five research chapters, this dissertation explored and analyzed various aspects of chemical/visual ecology and predator-induced defenses in zooplankton. Here, I briefly summarize these results and their implications to the evolution of nervous systems, predicting biological responses to environmental change, as well as the ecology of predator-prey interactions in estuarine and marine ecosystems. In addition, I provide my recommendations for future work.

First, I used similar behavioral and physiological techniques to assess the mechanism by which kairomones amplify photobehavior in the larvae of two marine crab species (Chapter 2) as well as in a branchiopod zooplankter from an endorheic saltwater lake (Chapter 3). In all tested species, kairomone-induced photobehavior is mediated, at least in part, by increased visual sensitivity at the photoreceptor level. However, the specific mechanism differs slightly, where structural changes in the rhabdom of crab larvae are absent in brine shrimp adults. In addition, the ubiquitous neurotransmitter, γ-aminobutyric acid (GABA), is required for the onset of fish predator-induced defenses in a freshwater branchiopod (*Daphnia pulex*; Weiss et al. 2012) and for the detection/processing of fish kairomones in a larval malacostracan (*Hemigrapsus sanguineus*, Charpentier and Cohen 2016 [Chapter 4]). Similarities between these two crustacean lineages suggest conservation of an olfactory-visual-motor circuit and thereby migration-related photobehavior. Alternatively, interconnected neural and endocrine pathways may also mediate kairomone-induced

defenses, as has been shown in *D. pulex* and *Daphnia longicephala* (Weiss et al. 2015). Given the described kairomone effect on extracellular physiology in the retina (crab larvae, brine shrimp) and to morphology of the rhabdom (crab larvae), future work would benefit from intracellular recording within individual photoreceptor cells (e.g. Barlow et al. 1987) as well as the use of immunohistochemistry in neurotransmitter identification and use of pharmacological agents to verify/control behavior at the neural level. Similar techniques have been used to identify visual-motor circuits in a more primitive zooplankton model, larval annelid *Platynereis dumerilii* (Conzelmann et al. 2011; Jékely et al. 2008). In addition, it would be interesting to determine whether the physiological response to kairomones persists throughout onteny in crabs (e.g. juveniles, adults), similarly to behavioral responses in *Artemia* spp. (here [Chapter 3]; Forward and Rittschof 1993).

As discussed in Chapter 4, crab larvae require GABAergic signaling for detection and/or processing of fish kairomones. The role of GABA in inducible defenses may be common in both marine and freshwater crustacean zooplankton, given that GABA also mediates fish-induced life history changes in *Daphnia* (Weiss et al. 2012). In addition, the kairomone effect to photobehavior was lost after exposure to acidified seawater, over timescales that reflect diel/tidal pH cycles. Contrary to Nilsson et al.'s (2012) GABA hypothesis, however, the addition of a GABA antagonist (gabazine) did not restore the kairomone effect to photobehavior, and I did not observe a depletion of extracellular chloride after exposure to acidified seawater. Nilsson et al.'s GABA hypothesis has been primarily tested in fish (Clements and Hunt 2015). Although fish and crustaceans similarly adjust ion concentrations (e.g. chloride, bicarbonate) after an acid disturbance (Brauner and Baker 2009; Henry et al.

2012), ion regulation is limited during larval development in crabs (Anger et al. 2008). This may explain why my results varied from Nilsson et al. However, Watson et al. (2014) found that gabazine did restore behavioral function in a gastropod mollusk, following exposure to acidified seawater. This result is certainly curious, as gastropods have a low capacity for ion and acid-base regulation, compared to fishes (Parker et al. 2014). In Chapter 4, I suggest that Nilsson et al.'s GABA hypothesis is not universal amongst marine fish, molluscs, and crustaceans. Future work should include measurements of intra- and/or extracellular ion concentrations (e.g. Damsgaard et al. 2015; Regan et al. 2016).

In Chapter 4, I also describe how loss of kairomone-induced photosensitivity may actually be adaptive in zooplankton that experience present-day diel fluctuations in pH. When describing similar behavioral responses to acidification, prior study has focused on deleterious pH effects in the context of global climate change. In most of these studies, animals are exposed to a single, constant stressor (e.g. acidification) over relatively short timescales (days to weeks; Clements and Hunt 2015). These exposures are unrealistic, especially in coastal ecosystems, where multiple environmental parameters fluctuate over diel, seasonal, and interannual timescales, and such fluctuations may or may not be synchronized (Baumann et al. 2014). Hence, future study in ecophysiology of coastal species should employ multiple, fluctuating environmental stressors over relevant timescales. Admittedly, analyzing the methods of ocean acidification studies was not the focus of my dissertation. Regardless, a lack of consistency (e.g. carbonate chemsitry) and relevance (e.g. exposure time) in these studies was one of the most common weaknesses that I found in the literature. My

conclusion is not novel (Todgham and Stillman 2013; Gunderson et al. 2016), and recent reports reflect the importance of multiple stressors (e.g. Paganini et al. 2014).

Switching gears in Chapter 5, I found that developmental exposure to kairomones resulted in slight elongation of spines in marine crab larvae and decreased predation by a planktivorous fish. However, this kairomone effect on spine morphology was only detected in one of the two tested crab species. To my knowledge, this is the first suggestion of kairomone-induced morphological defenses in marine crustacean zooplankton. In a larval mollusk, however, Vaughn (2007) reported similar phenotypic plasticity after exposure to predator kairomones. Hence, kairomone-induced morphology may be widespread in marine zooplankton, opening an avenue for future comparisons amongst diverse taxa. Though, more examples are needed to explore the evolution of morphological responses and their role in predator-prey interactions in marine pelagic ecosystems. In freshwater zooplankton, kairomone-induced morphology is well known, and *Daphnia* spp. are a textbook example of phenotypic plasticity. Hence, there is rich body of literature on this topic, discussing the cost, physiological mechanism, and adaptive significance of *Daphnia*'s morphological responses (e.g. Tollrian and Dodson 1999; Riessen 2012; Weiss et al. 2015). Reports on freshwater zooplankton provide methodology for future analyses of the proximate and ultimate mechanisms of predator-induced morphological defenses in marine zooplankton.

In marine zooplankton, laboratory studies report kairomone-induced defenses and the characteristics/origin of kairomone molecules (e.g. Forward and Rittschof 2000). However, we lack an understanding of kairomone concentrations in marine ecosystems. To address this issue, I report a simple approach for quantifying the

relative concentration of fish kairomones in an estuarine environment (Chapter 6). Field glycosaminoglycan ("kairomone") concentrations were similar to those in the crude mucus solutions used in previous laboratory studies. This supports the hypothesis that kairomone-induced photosensitivity functions in the field. Hence, my methodology and data provide the foundation for future work in the field, verifying that kairomones alter predator avoidance behaviors, such as vertical migration. To support this hypothesis, zooplankton depth should be compared to parameters of light penetration, predation risk (e.g. fish quantity, sGAG concentration), and behavioral threshold. Given that kairomones induce photosensitivity in the laboratory, I would expect zooplankton to migrate to deeper depths when kairomone (i.e. fish) concentration increases. Acoustic methods present an interesting option for measurement of zooplankton depth, because they are non-invasive, provide high spatial and temporal resolution, and can be used to track both fish and zooplankton distributions (Benoit-Bird and Lawson 2016).

In summary, the results of this dissertation provide evidence of intermediate steps in the neural pathway that contributes to kairomone-induced photosensitivity, and thereby vertical migration, as well as an evolutionary comparison between marine and endorheic, saltwater zooplankton. I also offer an *adaptive* perspective on the consequences of acidification to behavior induced by kairomones. In addition, my data support the hypothesis that kairomones induce morphological defenses in some marine crustacean zooplankton. Lastly, I quantified fish kairomones in the field, and conclude that relevant kairomone concentrations were used in previous laboratory studies. Describing inducible defenses and understanding the mechanisms that mediate migration behavior in diverse zooplankton species will provide insight into nutrient

cycling and trophic interactions in aquatic ecosystems (Busch and Mehner 2011; Stukel et al. 2013). Further, predicting biological responses is particularly pressing in our changing ocean climate, as sensation and behavior are impacted by acidification. Now and in the future, it is essential to understand the role of these universal signaling paradigms (e.g. kairomone-induced defenses) in successful recruitment, and potentially biodiversity of marine ecosystems. After all, aquatic organisms of all shapes and sizes rely on chemical communication to feed, mate, find home, avoid predation, and ultimately survive.

REFERENCES

Anger, K., Torres, G., Charmantier-Daures, M., and Charmantier, G. (2008). Adaptive diversity in congeneric coastal crabs: Ontogenetic patterns of osmoregulation match life-history strategies in *Armases* spp (Decapoda, Sesarmidae). *J. Exp. Mar. Biol. Ecol.* 367, 28–36.

Barlow, R. B., Kaplan, E., Renninger, G. H., and Saito, T. (1987). Circadian rhythms in *Limulus* photoreceptors. I. Intracellular studies. *J. Gen. Physiol.* 89, 353–78.

Baumann, H., Wallace, R. B., Tagliaferri, T., and Gobler, C. J. (2014). Large natural pH, CO_2 and O_2 fluctuations in a temperate tidal salt marsh on diel, seasonal, and interannual time scales. *Estuar. Coast.*, 38, 220–231.

Benoit-Bird, K. J., and Lawson, G. L. (2016). Ecological insights from pelagic habitats acquired using active acoustic techniques. *Annu. Rev. Mar. Sci*. 8, 463–490.

Brauner, C.J. and Barker, D. W. (2009). Patterns of acid-base regulation during exposure to hypercarbia in fishes. In *Cardio-respiratory control in vertebrates* (eds. M. L. Glass and S. C. Wood), pp. 43–63. Berlin, Germany: Springer.

Busch, S., and Mehner, T. (2011). Size-dependent patterns of diel vertical migration: smaller fish may benefit from faster ascent. *Behav. Ecol.* 23, 210–217.

Clements, J. C. and Hunt, H. L. (2015). Marine animal behaviour in a high CO_2 ocean. *Mar. Ecol. Prog. Ser*. 536, 259–279.

Conzelmann, M., Offenburger, S., Asadulina, A., Keller, T., Münch, T. A., and Jekely, G. (2011). Neuropeptides regulate swimming depth of *Platynereis* larvae. *PNAS* 108, E1174–E1183.

Damsgaard, C., Gam, L. T. H., Dang, D. T., Van Thinh, P., Huong, D. T. T., Wang, T., and Bayley, M. (2015). High capacity for extracellular acid-base regulation in the air-breathing fish Pangasianodon hypophthalmus. *J. Exp. Biol.* 218, 1290–1294.

Forward, R. B. and Rittschof, D. (1993). Activation of photoresponses of brine shrimp nauplii involved in diel vertical migration by chemical cues from fish. *J. Plankton Res.* 15, 693–701.

Forward, R. B., and Rittschof, D. (2000). Alteration of photoresponses involved in diel vertical migration of a crab larva by fish mucus and degradation products of mucopolysaccharides. *J. Exp. Mar. Biol. Ecol.* 245, 277–292.

Gunderson, A. R., Armstrong, E. J., and Stillman, J. H. (2016). Multiple stressors in a changing world: The need for an improved perspective on physiological responses to the dynamic marine environment. *Ann. Rev. Mar. Sci.* 8, 357–378.

Henry R. P., Lucu, C., Onken, H., and Weihrauch, D. (2012). Multiple functions of the crustacean gill: osmotic/ionic regulation, acid-base balance, ammonia excretion, and bioaccumulation of toxic metals. *Front. Physiol*. 3, 431.

Jékely, G. (2009). Evolution of phototaxis. *Proc. R. Soc. B* 364, 2795–2808.

Nilsson, G. E., Dixson, D. L., Domenici, P., McCormick, M. I., Sørensen, C., Watson, S.-A., and Munday, P. L. (2012). Near-future carbon dioxide levels alter fish behaviour by interfering with neurotransmitter function. *Nat. Clim. Change* 2, 201–204.

Paganini, A. W., Miller, N. A., and Stillman, J. H. (2014). Temperature and acidification variability reduce physiological performance in the intertidal zone porcelain crab *Petrolisthes cinctipes*. *J. Exp. Biol.* 217, 3974–3980.

Parker, L. M., Ross, P. M., O'Connor, W. A, Pörtner, H. O., Scanes, E., and Wright, J. M. (2013). Predicting the response of molluscs to the impact of ocean acidification. *Biol.* 2, 651–692.

Regan, M. D., Turko, A. J., Heras, J., Andersen, M. K., Lefevre, S., Wang, T., Bayley, M. Brauner, C. J., Huong, D. T. T., Phuong, N. T., and Nilsson, G. E. (2016). Ambient CO_2, fish behaviour and altered GABAergic neurotransmission: exploring the mechanism of CO_2-altered behaviour by taking a hypercapnia dweller down to low CO_2 levels. *J. Exp. Biol.* 219, 109–118.

Riessen, H. P. (2012). Costs of predator-induced morphological defences in Daphnia. *Freshwater Biol.* 57, 1422–1433.

Stukel, M., Ohman, M., Benitez-Nelson, C., and Landry, M. (2013). Contributions of mesozooplankton to vertical carbon export in a coastal upwelling system. *Mar. Ecol. Prog. Ser.* 491, 47–65.

Todgham, A. E. and Stillman, J. H. (2013). Physiological responses to shifts in multiple environmental stressors: Relevance in a changing world. *Integr. Comp. Biol.* 53, 539–544.

Tollrian, R. and Dodson, S. I. (1999). Inducible defenses in Cladocera: constraints, costs, and multipredator environments. In *The Ecology and Evolution of Inducible Denfenses* (eds. R. Tollrian and C.D. Harvell), pp. 177– 202. Princeton: Princeton University Press.

Vaughn, D. (2007). Predator-induced morphological defenses in marine zooplankton: a larval case study. *Ecol.* 88, 1030–1039.

Watson, S.-A., Lefevre, S., McCormick, M. I., Domenici, P., Nilsson, G. E., and Munday, P. L. (2014). Marine mollusc predator-escape behaviour altered by near-future carbon dioxide levels. *Proc. R. Soc. B* 281, 1–8.

Weiss, L. C., Kruppert, S., Laforsch, C., and Tollrian, R. (2012). *Chaoborus* and *gasterosteus* anti-predator responses in *Daphnia pulex* are mediated by independent cholinergic and gabaergic neuronal signals. *PloS One* 7, e36879.

Weiss, L. C., Leese, F., Laforsch, C., and Tollrian, R. (2015). Dopamine is a key regulator in the signalling pathway underlying predator- induced defences in *Daphnia*. *Proc. R. Soc. B* 282, 20151440.

Appendix A

CHAPTER 4 SUPPLEMENTARY MATERIALS

A.1 Supplemental Methods

A.1.1 The pH experiment

Though I did not measure oxygen during the pH experiment, potential changes to dissolved oxygen (DO) in my sealed containers would have been minimal. In both pH treatments, I placed ~ 65 zoeae in 4 L of artificial seawater (Instant Ocean, Spectrum Brands, Blacksburg, VA, USA) for 12 h at 32 practical salinity units (psu) and 22 °C. During the third zoeal stage, Marsh et al. (2001) found that zoeae consume approximately 6 *n*mol O_2 h^{-1} $zoea^{-1}$ at a similar temperature (21 °C). Artificial seawater at 32 psu and 22 °C has a DO concentration of ~ 7.0 mg L^{-1} (6600-V2 sonde with 6589 Fast-Response pH sensor; YSI Incorporated, Yellow Springs, OH, USA). Using the simple calculation shown below, I determined that DO should have decreased by only 0.04 mg L^{-1} during the 12 h exposure, resulting in a percent decrease of 0.5%.

$$\Delta DO = O_2 \text{ consumption } \left(\frac{\text{mol } O_2}{\text{h} \times \text{zoea}}\right) \times \text{Molar mass } \left(\frac{\text{mg } O_2}{\text{mol } O_2}\right) \times \frac{\text{\# of zoeae}}{\text{Volume (L)}} \times \text{Time (h)}$$

A.1.2 Analysis of extracellular fluid

I multiplied all values for osmolality and Cl^- by a common faction (1.99), because the original concentrations were lower than expected values for larval crab extracellular fluid (ECF), nearly isosmotic to seawater (Anger et al. 2008). Here, I

defend that these corrections had no effect on the outcome of my statistical comparisons. Further, I extracted ECF following the pH behavioural assay. Mean ± se ECF Cl^- concentrations were 146 ± 40 m*M* in ambient pH and 141 ± 47 m*M* in low pH before the correction. Following the correction, concentrations were 292 ± 63 m*M* in ambient pH and 282.0 ± 94 m*M* in low pH. To ensure that this correction did not alter my statistical interpretations, I conducted t-tests comparing Cl^- concentrations between pH treatments before and then after the correction. In both analyses, I found no significant difference between the two pH treatments ($t(8) = 0.08$, $P = 0.93$). This statistical analysis was conducted in R (R Core Team, 2015, Vienna, Austria).

A.1.3 Seawater chemistry

The total alkalinity (TA) values of the ambient pH treatment were higher than expected, given a salinity of 32 practical salinity units (psu, Table 1). With few exceptions (e.g. calcium carbonate dissolution), TA is generally conservative and correlated with salinity. As mentioned in the methods section [Chapter 4], the same salinity and artificial seawater mix (Instant Ocean, Spectrum Brands, Blacksburg, VA, USA) were used in both the ambient and low pH treatments. However, the seawater for the low pH treatment was extracted from a system that had been circulating in a large sump for several weeks, while seawater for the ambient pH treatment was made on the day of use. Though Instant Ocean salt mix and deionized water were mixed until the solution was clear (i.e. no visible salt crystals), it is possible that salt continued to dissolve far after my initial mix, which would impact salinity and therefore TA. Further, TA was analyzed several weeks after completion of behavioural experiments. Fortunately, salinity of Instant Ocean seawater did not increase significantly over a 24 h period (table A.1). Hence, my behavioural and ECF Cl^-

results should not have been influenced by salinity differences between the two pH treatments. To further investigate whether TA of recently mixed Instant Ocean salt mix changes over longer time periods in storage, I analyzed TA of samples at 32 psu and found that TA was 2365 and 3253 μmol kg^{-1}, 24 and 72 h after solution was made, respectively. This could explain higher TA values at ambient pH. Regardless, pH should have been maintained over this time period, because (1) I properly eliminated biologically-induced changes to carbonate chemistry (e.g. addition of saturated mercury bichloride) and (2) seawater has a high buffering capacity, where increases in TA are correlated with dissolved inorganic carbon (DIC) as HCO_3^- contributes significantly to both. As secondary evidence for this, the mean ± se pH_{NBS} measurements at the time of the experiment were similar (8.1 ± 0.02) to calculated values of pH_T shown in Table A.1 (8.1 ± 0.06).

Table A.1: Salinity of artificial seawater (Instant Ocean) at 0 and 24 h after dissolution of salt mixture into deionized water

Initial salinity (0 h)	Salinity after 24 h
32.4	32.4
32.3	32.7
29.1	29.1

Seawater was considered "dissolved" after mixture was clear (i.e. no apparent salt crystals), and salinity was measured with a handheld meter (Pro2030; YSI Incorporated, Yellow Springs, OH, USA). There were no significant differences in salinity between 0 and 24 h after dissolution ($t(2) = -1$, $P = 0.4$; paired t-test).

REFERENCES

Anger, K., Torres, G., Charmantier-Daures, M., and Charmantier, G. (2008). Adaptive diversity in congeneric coastal crabs: Ontogenetic patterns of osmoregulation match life-history strategies in *Armases* spp (Decapoda, Sesarmidae). *J. Exp. Mar. Biol. Ecol*. 367, 28–36.

Marsh, A. G., Cohen, S., and Epifanio, C. E. (2001). Larval energy metabolism and physiological variability in the Asian shore crab *Hemigrapsus sanguineus*. *Mar. Ecol. Prog. Ser.* 218, 303–309.

Appendix B

CHAPTER 5 SUPPLEMENTARY MATERIALS

B.1 Animal rearing and maintenance

Prior to experiments, I collected ovigerous female crabs from either Broadkill River estuary, DE, USA (*Rhithropanopeus harrisii*) or Roosevelt Inlet, DE, USA (*Hemigrapsus sanguineus*) during summer (May – September) of 2012, 2013, and 2016. In the laboratory, *R. harrisii* and *H. sanguineus* were kept in seawater with a salinity of 20 and 30, respectively. On the day of hatching, larvae from single female broods were split into control seawater and kairomone treatments and maintained in ~500 mL of their respective treatment solutions in fingerbowls throughout development. Water was changed 3 times per week for animals in control seawater and daily for those exposed to kairomones to ensure the presence of active mucus compounds. For water changes, larvae were gently transferred to a new bowl using a wide mouth 25 mL pipette to minimize mechanical disturbance. Throughout rearing, larvae were fed newly hatched brine shrimp (*Artemia* spp.) nauplii *ad libitum*.

Juvenile silversides, *Menidia menidia* (56 – 86 mm, standard length) were collected with a seine net (3×1.2 m) from Roosevelt Inlet, DE, USA during the summer (May – September) of 2016. Fish were transported back to the lab under gentle aeration and moved into a 38-L aquarium under a 14:10 h light:dark cycle at ~ 24 °C for 24 h before the start of feeding experiments. During this time, fish were not fed and remained in their collection seawater. At the time of collection, temperature,

salinity, and dissolved oxygen were measured with a handheld meter (Pro2030, YSI Incorporated, Yellow Spring, OH, USA) and ranged from 23 – 28 °C, 27 – 30 salinity, and 5.2 – 7.4 mg O_2 L^{-1}, respectively.

B.2 Predation experiment

B.2.1 Fish morphology

To ensure that fish size did not impact consumption rate, I determined whether fish morphology varied between treatments during the predation experiment. Further, I measured the standard length and vertical mouth gape of all *M. menidia* used in feeding assays with a digital caliper (Table B.1). Fish length and mouth gape did not vary between fish that fed on zoeae exposed to control or kairomone treatments ($F(2,27)<0.4$, $P>0.7$, one-way ANOVA).

Table B.1: Sizes (mm) of *Menidia menidia* used in the predation experiment, given *Z3 Rhithropanopeus harrisii* that had been previously exposed to control seawater or kairomones over two timescales, developmental (since time of hatching) and acute (1 – 3 h)

	Control	Developmental	Acute
Standard length	69.0 ± 3.06	69.2 ± 2.29	68.7 ± 1.84
Vertical mouth gape	5.1 ± 0.26	5.3 ± 0.25	5.4 ± 0.15

Values are mean ± standard error (n = 10).

B.2.2 Experimental chamber

I conducted feeding assays in an apparatus that mimics the underwater angular light distribution, similar to Forward et al. (1984). Briefly, experimental light, produced by a 300 W ozone-free Xe Arc Lamp (6258; Oriel Instruments, Stratford,

CT, USA), passed through a collimating lens, reflected off a mirror into a light-tight enclosure, and ultimately passed through a white acrylic diffuser into an acrylic water bath painted flat black (40×40×15 cm; ~23°C). During experiments, both larvae and fish were placed in a transparent acrylic chamber (20×20×8 cm) with a removable insert of the same material at the center (10×10×8 cm), all of which was centered within the water bath. The described light assembly generates a relatively diffuse, spectrally flat, downwelling white light source, entering an otherwise dark chamber. Feeding behavior was recorded through two transparent sections of the water bath on an analog camera (TK-C9200U; JVC, Wayne, NJ, USA) with a 5.0–50 mm varifocal lens (Pelco, Clovis, CA, USA), backlit by an infrared LED array (880 nm; Advanced Illumination, Rochester, VT, USA).

In order to mimic natural turbidity levels, feeding assays were conducted in seawater collected from Roosevelt Inlet, DE, USA and aged for at least one week in darkness, hereafter referred to as 'field seawater'. Field seawater ranged in salinity from 19.8 to 24.3. Prior to predation experiments, downwelling irradiance was measured at the center of the animal chamber, under field seawater, using a cosine-corrected optical fiber on a spectroradiometer (QE Pro, Ocean Optics, Dunedin, FL, USA) calibrated for absolute irradiance. All experiments were conducted under white light with an irradiance of 1.92×10^{16} photons $m^{-2}s^{-1}$ (integrated from 400-700 nm). To provide some environmental context, I compared spectral irradiance between the animal chamber and the Broadkill River (animal collection site) at midday and sunset ± 0.5 h (Fig. B.1). Field measurements were taken with a cosine-corrected spectroradiometer (HydroRad; HobiLabs, Inc, Tucson, AZ, USA) on September 13th 2016 with < 10% cloud cover. Values of spectral irradiance used within the chamber

were similar to those observed during civil twilight (Fig. B.1d). Twilight is an important time of day for many zooplankton, which commence upward vertical migrations at this time (Cohen and Forward 2009).

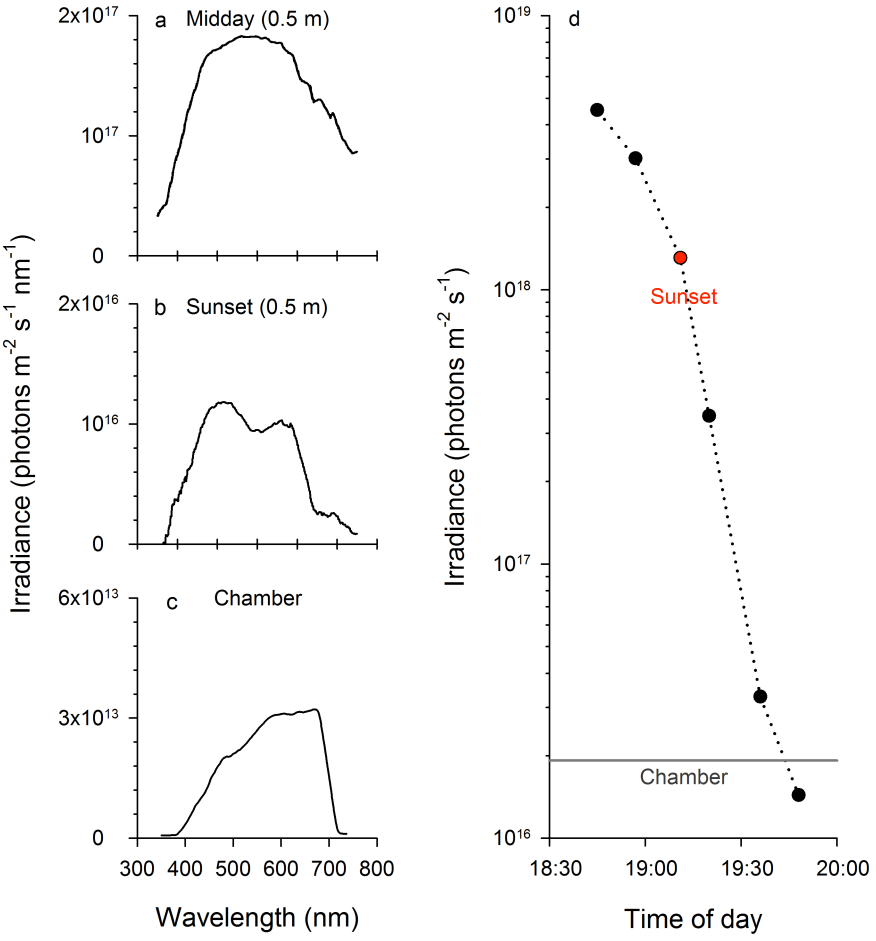

Figure B.1: Comparison of irradiance in the field to the predation experiment chamber. Moving average (1 nm) of spectral irradiance in the Broadkill River, DE, USA at a depth of 0.5 m during (a) midday (12:00) and (b) sunset (19:11), and (c) at the center of the experimental chamber. Field irradiance measurements were also taken over time at 0.5 m (d), at ± 0.5 h around sunset and ending at the conclusion of civil twilight (integrated from 400 – 700 nm). Highlighted values represent the irradiance at the time of sunset (red) and within the animal chamber (gray). Note scale differences in irradiance for each panel.

B.2.3 Larval morphology and swimming speed

Here, I investigated whether kairomones affected larval morphology and/or swimming speed during the predation experiment. Prior to feeding assays, 10 larvae were removed from the control and kairomone (developmental) treatments. Morphological measurements were conducted using the same methods described in the morphology experiment. Following feeding assays, swimming speed of zoeae was measured using the above-described video recordings for 6 of the 10 replicates. Ten minutes after the start of each predation trial, swimming speed was calculated by measuring the distance moved over a duration of 1 – 3 s for the first 10 zoeae that were visible (Forward et al. 1984). Zoeae near the top or edges of the chamber were not included. Differences in morphology and speed were assessed using mixed models with likelihood ratio tests (Bolker et al. 2008), comparing these parameters between control and kairomone treatments with brood as a random effect. Mixed models were conducted in R (R Core Team 2016) with the lme4 package (Bates et al. 2015). Here, I found that larval morphology and swimming speed did not differ between treatments in the predation experiment ($\chi^2(2)>3.3$, $P>0.1$, mixed model). However, mean spine

length was 2% greater in Z3 *R. harrisii* exposed to kairomones throughout development (Table B.2).

Table B.2: Morphology and swimming speed of Z3 *Rhithropanopeus harrisii* given control seawater or kairomones at two timescales, developmental (since time of hatching) and acute (1 – 3 h), prior to the predation experiment

	Control	Developmental	Acute
Body length (mm)	0.79 ± 0.01	0.80 ± 0.01	
Spine length (mm)	2.69 ± 0.04	2.75 ± 0.03	
Spine:body length	3.37 ± 0.04	3.41 ± 0.06	
Swimming speed (mm s^{-1})	6.9 ± 0.6	6.3 ± 0.3	6.6 ± 1.0

Values are mean ± standard error (n = 10 for morphology, n = 6 for speed). Morphology of acute-exposed zoeae was not measured separately, as they were pulled from the control group just 1 – 3 h before experiments.

B.3 Power analysis

As described in the results of the morphology experiment, kairomones did not significantly impact spine length in *H. sanguineus* during larval development ($\chi^2(5) = 7.1$, $P = 0.2$; linear mixed model), although the mean spine length of Z3 and Z4 larvae was approximately 3.8% larger in kairomone-exposed animals. Using the same statistical model, I identified 2-3% increases in spine length in larval *R. harrisii* ($\chi^2(4) = 11.2$, $P = 0.02$). In addition, variation in spine length was consistently lower in *R. harrisii* than in *H. sanguineus* (Fig. 1e,f). Hence, it is possible that I were unable to detect a kairomone effect in *H. sanguineus* due to greater variability. Following the initial mixed model analyses, I conducted power analyses to assess whether the data, model, and sample size were sufficient to detect a 2-4% difference in *H. sanguineus*, using the longpower package (Donohue and Edland 2016) in R (R Core Team 2016).

Power ranged from 0.40 to 0.90 to detect a 2-4% difference in spine length, respectively. Further, the difference would need to exceed 3% to achieve a power of 0.80. Given differences similar to *R. harrisii* (2-3%), these results suggest that the statistical power of my *H. sanguineus* model would be relatively low (< 0.80). Therefore, it is possible that kairomones do induce spine elongation in *H. sanguineus*, but I was unable to detect this effect (i.e. type II error).

REFERENCES

Bates, D., Maechler, M., Bolker, B., and Walker, S. (2015). Fitting linear mixed-effects models using lme4. *J. Stat. Softw*. 67, 1–48.

Bolker, B. M., Brooks, M. E., Clark, C. J., Geange, S. W., Poulsen, J. R., Stevens, M. H. H., and White, J-S. S. (2009). Generalized linear mixed models: a practical guide for ecology and evolution. *Trends Ecol. Evol*. 24, 127–135.

Cohen J. H. and Forward, R. B. (2009). Zooplankton diel vertical migration: a review of proximate control. *Oceanogr. Mar. Biol. Ann. Rev*. 47, 77–110.

Donohue, M. C. and Edland, S. D. (2016). longpower: Power and sample size calculators for longitudinal data. R package version 1.0-16.

Forward, R. B., Cronin, T. W., and Stearns, D. E. (1984). Control of diel vertical migration : Photoresponses of a larval crustacean. *Limnol. Oceanogr*. 29, 146–154.

R Core Team, (2016). R: A language and environment for statistical computing. R Foundation for Statistical Computing, Vienna, Austria. URL http://www.R-project.org/.

Appendix C

CHAPTER 6 SUPPLEMENTARY MATERIALS

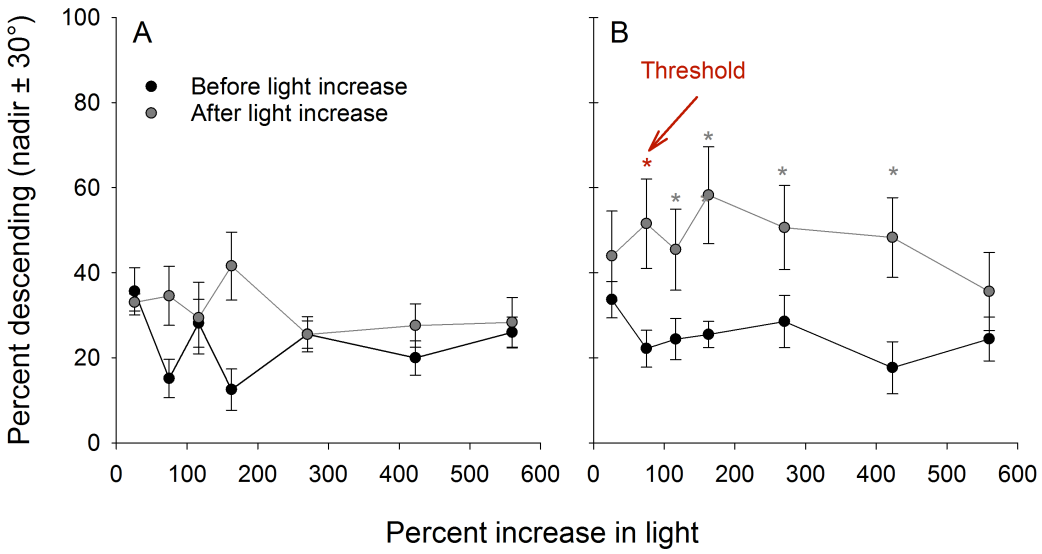

Figure C.1: Determination of the behavioral threshold. Mean ± se percentage of animals descending (nadir ± 30°) before (black) and after (gray) an increase in light. Prior to experiments, animals were exposed to either (A) control or (B) field seawater for 1 – 3 h. Field seawater was collected on August 28th, 2014, and the example dataset shown here was included in my analysis. Significant differences in the percentage descending before and after light stimulation were determined by one-way repeated measures ANOVAs with Holm–Šidák *post hoc* tests and accepted at $P < 0.05$. The behavioral threshold, or lowest light increase to induce a descent response, is labeled in red. Note that animals in control seawater did not exhibit a significant descent response to increases in light.

Table C.1: Descent responses and behavioral thresholds of *Artemia* spp. nauplii after a 1 – 3 h exposure to field water from samples taken in 2014 and 2015.

Year	Month/Day	Response to field water (Signficant descent, nadir ± 30°)	Threshold (% increase in light)
2014	08/28	Y	26
	09/03	Y	77
	09/09	N	–
	09/18	Y	77
	09/24	Y	120
	10/02	N	–
	10/08	Y	77
	10/16	N	–
	10/22	Y	77
	10/30	N	–
2015	05/27	Y	75
	06/03	Removed	
	06/10	Y	163
	06/18	Y	75
	06/23	Removed	
	06/30	Y	116
	07/08	Y	116
	07/13	Y	75
	07/22	Y	75
	07/28	Y	26
	08/06	Y	116
	08/11	Y	75
	08/21	Y	116
	08/27	Y	75
	09/03	Y	75
	09/09	Y	116
	09/14	Y	116
	09/22	Y	75
	09/29	Y	75
	10/06	Y	26
	10/13	Y	26
	10/22	Y	75
	10/29	Y	75

Significant descent responses (e.g Fig. C.1) are denoted by "Y", whereas no response to field water is represented by "N". Behavioral thresholds (% increase in light) are shown for each week in which *Artemia* spp. responded to field water. If no response/threshold (−), samples were given a behavioral threshold of 175% for analyses, as this percent increase in light was greater than thresholds of responding individuals. Two samples were removed in 2015, because animals also exhibited a descent response in the control.

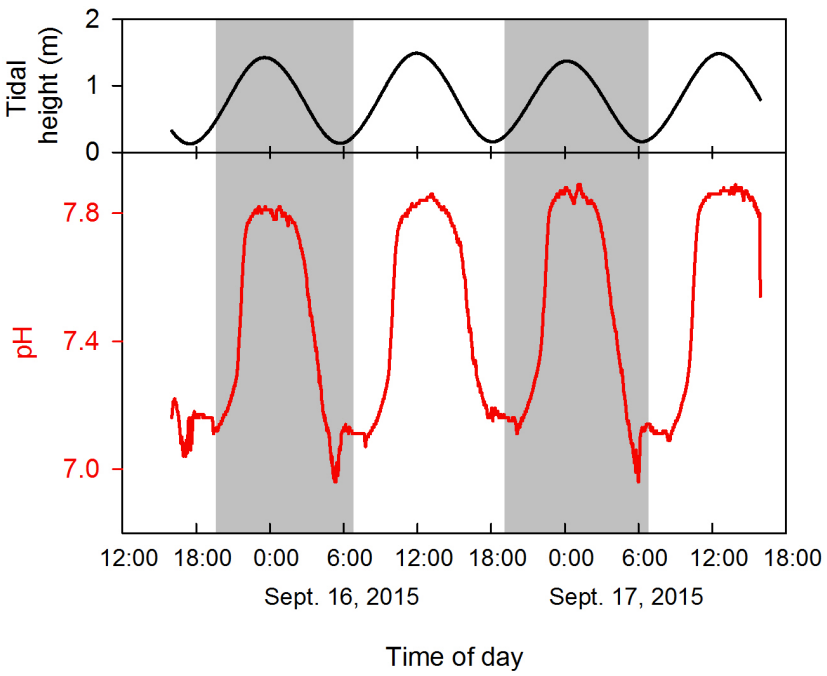

Figure C.2: Tidal and diel fluctuations in pH. Time series of pH (red), tidal height (m above mean lower low water, black), and day (white) versus night (gray), measured from September 15th, 2015 to September 17th, 2015 in Broadkill River, Delaware, USA (38.802583°, -75.203183°). Measurements of pH were made with a Sonde (6600-V2; YSI Incorporated, Yellow Springs, OH, USA).

Appendix D

RIGHTS AND PERMISSIONS OF PUBLISHED CHAPTERS

D.1 Journal of Experimental Biology (Ch. 2)

Text below describes the rights and permissions of the Journal of Experimental Biology, and was found at http://jeb.biologists.org/content/rights-permissions:

At JEB, we realise that different authors may have different needs when it comes to article access policies.

If your funder or institute mandate any aspect of Open Access, we recommend that you select the journal's Gold Open Access option during submission. Your article will be published under a CC-BY licence and research papers will be deposited into PMC for immediate release. JEB charges an article processing fee of £2,500 (plus VAT if applicable) for this Gold Open Access option. If you pay for Open Access publication and we fail to fulfil these Open Access commitments, an APC rebate is available – please contact the editorial office.

If you do not have any specific Open Access needs, your article will be published automatically under the Green Open Access model. For the first six months your article will only be accessible by subscribers of the journal. After six months, the article will be made freely available for everyone. Publishing under the Green Open Access model in JEB is completely free.

If you do not want your article to be Gold Open Access, but must comply with PMC deposition mandates, it is essential that you fully and correctly indicate all

funder/institute PMC mandates for all authors as part of the submission process. Your research paper will then be deposited in PMC for release after 6 or 12 months as mandated. This is a free service offered to authors of research papers who require deposition. If you fail to select the correct options during submission and PMC deposition is requested at a later stage, we reserve the right to charge $50 for the PMC deposition service.

We are also a member of CHORUS and will ensure that your article complies with US public access mandates.

These options should allow you to comply with any funder / institute mandates.

Authors should be aware that some article types are already free to read on our site: Editorial, Publisher's Note, Correction, Retraction, Obituary, Inside JEB, Outside JEB, Special Issues and occasional other selected articles.

Further details on our Gold Open Access and Green Open Access options are listed in the table below.

Table D.1: Rights and permissions as described by the Journal of Experimental Biology

	Gold Open Access	Green Open Access (this is applied to all other papers)
Author information		
Fees	Article Processing Charge (APC): £2,500 (plus VAT if applicable)	FREE to the author
License	CC-BY license	Company of Biologists Publication Agreement
Copyright owner	The author.	The author.
Preprint servers	This journal allows posting of research manuscripts in preprint servers.	This journal allows posting of research manuscripts in preprint servers.

Content freely available on journal website	Immediately upon publication.	FREE to read 6 months after publication; Company of Biologists retains exclusive license.
Use in other articles created by the author	Allowed by CC-BY license.	Data, figures and tables created by the author can be reused in other articles by that author.
FREE deposition in PMC	FREE author service. Immediately upon publication. Final published PDF.	FREE author service for research papers where mandated by funder or institution.
Self archiving		
Posting on author's website	Immediately upon publication. Any version, including final published PDF. Must attribute source e.g. by citing doi and linking to the published article on the journal website.	Immediately upon publication. Any version, including final published PDF. Must link to published article on journal website.
Inclusion in thesis	Immediately upon publication. Any version, including final published PDF. Must attribute source e.g. by citing doi and linking to the published article on the journal website.	Immediately upon publication. Any version, including final published PDF. Must link to published article on journal website.
Institutional repository, thesis repository or PMC Europe	Immediately upon publication. Any version, including final published PDF. Must attribute source e.g. by citing doi and linking to the published article on the journal website.	If mandated by funder or institute. 12 months after publication unless otherwise mandated. Any version, including final published PDF. Must link to published article on journal website.
Use by parties other than the authors		
Teaching purposes	Allowed by CC-BY license.	Use for bona fide teaching is allowed on the condition that it is non-commercial.
Commercial use	Allowed by CC-BY license.	Permission requests via CCC.
Third party article collections	Allowed by CC-BY license.	Permission requests via CCC.
Responsible text and data mining	Allowed by CC-BY license.	Responsible TDM allowed on the condition that it is non-commercial.

D.2 Royal Society Open Science (Ch. 4)

The text below describes the rights and permissions of Royal Society Open Science, and was found at https://royalsociety.org/journals/authors/open-access/:

Authors who choose open access publication are likely to benefit from increased dissemination and citation.

We apply exactly the same standards of high-quality, rapid peer review and production to all papers, whether they are available under open access or subscription only.

If you choose open access, for relevant journals we will deposit the article in PubMedCentral on your behalf. You'll also benefit from a liberal licensing and re-use policy through Creative Commons licence CC-BY 4.0 (https://creativecommons.org/licenses/by/4.0/legalcode).

Our open access policies are fully compliant with the requirements of a range of funders including the Wellcome Trust, HEFCE (REF 2020), NIH, HHMI, RCUK, European Commission, MRC, NERC, STFC, ESRC, EPSRC and BBSRC. For a full list of funders with open access requirements, please visit the SHERPA/JULIET website.

We have recently also partnered with CHORUS and FundRef, enabling us to better capture and record funding information on individual articles.

Appendix E

ANIMAL CARE APPROVAL

University of Delaware
Institutional Animal Care and Use Committee
Request to Amend an Animal Use Protocol

RECEIVED
MAY 11 2016
IACUC JH

Title of Protocol: Body mucus collection from an estuarine fish	
AUP Number: 1236-2016-A	← **(4 digits only)**
Principal Investigator: Jonathan H. Cohen	

Requested Changes

I am requesting a change to: ***(Check all that apply)***

- ☒ Animal Species *(Complete Section 1)*
- ☒ Animal Numbers *(Complete Section 2)*
- ☒ Animal Procedures *(Complete Section 3)*
- ☐ Therapeutic or Experimental Agents *(Complete Section 4)*
- ☐ Pain Category *(Complete Section 5)*
- ☐ Use of Biological Material, Hazardous Agents or Radiation *(Complete Sections 4 & 6)*
- ☐ Other *(Specify)* Click here to enter text.

(Complete Section 7)

Changes MUST NOT be initiated until IACUC approval is granted

Official Use Only

IACUC Approval Signature: Jon Talbot, DVM

Date of Approval: 5/16/16